

Non-minimally coupled scalar field dark sector of the universe: in-depth (Einstein frame) case study

Marcin Postolak^{1,*}

¹*Institute of Theoretical Physics, Faculty of Physics and Astronomy,
University of Wrocław, pl. M. Borna 9, 50-204 Wrocław, Poland*

(Dated: May 13, 2025)

We revisit non-minimally coupled scalar field cosmologies in the Einstein frame and present a comprehensive analysis that spans background dynamics, linear perturbations, thermodynamics, quantum gravity constraints and baryogenesis. Using a dynamical systems approach, we classify all analytical critical points for a representative set of scalar field potentials: axions/ALPs, cyclic ekpyrotic, exponential/ekpyrotic with Λ , quintessence, and scalar field dark matter. We show that a chameleon-like coupling $f(\phi) = e^{\beta\phi}$ modifies both the expansion history and the growth of structure in a way that remains compatible with current fifth force searches. Analytical transfer matrices for primordial tensor modes are derived, revealing a scale-dependent break in the gravitational wave spectrum whose position and amplitude are fixed by the coupling parameter β . A causal Israel–Stewart treatment demonstrates that the same coupling supplies an effective bulk pressure that drives a smooth bounce while respecting quantum energy inequalities. Penrose’s Weyl-curvature hypothesis is recovered dynamically: during an ekpyrotic phase with $\omega \gg 1$ the Weyl invariant decays as $a^{-6(1+\omega)}$, resetting gravitational entropy without violating the generalized second law. A time-varying ϕ simultaneously generates an effective chemical potential $\mu_B \simeq \beta\dot{\phi}/M_*^2$, allowing for spontaneous high-scale baryogenesis whose back reaction on ϕ is negligible for $M_* \gtrsim 10^{15}\sqrt{\beta}$ GeV. Swampland distance and de Sitter criteria are automatically satisfied because the ekpyrotic phase confines the field excursion to $\Delta\phi \lesssim \mathcal{O}(1)M_{\text{Pl}}$. These results establish new links between dark sector interactions, entropy production, and late-time acceleration while identifying observational windows: CMB B-modes, PTA and LISA frequency bands, BAO and growth rate measurements where the predictions can be tested in the near future.

I. INTRODUCTION

A. Cosmological context and open problems

The Λ -CDM (LCDM) cosmological concordance model provides a remarkably efficient fit to a plethora of observations, yet its phenomenological success conceals a set of deep theoretical puzzles that collectively motivate the scalar–tensor (ST) gravity/cosmology framework explored in this article. Foremost among these is the vacuum energy crisis: quantum field theory (QFT) estimates of the zero-point energy are roughly 10^{60} – 10^{120} times larger than the energy density inferred from late-time cosmic acceleration, a discrepancy recognized as the *cosmological constant problem* [1–4] (“*the worst theoretical prediction in the history of physics*” [5] or “*the largest discrepancy between theory and experiment in all of science*” [6]). Dynamical dark energy (DE) proposals attempt to reconcile this mismatch by promoting the cosmological constant to a field whose stress–energy evolves on cosmological timescales; minimally coupled quintessence, Galileons, $f(R)$ gravity and related constructions have all been shown to track the background expansion while remaining consistent with supernovae, cosmic microwave background (CMB) and baryon acoustic oscillations (BAO) data [7–10]. Non-minimally cou-

pled (NMC) scalars occupy a particularly attractive corner of theory space because the conformal coupling potentially could simultaneously suppress vacuum contributions in high-curvature environments, thereby evading stringent Solar System tests, while allowing for an order-one effective equation of state on Hubble scales, thus providing a technically natural handle on the cosmological constant problem.

A second, equally pressing challenge arises from the nature of dark matter (DM). Three decades of dedicated direct, indirect and collider searches have yet to reveal the *weakly interacting massive particles* (WIMPs) that once dominated the theoretical discourse [11–17]. Alternatives collectively referred to as *very weakly interacting slim particles* (WISPs)¹ based on ultra-light axions and scalar field dark matter emerge naturally in string-theoretic compactifications and in the Peccei–Quinn mechanism; such fields exhibit de Broglie wavelengths on kiloparsec scales, leading to solitonic cores that can alleviate the core-cusp, too-big-to-fail and missing-satellite problems that plague collisionless cold dark matter (CDM) simulations [18–25]. When endowed with a conformal coupling, these axion-like fields inherit the same screening mechanisms as their dark energy counterparts, thereby evading equivalence principle violations while leaving testable im-

¹ More information can be found on the website of *COST Action CA21106* – “*COSMIC WISPs in the Dark Universe: Theory, astrophysics and experiments*” - <https://cosmicwisps.eu/>.

* marcin.postolak@uwr.edu.pl

prints in pulsar-timing arrays (PTA), 21-cm surveys and precision reionization data.

The observational frontier has now entered a sub-percent precision regime, driven by large-scale structure (LSS) and late-universe probes such as DESI (*Dark Energy Spectroscopic Instrument*), DES (*Dark Energy Survey*), KiDS (*Kilo-Degree Survey*), HSC (*Hyper Suprime-Cam*) and recent analyses [26–34]. Paradoxically, the very success of these surveys has sharpened internal inconsistencies within Λ -CDM, most notably the H_0 and S_8 tensions² [35]: local determinations of the Hubble constant based on Cepheid-calibrated supernovae and the amplitude of matter clustering inferred from weak lensing disagree with Planck’s base Λ -CDM values at the $2\sigma - 4\sigma$ level [35–37]. Rolling scalar fields that couple differentially to baryons and dark matter can reconcile these anomalies by modifying the background expansion during the matter-dominated era and by altering the growth index in a scale-dependent manner. Such mechanisms are naturally embedded in the NMC framework studied here, and forthcoming Euclid, Roman and CMB-S4 data will critically test their viability.

At even earlier epochs, the inflationary paradigm elegantly explains the spatial flatness, homogeneity and isotropy of the universe and predicts an almost scale-invariant spectrum of curvature perturbations [38–41]. Nonetheless, inflation inherits two conceptual hurdles: it does not eliminate the initial singularity, it merely pushes it to earlier times, and it is acutely sensitive to ultraviolet (UV) physics, raising concerns about radiative stability and the trans-Planckian problem [42–44]. Alternatives based on ekpyrotic or cyclic cosmologies replace the inflationary epoch with a phase of slow, ultra-stiff contraction followed by a non-singular bounce (ekpyrotic models) [45–53], or iterate through infinite cycles (conformal cyclic cosmology) [54, 55]. These scenarios suppress primordial anisotropies and potentially realize Penrose’s low-entropy initial state [56–60], but they require a brief violation of the null energy condition (NEC). NMC scalars offer a radiatively stable avenue for NEC violation, permitting smooth, ghost-free bounces that pass quantum stability conditions [61–64]. The same coupling that screens vacuum energy at late times thus plays a pivotal role in the earliest moments of cosmic history, unifying early- and late-time dynamics within a single effective field theory (EFT) description [10, 65, 66].

From the perspective of linear perturbation theory, primordial fluctuations originate in an approximately Bunch–Davies vacuum [67] and evolve through horizon crossing to seed the temperature anisotropies and polarization patterns observed in the CMB, as well as the formation of LSS. The conformal coupling modifies

both scalar and tensor transfer functions, enhancing the high-frequency tail of the stochastic gravitational wave (GW) background and generating potentially observable signals in LISA, DECIGO, SKA and PTA experiments [68–70]. A self-consistent treatment must combine quantum field theory in curved spacetime with thermodynamic considerations at causal horizons [71–77]. Viability additionally demands compliance with classical energy conditions, a well-behaved autonomous dynamical system, and compatibility with Swampland constraints that restrict low-energy effective theories in quantum gravity [78–93]. Simultaneously, the model must furnish a mechanism for baryogenesis and satisfy stringent fifth force and equivalence principle bounds from laboratory and satellite experiments [94–101].

Against this backdrop, the exponential non-minimally coupled scalar sector developed in the present work is designed to address, within a unified and empirically testable framework, the dark energy problem, the particle nature of dark matter, the emerging H_0 and S_8 tensions, the trans-Planckian sensitivity of the early universe, and the cosmological implications of Swampland conjectures. By confronting these interlocking problems with current data and outlining falsifiable predictions for forthcoming surveys, we aim to advance the programme of high-precision cosmology beyond Λ -CDM while maintaining rigorous theoretical consistency.

B. Aim and outline of this work

Guided by the above considerations, we perform an in-depth Einstein frame analysis of a NMC to matter (baryons) scalar field with exponential coupling that significantly expands the previously considered models [102].

Section II derives the exact background equations, highlighting the modified baryon scaling $\rho_b \propto a^{-3}e^{\beta\phi}$. In Sec. III we compute the full linear perturbation system, including new β -dependent source terms. Section IV reviews dynamical systems tools [80, 81] and Sec. V formulates the autonomous system whose critical points are classified, for each potential in Sec. VI, in Tables I–XIV. Section VII traces representative cosmological trajectories, while Secs. VIII–IX confront the model with fifth force tests [98] and primordial gravitational waves (PGWs) predictions [68]. A detailed analysis of the evolution of possible trajectories in phase space was carried out in Sec. X. The effect of non-minimal coupling on the cosmological tension issue and the ultra light dark matter (ULDM) model is described in Sec. XI and Sec. XII, respectively. Thermodynamic and quantum gravity aspects, including entropy production, causal bulk viscosity, energy conditions diagnostics and Swampland constraints, are unified in Secs. XIII–XV. The generation of the baryon asymmetry via a time-dependent chemical potential is presented in Sec. XVI and the Weyl curvature hypothesis is recovered dynamically in Sec. XVII. Finally,

² More information can be found on the website of *COST Action CA21136 – “Addressing observational tensions in cosmology with systematics and fundamental physics (CosmoVerse)”* - <https://cosmoversetensions.eu/>.

Sec. XVIII summarizes the new insights and enumerates future directions, ranging from DESI/DES consistency tests to PTA constraints on blue-tilted tensor spectra.

II. BACKGROUND LEVEL

In this section, we present the background-level equations for a spatially flat FLRW universe in the presence of a NMC scalar field ϕ . We closely follow the notation of [102, 103].³

A. Action and NMC

We consider the following general form of the action:

$$S[g_{\mu\nu}, \phi, \chi] = \frac{1}{2\kappa^2} \int d^4x \sqrt{-g} [R - g^{\mu\nu} \partial_\mu \phi \partial_\nu \phi - \mathcal{V}(\phi)] + S_m[f^2(\phi)g_{\mu\nu}, \chi], \quad (1)$$

where:

$$f(\phi) \equiv e^{\beta\phi}. \quad (2)$$

Throughout this article, we use normalization of the reduced Einstein gravitational constant, namely:

$$\kappa^2 \equiv \frac{8\pi G}{c^4} = 1. \quad (3)$$

A crucial effect of the coupling is that the (baryonic) matter fields effectively 'see' the *transformed metric* - the *dark sector metric*:

$$\tilde{g}_{\mu\nu} \equiv f^2(\phi)g_{\mu\nu}, \quad (4)$$

modifying the usual:

$$\rho_b \propto a^{-3} \quad (5)$$

scaling for baryons.

B. Constraints and fluid equations

We include radiation and baryons, with energy densities ρ_r and ρ_b , respectively. Setting the equation of state for radiation to $\omega_r = 1/3$ and for baryons to $\omega_b = 0$, one obtains the Friedmann equation:

$$3H^2 = \sum_i [\rho_i(a, \phi)] + \frac{1}{2}\dot{\phi}^2 + \frac{1}{2}\mathcal{V}(\phi), \quad (6)$$

where $i = r, b$. From [102] (see *Proposition 2.1.*), the background densities obey:

$$\dot{\rho}_r = -3H\rho_r(1 + \omega_r) = -4H\rho_r, \quad (7)$$

$$\dot{\rho}_b + 3H\rho_b(1 + \omega_b) = -\frac{\dot{f}}{f}\rho_b(3\omega_b - 1) = \dot{\phi}\frac{f'(\phi)}{f(\phi)}\rho_b, \quad (8)$$

and the general solution takes the form of:

$$\rho_i(a, \phi) \equiv f^4(\phi)\rho_i[af(\phi)]. \quad (9)$$

C. Baryons and radiation

Solving the continuity (7) and non-continuity equation (8) leads to:

$$\rho_r(a, \phi) \equiv \rho_{r0}f^4(\phi)[af(\phi)]^{-4} = \rho_{r0}a^{-4} \equiv \rho_r(a), \quad (10)$$

$$\rho_b(a, \phi) \equiv \rho_{b0}f^4(\phi)[af(\phi)]^{-3} = \rho_{b0}f(\phi)a^{-3}, \quad (11)$$

so that radiation retains the usual $\propto a^{-4}$ dependence, while baryons gain an extra factor $f(\phi) = e^{\beta\phi}$.

D. Equations of motion

In the homogeneous spatially flat FLRW background, the relevant equations become of the form:

$$\begin{aligned} 2\dot{H} + 3H^2 &= -\sum_i [p_i(a, \phi)] - \frac{1}{2}\dot{\phi}^2 + \frac{1}{2}\mathcal{V}(\phi) \\ &= -\sum_i [\omega_i\rho_i(a, \phi)] - \frac{1}{2}\dot{\phi}^2 + \frac{1}{2}\mathcal{V}(\phi), \end{aligned} \quad (12a)$$

$$\begin{aligned} \ddot{\phi} + 3H\dot{\phi} + \frac{1}{2}\mathcal{V}'(\phi) &= -f'(\phi)\rho_b(a, \phi)(1 - 3\omega_b) \\ &= -f'(\phi)\rho_b(a, \phi) \\ &= -f'(\phi)f(\phi)\rho_b(a). \end{aligned} \quad (12b)$$

E. Conformal time representation

Introducing the conformal time, τ , by the relation:

$$\frac{d}{d\tau} \equiv (\cdot)' \equiv a\frac{d}{dt}, \quad (13)$$

one could obtain:

$$3\mathcal{H}^2 = a^2 \sum_i [\rho_i(a, \phi)] + \frac{1}{2}\phi'^2 + \frac{1}{2}\mathcal{V}(\phi)a^2, \quad (14)$$

³ In contrast to [103], the non-minimal coupling between matter sector and the scalar field is described by the functional dependence $f^2(\phi)$ in this article.

$$\begin{aligned}
2\mathcal{H}' + \mathcal{H}^2 &= -a^2 \sum_i [p_i(a, \phi)] - \frac{1}{2}\phi'^2 + \frac{1}{2}\mathcal{V}(\phi)a^2 \\
&= -a^2 \sum_i [\omega_i \rho_i(a, \phi)] - \frac{1}{2}\phi'^2 + \frac{1}{2}\mathcal{V}(\phi)a^2,
\end{aligned} \tag{15a}$$

$$\phi'' + 3\mathcal{H}\phi' + \frac{1}{2}\mathcal{V}'(\phi)a^2 = -a^2 f'(\phi)\rho_b(a, \phi). \tag{15b}$$

Here:

$$\mathcal{H} \equiv \frac{a'}{a} \tag{16}$$

is the conformal Hubble parameter and:

$$f'(\phi) \equiv \frac{df(\phi)}{d\phi}. \tag{17}$$

In the simplest scenario of the chameleon-like mechanism (exponential coupling) that will be employed in this work:

$$\beta(\phi) = \beta = \text{const.} \tag{18}$$

These equations set the stage for our dynamical investigation in subsequent sections, where we introduce dimensionless variables to study fixed points and for analyzing how perturbations evolve in the presence of a non-minimal coupling.

III. COSMOLOGICAL PERTURBATIONS

We turn now to the perturbative regime, examining the linearized fluctuations of the metric and matter fields in the presence of a chameleon-like scalar field. Our presentation follows standard treatments [104–108], specialized to synchronous gauge and explicitly including the modifications induced by $f(\phi) = \exp(\beta\phi)$ in the baryonic sector.

A. Perturbed metric in synchronous gauge

The line element is written as:

$$ds^2 = a^2(\tau) [-d\tau^2 + (\delta_{ij} + h_{ij}) dx^i dx^j], \tag{19}$$

where h_{ij} can be decomposed in terms of Fourier modes:

$$\begin{aligned}
h_{ij}(\vec{x}, \tau) = \\
\int d^3k e^{i\vec{k}\cdot\vec{x}} \left[\hat{k}_i \hat{k}_j h(\vec{k}, \tau) + \left(\hat{k}_i \hat{k}_j - \frac{1}{3}\delta_{ij} \right) 6\eta(\vec{k}, \tau) \right]
\end{aligned} \tag{20}$$

with:

$$\vec{k} = k\hat{k}. \tag{21}$$

The scalar field is split into:

$$\phi(\tau, \vec{x}) = \bar{\phi}(\tau) + \delta\phi(\tau, \vec{x}), \tag{22}$$

and the matter density fluctuations are quantified by the density contrast:

$$\delta_i \equiv \frac{\delta\rho_i}{\bar{\rho}_i}, \tag{23}$$

while velocity perturbations enter via velocity divergence:

$$\theta_i \equiv ik^j \delta u_j^{(i)}. \tag{24}$$

B. Linearized field equations

In the synchronous gauge, the perturbed Einstein equations yield relations such as [106]:

$$\delta G^\mu{}_\nu = \delta T^\mu{}_\nu, \tag{25}$$

$$k^2\eta - \frac{1}{2}\mathcal{H}h' = \frac{1}{2}a^2[\delta\rho_r + \delta\rho_b + \delta\rho_\phi], \tag{26}$$

where:

$$\delta\rho_\phi = a^{-2}\bar{\phi}'\delta\phi' + \frac{1}{2}\mathcal{V}'(\bar{\phi})\delta\phi. \tag{27}$$

Likewise:

$$\begin{aligned}
k^2\eta' &= \frac{a^2}{2} \left[(\bar{\rho}_r + \bar{p}_r)\theta_r + (\bar{\rho}_b + \bar{p}_b)\theta_b + \frac{k^2}{a^2}\bar{\phi}'\delta\phi \right] \\
&= \frac{a^2}{2} \left[\frac{4}{3}\bar{\rho}_r\theta_r + \bar{\rho}_b\theta_b + \frac{k^2}{a^2}\bar{\phi}'\delta\phi \right].
\end{aligned} \tag{28}$$

Another key relation is:

$$\begin{aligned}
h'' + 2\mathcal{H}h' - 2k^2\eta &= -3a^2(\delta p_r + \delta p_\phi) \\
&= -3a^2\left(\frac{1}{3}\delta\rho_r + \delta p_\phi\right),
\end{aligned} \tag{29}$$

with:

$$\delta p_\phi = a^{-2}\bar{\phi}'\delta\phi' - \frac{1}{2}\mathcal{V}'(\bar{\phi})\delta\phi. \tag{30}$$

C. Klein-Gordon equation with exponential coupling

When the chameleon-like factor $f(\phi)$ multiplies the baryon sector, the scalar field's linearized equation includes:

$$\delta[f'(\phi)\rho_b] = f'(\bar{\phi})\delta\rho_b + f''(\bar{\phi})\bar{\rho}_b\delta\phi, \tag{31}$$

and thus the Klein-Gordon equation takes the form:

$$\begin{aligned}
\delta\phi'' + 2\mathcal{H}\delta\phi' + \left[k^2 + \frac{a^2}{2}\mathcal{V}''(\bar{\phi}) \right] \delta\phi - \frac{1}{2}\bar{\phi}'h' \\
= -a^2 \left[f'(\bar{\phi})\delta\rho_b + f''(\bar{\phi})\bar{\rho}_b\delta\phi \right].
\end{aligned} \tag{32}$$

In the specific case of $f(\phi) = \exp(\beta\bar{\phi})$, one has $f'(\bar{\phi}) = \beta e^{\beta\bar{\phi}}$, $f''(\bar{\phi}) = \beta^2 e^{\beta\bar{\phi}}$. The above equation then reduces to:

$$\begin{aligned} \delta\phi'' + 2\mathcal{H}\delta\phi' + \left[k^2 + \frac{a^2}{2}\mathcal{V}''(\bar{\phi})\right]\delta\phi - \frac{1}{2}\bar{\phi}'h' \\ = -a^2\left(\beta\delta\rho_b + \beta^2\bar{\rho}_b\delta\phi\right). \end{aligned} \quad (33)$$

D. Perturbed fluid equations

1. Radiation perturbations

For radiation, the linearized continuity and Euler equations read:

$$\delta_r' = -\frac{4}{3}\left(\theta_r + \frac{1}{2}h'\right), \quad (34)$$

$$\theta_r' = \frac{1}{4}k^2\delta_r. \quad (35)$$

These maintain the standard form since radiation does not couple directly to ϕ in this setup (if only baryons are coupled).

2. Baryon perturbations

In contrast, baryons acquire additional terms from the explicit ϕ -dependence of ρ_b . The continuity equation is:

$$\begin{aligned} \delta_b' = -\theta_b - \frac{1}{2}h' + \frac{f'(\bar{\phi})}{f(\bar{\phi})}\left(\delta\phi' - \bar{\phi}'\delta_b\right) \\ + \bar{\phi}'\left[\frac{f''(\bar{\phi})}{f(\bar{\phi})} - \frac{f'(\bar{\phi})^2}{f(\bar{\phi})^2}\right]\delta\phi, \end{aligned} \quad (36)$$

and the Euler equation is:

$$\theta_b' = -\mathcal{H}\theta_b + \frac{f'(\bar{\phi})}{f(\bar{\phi})}k^2\delta\phi. \quad (37)$$

Specifically, in our case, one obtains:

$$\delta_b' = -\theta_b - \frac{1}{2}h' + \beta\left(\delta\phi' - \bar{\phi}'\delta_b\right), \quad (38)$$

$$\theta_b' = -\mathcal{H}\theta_b + \beta k^2\delta\phi. \quad (39)$$

These new terms affect both the growth rate of baryon overdensities and the scalar fluctuations. In the next sections, we use the dynamical-systems framework (Sec. V) and the choice of specific scalar field potentials (Sec. VI) to analyze the resulting modified evolution of perturbations, structure formation, and possible observational signatures.

E. Physical implications

The modifications introduced by the NMC not only affect the background evolution but also leave important imprints on the dynamics of cosmological perturbations. These modifications have several key physical implications:

a. Impact on structure formation: The extra terms in the baryon continuity and Euler equations, modify the evolution of baryonic density fluctuations, leading to scale-dependent alterations of the matter power spectrum. Such modifications may shift the amplitude and peak position of the BAO and affect the growth rate of structures, as discussed in [106, 107]. These effects can be probed by future large-scale structure surveys such as DESI and Euclid, allowing tests of the strength of the non-minimal coupling.

b. Effects on CMB anisotropies: The modified dynamics of scalar perturbations influence the gravitational potential fluctuations and thus imprint changes on the CMB anisotropy spectrum. In particular, alterations in the Integrated Sachs-Wolfe (ISW) effect due to the modified evolution of the metric perturbations (notably through the coupling-induced changes in h' and η') can leave detectable signals in the low multipoles of the temperature and polarization spectra [105, 108]. Precise measurements of these large-angle anisotropies may therefore provide indirect constraints on β .

c. Gravitational waves (tensor modes) signatures: While the evolution equation for tensor perturbations retains its canonical form in the synchronous gauge, the modified background dynamics induced by $f(\phi)$ affect the evolution of the scale factor $a(\tau)$ and the conformal Hubble parameter \mathcal{H} . This, in turn, alters the amplitude and spectral tilt of primordial gravitational waves [70]. In particular, the modifications can lead to deviations from the nearly scale-invariant tensor spectrum predicted by inflation, with possible blue tilts characteristic of ekpyrotic or bouncing models [109–111]. Future CMB polarization experiments and gravitational wave observatories could be sensitive to such signatures.

IV. DYNAMICAL SYSTEMS: THEORETICAL BACKGROUND

The use of dynamical systems methods in cosmology has proven to be an efficient way to classify the asymptotic (early- and late-time) behavior of solutions to the underlying field equations; see, e.g., [80–83, 86] and references therein. In this section, we summarize the main mathematical concepts required for the subsequent analysis in this article.

A. General setup

A *dynamical system* in (continuous) time⁴ can be written as:

$$\dot{\mathbf{x}} = \mathbf{f}(\mathbf{x}) \quad \wedge \quad \mathbf{x} \in \mathbb{R}^n, \quad (40)$$

where the dot denotes differentiation with respect to time t , and:

$$\mathbf{f} : \mathbb{R}^n \rightarrow \mathbb{R}^n \quad (41)$$

is assumed to be sufficiently smooth. A point \mathbf{x}_0 is called a *fixed point* (*equilibrium point* or *critical point*) if:

$$\mathbf{f}(\mathbf{x}_0) = \mathbf{0}. \quad (42)$$

From a cosmological perspective, these fixed points often correspond to asymptotic states (e.g., matter domination, radiation domination, de Sitter phases, etc.). Studying their existence and stability thus provides valuable information about long-term cosmic behavior.

B. Linear stability

To assess the stability of a fixed point \mathbf{x}_0 , one typically studies the linearization of (40) near \mathbf{x}_0 . Writing:

$$\mathbf{x} = \mathbf{x}_0 + \boldsymbol{\varepsilon}, \quad \|\boldsymbol{\varepsilon}\| \ll 1, \quad (43)$$

and expanding $\mathbf{f}(\mathbf{x})$ to first order, we get:

$$\dot{\boldsymbol{\varepsilon}} = D\mathbf{f}(\mathbf{x}_0)\boldsymbol{\varepsilon} + \mathcal{O}(\|\boldsymbol{\varepsilon}\|^2), \quad (44)$$

where $D\mathbf{f}(\mathbf{x}_0)$ is the Jacobian matrix of partial derivatives evaluated at \mathbf{x}_0 . Therefore, the local behavior of solutions near \mathbf{x}_0 is governed by the linear system:

$$\dot{\boldsymbol{\varepsilon}} = A\boldsymbol{\varepsilon}, \quad \text{where } A := D\mathbf{f}(\mathbf{x}_0). \quad (45)$$

1. Classification of fixed points

The matrix A has n (possibly complex) eigenvalues λ_i . Based on these, the following classification of critical points is made:

1. **Stable (attracting) node:** If all eigenvalues have strictly negative real parts, $\Re(\lambda_i) < 0$, then \mathbf{x}_0 is asymptotically stable (i.e. small perturbations decay to \mathbf{x}_0).
2. **Unstable (repelling) node:** If all eigenvalues have strictly positive real parts, \mathbf{x}_0 is unstable (perturbations grow away from \mathbf{x}_0).

3. **Saddle:** If at least one eigenvalue has positive real part and at least one has negative real part, \mathbf{x}_0 is a saddle. Solutions approach \mathbf{x}_0 along stable directions and depart along unstable directions.

4. **Center-type (oscillatory):** If purely imaginary eigenvalues occur with no zero real parts of other eigenvalues, one obtains neutral stability (typical in oscillatory phenomena). Higher-order terms are needed to decide long-term behavior, often using normal form or center manifold methods [82, 83].

5. **Degenerate/critical cases:** If one or more eigenvalues vanish, or if complex eigenvalues have zero real part, a deeper analysis (e.g., center manifold or Lyapunov functions) is required.

In cosmic applications, stable fixed points often represent late-time attractors such as de Sitter phases, whereas saddle and unstable can correspond to transient eras (e.g. radiation or matter domination).

C. Center manifold analysis

When the Jacobian matrix $D\mathbf{f}(\mathbf{x}_0)$ at a fixed point (equilibrium) \mathbf{x}_0 (i.e., $\mathbf{f}(\mathbf{x}_0) = \mathbf{0}$) has one or more eigenvalues with *zero* real part, the standard linear stability classification is inconclusive. To proceed, one applies the *center manifold theorem* [82, 83, 112].

1. Center, stable and unstable subspaces

Let $A = D\mathbf{f}(\mathbf{x}_0)$ be the Jacobian evaluated at the equilibrium $\mathbf{x}_0 \in \mathbb{R}^n$. Suppose the eigenvalues of A are separated into three (possibly empty) sets:

- **Stable:** Eigenvalues whose real parts are strictly negative.
- **Unstable:** Eigenvalues whose real parts are strictly positive.
- **Center:** Eigenvalues whose real parts are exactly zero.

Accordingly, \mathbb{R}^n can be decomposed as a direct sum of the *stable*, *unstable*, and *center* subspaces:

$$\mathbb{R}^n = E^s \oplus E^u \oplus E^c, \quad (46)$$

where E^s , E^u , and E^c are spanned by the eigenvectors associated with stable, unstable, and center eigenvalues, respectively.

⁴ It is important to note that the time "t" does not necessarily have to be the *physical time* (as will be the case here).

2. Normal form near the equilibrium

By an appropriate local change of coordinates⁵ near \mathbf{x}_0 , we can write the dynamical system as:

$$\begin{pmatrix} \dot{\mathbf{s}} \\ \dot{\mathbf{c}} \\ \dot{\mathbf{u}} \end{pmatrix} = \begin{pmatrix} A_s & 0 & 0 \\ 0 & A_c & 0 \\ 0 & 0 & A_u \end{pmatrix} \begin{pmatrix} \mathbf{s} \\ \mathbf{c} \\ \mathbf{u} \end{pmatrix} + \Phi(\mathbf{s}, \mathbf{c}, \mathbf{u}), \quad (47)$$

where

- $\mathbf{s} \in \mathbb{R}^s$ (the “stable” variables) satisfy $\Re(\text{spec}(A_s)) < 0$,
- $\mathbf{u} \in \mathbb{R}^u$ (the “unstable” variables) satisfy $\Re(\text{spec}(A_u)) > 0$,
- $\mathbf{c} \in \mathbb{R}^c$ (the “center” variables) satisfy $\Re(\text{spec}(A_c)) = 0$,
- Φ contains the nonlinear terms that vanish to second order at $(\mathbf{s}, \mathbf{c}, \mathbf{u}) = \mathbf{0}$ (which corresponds to the equilibrium \mathbf{x}_0 in the original coordinates).

The dimensions add up as $s + c + u = n$.

3. Existence of the center manifold

The *center manifold* $\mathcal{W}^c(\mathbf{x}_0)$ is an invariant manifold of dimension c that is tangent at \mathbf{x}_0 to E^c . In a neighborhood of \mathbf{x}_0 , one can typically express the stable and unstable variables as functions of the center variables:

$$\mathbf{s} = \mathbf{h}_s(\mathbf{c}), \quad \mathbf{u} = \mathbf{h}_u(\mathbf{c}), \quad (48)$$

with $\mathbf{h}_s(\mathbf{0}) = \mathbf{0}$, $\mathbf{h}_u(\mathbf{0}) = \mathbf{0}$, and $D\mathbf{h}_s(\mathbf{0}) = D\mathbf{h}_u(\mathbf{0}) = \mathbf{0}$. Substituting these into (47), one obtains a *reduced system* in terms of only \mathbf{c} (the center directions). That smaller system then governs the local evolution on the center manifold.

4. Dynamical consequences

Once $\mathcal{W}^c(\mathbf{x}_0)$ is known (or approximated):

- *Stable directions* (\mathbf{s}): small perturbations in E^s decay exponentially to \mathbf{x}_0 , hence these do not affect asymptotic behavior on \mathcal{W}^c .
- *Unstable directions* (\mathbf{u}): small perturbations in E^u grow exponentially, so \mathbf{x}_0 is repelling along those directions.

- *Center directions* (\mathbf{c}): the evolution is *neutral* to first order, so nonlinear terms determine whether nearby trajectories approach, depart from, or remain oscillatory around \mathbf{x}_0 .

In cosmology, a non-hyperbolic equilibrium (with zero real part eigenvalues) may signal a transition or “tracking” behavior, commonly encountered in certain scalar field and modified gravity models [80, 81]. The center manifold thus captures the subtlety of these borderline cases, which often cannot be assessed by linearization alone.

D. Global attractors and invariant submanifolds

A system may have invariant submanifolds defined by constraints in phase space. For instance, in cosmological models, an equation of state or a scalar field potential might define submanifolds (e.g., $\Omega_r = 0$). A *global attractor* is a fixed point (or a set) such that all solutions converge to it (or remain in it) for large time. Examples in cosmology include de Sitter expansion or Minkowski vacuum, depending on the sign of the potential and the underlying model [103, 113, 114].

These techniques underpin the standard procedure for studying the cosmic evolution of NMC scalar field theories, quintessence, ekpyrotic models, etc. In the next sections, we apply this machinery to specific SF potentials and couplings of physical interest.

V. DYNAMICAL SYSTEM

We now formulate the relevant scalar field equations as an autonomous dynamical system, facilitating the classification of equilibrium points (i.e. fixed points) and their stability. In doing so, we explicitly retain the non-minimal coupling (NMC) factor introduced in (2) (see also [102, 103, 115, 116]).

A. Dimensionless variables

First, we define a new time variable based on the e-folding function of the scale factor:

$$N \equiv \ln a. \quad (49)$$

Differentiation with respect to N thus translates time derivatives $\dot{X} = \frac{dX}{dt}$ into:

$$\frac{dX}{dN} = \frac{1}{H} \frac{dX}{dt}. \quad (50)$$

The next step is to introduce dimensionless variables that encapsulate the ratio of the scalar field kinetic and

⁵ One shifts the origin to \mathbf{x}_0 and applies a linear transformation whose matrix blocks diagonalize A .

potential energies to the critical density, as well as any coupling-dependent terms. Specifically, we define⁶⁷:

$$\Omega_b \equiv \frac{\rho_b f(\phi)}{3H^2} \quad \wedge \quad x \equiv \frac{\dot{\phi}}{\sqrt{6}H} \quad \wedge \quad y \equiv \frac{\sqrt{|\mathcal{V}|}}{\sqrt{6}H}. \quad (51)$$

Here, Ω_b stands for baryonic matter with modified density $\rho_b f(\phi)$, x characterizes the kinetic energy of the SF, and y represents the potential energy. Additionally, we define:

$$\lambda_\phi \equiv -\frac{\mathcal{V}'(\phi)}{\mathcal{V}(\phi)} \quad \wedge \quad \Gamma_\phi(\lambda_\phi) \equiv \frac{\mathcal{V}''(\phi)\mathcal{V}(\phi)}{\mathcal{V}'(\phi)^2}, \quad (52)$$

$$\sigma_\phi \equiv \frac{f'(\phi)}{f(\phi)} \quad \wedge \quad \Delta_\phi(\sigma_\phi) \equiv \frac{f''(\phi)f(\phi)}{f'(\phi)^2}. \quad (53)$$

These parameters naturally appear in many chameleon-like or quintessence-like models. In particular, for exponential couplings $f(\phi) = \exp(\beta\phi)$, $\sigma_\phi = \beta$ remains constant, significantly simplifying the resulting system (reduction of the dimensionality of the dynamical system).

B. Basic relations

For later convenience, let us list the following useful relations that emerge from rewriting the Friedmann and Klein-Gordon equations in terms of (x, y, Ω_r, \dots) . First, the Hubble rate evolution becomes:

$$\frac{\dot{H}}{H^2} = \frac{1}{2} [3(-1 - x^2 + y^2) - \Omega_r]. \quad (54)$$

Likewise, from the scalar field equation of motion, one finds an expression for $\frac{\ddot{\phi}}{H\dot{\phi}}$:

$$\frac{\ddot{\phi}}{H\dot{\phi}} = -3 + \frac{\sqrt{\frac{3}{2}} [y^2 (2\lambda_\phi + \sigma_\phi) + \sigma_\phi (x^2 + \Omega_r - 1)]}{x}. \quad (55)$$

These relations highlight the interplay between the kinetic energy ratio x , the potential energy ratio y , and the radiation fraction Ω_r . The dependence on λ_ϕ and σ_ϕ reflects both the slope of the potential and the non-minimal coupling factor, respectively.

C. Equations of the dynamical system

Putting these ingredients together, we obtain an autonomous system of differential equations in terms of the

variables $\{x, y, \Omega_r, \lambda_\phi, \sigma_\phi\}$. Explicitly:

$$\frac{dx}{dN} = \frac{1}{2} \left[3x^3 + \sqrt{6}\sigma_\phi x^2 + \sqrt{6}(y^2 (2\lambda_\phi + \sigma_\phi) + \sigma_\phi (\Omega_r - 1)) + x(-3(1 + y^2) + \Omega_r) \right] \quad (56a)$$

$$\frac{dy}{dN} = \frac{1}{2} y \left[3(x^2 - y^2 + 1) - \sqrt{6}x\lambda_\phi + \Omega_r \right] \quad (56b)$$

$$\frac{d\Omega_r}{dN} = \Omega_r [3(x^2 - y^2) + \Omega_r - 1] \quad (56c)$$

$$\frac{d\lambda_\phi}{dN} = -\sqrt{6}(\Gamma_\phi - 1)\lambda_\phi^2 x \quad (56d)$$

$$\frac{d\sigma_\phi}{dN} = \sqrt{6}(\Delta_\phi - 1)\sigma_\phi^2 x \quad (56e)$$

Equations (56) capture the coupled evolution of the scalar field, its potential shape, and the matter/radiation contents in a unified framework [82, 83]. Note that in our case, we set $\sigma_\phi = \beta = \text{const}$, so $\frac{d\sigma_\phi}{dN} = 0$. This truncates the system to four variables: $\{x, y, \Omega_r, \lambda_\phi\}$.

D. Physical quantities

Once $\{x(N), y(N), \Omega_r(N), \lambda_\phi(N)\}$ are found, one can reconstruct standard cosmological observables:

$$\Omega_\phi \equiv x^2 + y^2, \quad (57)$$

$$\omega_\phi \equiv \frac{x^2 - y^2}{x^2 + y^2}, \quad (58)$$

$$\Omega_b \equiv 1 - x^2 - y^2 - \Omega_r, \quad (59)$$

and:

$$\omega_{eff} \equiv \omega_b \Omega_b + \omega_r \Omega_r + \omega_\phi \Omega_\phi = \frac{1}{3} \Omega_r + x^2 - y^2. \quad (60)$$

Additionally, one must respect the physical constraints:

$$0 \leq \Omega_r + x^2 + y^2 = 1 - \Omega_b \leq 1, \quad (61)$$

which ensure that the total density fraction sums to unity in a spatially flat FLRW universe.

VI. SF POTENTIALS

In this section, we detail each of the scalar field potentials that will be considered in the subsequent analysis. We supplement each potential's defining equations (already provided below in their original form) with additional theoretical remarks on their cosmological implications when combined with the non-minimal coupling (NMC) $f(\phi) = e^{\beta\phi}$. As noted in Secs. IV and III, these potentials enter the dynamical system (56) via the auxiliary parameters λ_ϕ and Γ_ϕ , as well as through the chameleon-like factor σ_ϕ if $\beta \neq 0$.

⁶ In the context of potential scenarios involving a non-singular bounce, the point at which $H = 0$ is excluded.

⁷ In the case of ekpyrotic potentials, $\text{sgn}(\mathcal{V})$ function must be taken into account in the definition of y variable.

A. Axions/ALPs

A prominent example of a periodic scalar field potential is:

$$\mathcal{V}(\phi) = \Lambda_c^4 (1 - \cos \phi). \quad (62)$$

This form arises in QCD axion physics and more generally in axion-like particles (ALPs) [22]. If the field ϕ remains near a local minimum, one effectively obtains a slow-roll or pseudo-constant vacuum energy. For large excursions in ϕ , the potential is bounded from above by Λ_c^4 . In the presence of a non-minimal coupling, one must track the interplay between the axial oscillations and matter density transfer [115].

To characterize the slope, one identifies:

$$\lambda_\phi = -\cot\left(\frac{\phi}{2}\right), \quad (63)$$

$$\Gamma_\phi(\lambda_\phi) = \frac{1}{2} \left(1 - \frac{1}{\lambda_\phi^2}\right), \quad (64)$$

and hence obtains the evolution equation:

$$\frac{d\lambda_\phi}{dN} = \sqrt{\frac{3}{2}} x (1 + \lambda_\phi^2). \quad (65)$$

In many models, ϕ settles into slow oscillations, and the NMC factor modifies the effective mass in high-density regions, thus regulating possible fifth forces.

B. Cyclic ekpyrotic SF

A well-known potential that can produce a cyclic universe scenario (i.e. repeated expansions and contractions) is given by:

$$\mathcal{V}(\phi) = \mathcal{V}_0 (e^{b\phi} - e^{-c\phi}). \quad (66)$$

If b and c are chosen such that the term $-e^{-c\phi}$ dominates in a contracting phase, one obtains an ekpyrotic-like contraction and potentially a bounce, while the part $e^{b\phi}$ can support an expanding epoch [47, 52]. The non-minimal coupling can significantly affect the bounce condition by effectively shifting the matter density [102].

We define:

$$\lambda_\phi = -\frac{be^{(b+c)\phi} + c}{e^{(b+c)\phi} - 1}, \quad (67)$$

$$\Gamma_\phi(\lambda_\phi) = \frac{bc}{\lambda_\phi^2} + \frac{c-b}{\lambda_\phi}, \quad (68)$$

and the evolution in the dynamical system becomes:

$$\frac{d\lambda_\phi}{dN} = -\sqrt{6}x (b + \lambda_\phi)(c - \lambda_\phi). \quad (69)$$

These parameters encode how the field transits between the two exponential branches, enabling repeated cycles if sufficiently fine-tuned and if $|\beta|$ is not too large.

C. Ekpyrotic/Exponential with cosmological constant

Another variant, which combines a pure exponential with a cosmological constant, takes the form:

$$\mathcal{V}(\phi) = 2\Lambda \pm \mathcal{V}_0 e^{-c\phi}. \quad (70)$$

If the sign is minus, the negative exponential can drive a contracting phase (similar to ekpyrotic or bounce scenarios), after which $2\Lambda > 0$ governs a late-time de Sitter expansion [46]. If the sign is plus, one may obtain inflationary behavior or a standard monotonic expansion.

In the dynamical-system language, we set:

$$\lambda_\phi = \frac{c\mathcal{V}_0}{\mathcal{V}_0 \pm 2\Lambda e^{c\phi}}, \quad (71)$$

$$\Gamma_\phi(\lambda_\phi) = \frac{c}{\lambda_\phi}, \quad (72)$$

and the evolution equation is:

$$\frac{d\lambda_\phi}{dN} = \sqrt{6}x \lambda_\phi (\lambda_\phi - c). \quad (73)$$

Including the NMC factor can alter the bounce threshold, change the relative timing of the exponentially limited phase, and thus shift the universe's approach to Λ -dominated expansion.

D. Quintessence

Quintessence scenarios often rely on potentials that flatten at large field values, producing a slowly evolving vacuum energy. One such candidate is:

$$\mathcal{V}(\phi) = \mathcal{V}_0 [\sinh(\lambda\phi)]^n, \quad (74)$$

which has a tracking behavior for certain $n > 0$ [117–119]. If $\beta \neq 0$, the scalar couples to baryons, altering the usual quintessence evolution and potentially shifting the onset of late-time cosmic acceleration [116].

In the autonomous system, one has:

$$\lambda_\phi = -n\lambda \coth(\lambda\phi), \quad (75)$$

$$\Gamma_\phi(\lambda_\phi) = 1 - \frac{1}{n} + n \frac{\lambda^2}{\lambda_\phi^2} \quad (76)$$

and:

$$\frac{d\lambda_\phi}{dN} = \frac{\sqrt{6}x (\lambda_\phi^2 - n^2 \lambda^2)}{n}. \quad (77)$$

Depending on parameter choices, the field can remain subdominant until recently, then evolve to $\omega_\phi \approx -1$, with the exact trajectory regulated by the β -dependent energy exchange with matter.

E. SFDM

Finally, in the context of scalar field dark matter (SFDM), the following potential is particularly relevant:

$$\mathcal{V}(\phi) = \mathcal{V}_0 [\cosh(\lambda\phi) - 1]. \quad (78)$$

For small ϕ , we have $\mathcal{V}(\phi) \approx \frac{1}{2}m^2\phi^2$, giving $\omega_\phi \approx 0$ (mimicking CDM). For large values of ϕ , $\cosh(\lambda\phi) - 1$ saturates, therefore effectively $\omega_\phi \rightarrow -1$ [18, 120].

Mathematically, one obtains:

$$\lambda_\phi = -\lambda \coth\left(\frac{\lambda\phi}{2}\right), \quad (79)$$

$$\Gamma_\phi(\lambda_\phi) = \frac{1}{2} \left(1 + \frac{\lambda^2}{\lambda_\phi^2}\right) \quad (80)$$

and:

$$\frac{d\lambda_\phi}{dN} = \sqrt{\frac{3}{2}} x (\lambda_\phi^2 - \lambda^2). \quad (81)$$

When combined with $f(\phi) = e^{\beta\phi}$, the baryonic fluid can transfer energy to (or from) the scalar, effectively altering the redshift interval during which the field behaves like DM and/or DE. This can shift structure formation on small scales, subject to screening constraints if $|\beta| \gtrsim 1$ [19, 115, 116].

Overall remarks on the potentials. Each of these potentials provides a different cosmological phase structure (bounce, cycle, matter-era tracking, late-time acceleration, etc.). Their precise dynamics in the presence of the non-minimal coupling $f(\phi)$ is systematically captured by the dimensionless system (56) in Sec. V, whose fixed points and stability are summarized in Tables I–XIV. As we shall see, the NMC ensures that large β is viable only if screening is efficient in high-density environments, while small $|\beta|$ recovers near-minimal-coupling solutions with slight modifications.

VII. DETAILED EVOLUTION SCENARIOS

We now provide a systematic account of how each model's cosmic evolution (bounce, accelerated expansion, matter-dominated era, etc.) depends on the potential parameters and on the coupling β . Many of these scenarios were partially summarized in the fixed-point analysis (Tables I–XIV). Here, we outline the main transitions and stability features as the free parameters vary.

A. Axion-like potentials

- **Case I: small decay constant (Λ_c) and moderate β .** The axion field remains near its potential

minimum for most of cosmic time, giving an effectively cosmological constant-like behavior. The early universe remains radiation-dominated; a standard matter era follows if β is not too large.

- **Case II: large Λ_c and small β .** The oscillatory behavior of ϕ after crossing the potential maximum can lead to an intermediate era similar to matter or *kination* [121], depending on $\dot{\phi}$. If β is very small, baryons remain nearly decoupled, preserving standard structure formation.

B. Cyclic ekpyrotic potentials

- **Case I: $b, c > 0$ with $|b| \neq |c|$ and $|\beta| \ll 1$.** A stable bounce can occur due to the steep negative branch $-e^{-c\phi}$. Matter domination emerges post-bounce if β is small. If $b \neq c$, the amplitude of each cycle might change slightly, but the model remains stable in a repeating sequence of expansions and contractions.
- **Case II: $|\beta| \gtrsim 1$.** Large coupling can significantly transfer energy from the baryonic sector to ϕ near the bounce, possibly altering the duration of the contracting phase or the amplitude of the next expanding cycle. If β is too large, stable cycles might be replaced by singular or chaotic behavior.

C. Ekpyrotic/exponential potential with Λ

- **Case I: $\text{sign}(\mathcal{V}_0) = +1$.** In the presence of $\Lambda > 0$, a final de Sitter epoch emerges. Depending on c , an intermediate ekpyrotic contracting phase can occur. If $c < 0$, one obtains a standard inflationary-like solution instead.
- **Case II: $\text{sign}(\mathcal{V}_0) = -1$.** A negative exponential sector can trigger bounce or recollapse, but eventually the positive Λ term can dominate, leading to re-expansion. Parameter constraints can localize the bounce scale. Large β modifies the matter era onset, potentially shifting the time at which Λ dominates.

D. Quintessence potential

- **Case I: $n > 1$ and small λ .** The field can track radiation or matter initially, depending on initial conditions. Eventually, if ϕ crosses near the potential minimum, an accelerated expansion emerges. β modifies the effective matter coupling. If β is large, the matter era can be shortened.
- **Case II: $n < 1$ or λ large.** Steep potentials lead to a kination-like regime if $\dot{\phi}^2 \gg \mathcal{V}(\phi)$ [121]. If β

remains moderate, the usual matter-radiation eras remain intact, but the onset of acceleration may be delayed.

E. SFDM potential

- **Case I: small λ and moderate β .** The scalar first behaves like dust, $\omega_\phi \approx 0$, matching the cold dark matter era. At late times, the potential curvature drives $\omega_\phi \rightarrow -1$, giving a (mildly) accelerated expansion. The transition redshift depends on both λ and β .
- **Case II: large λ .** The slope of $\mathcal{V}(\phi)$ can be significant, potentially yielding a rapid quintessence-like era or even an early kination period. If β is large, additional couplings can spoil standard matter domination, possibly conflicting with structure-formation [122].

In all cases, consistency with current data restricts $|\beta| \lesssim \mathcal{O}(1)$ and certain intervals in potential parameters. Detailed constraints are model-specific and typically require numerical scans against cosmological data sets, as partially described in [123, 124].

F. Analytical insights into cyclic evolution

Throughout, we use the following definitions of the SF energy density and pressure:

$$\rho_\phi \equiv \frac{1}{2} \left(\dot{\phi}^2 + \mathcal{V}(\phi) \right). \quad (82)$$

$$p_\phi \equiv \frac{1}{2} \left(\dot{\phi}^2 - \mathcal{V}(\phi) \right). \quad (83)$$

1. Bounce Condition

At a non-singular bounce the Hubble parameter vanishes, so that:

$$3H^2 = \rho_{tot} \equiv \rho_r + \rho_b + \rho_\phi = 0. \quad (84)$$

Using (82) for ρ_ϕ , the total energy density is:

$$\rho_{tot} = \rho_r + \rho_b + \frac{1}{2} \left(\dot{\phi}^2 + \mathcal{V}(\phi) \right). \quad (85)$$

In ekpyrotic-type models the potential $\mathcal{V}(\phi)$ may become negative so that near the bounce we require:

$$\frac{1}{2} \left(\dot{\phi}^2 + \mathcal{V}(\phi) \right) \approx - \left[\rho_r + \rho_{b0} e^{\beta\phi} a^{-3} \right]. \quad (86)$$

A regular bounce further demands that the time derivative of the Hubble parameter is positive:

$$\dot{H} = -\frac{1}{2} \left(\rho_{tot} + p_{tot} \right) > 0. \quad (87)$$

2. Local scale factor expansion near the bounce

Suppose that the bounce occurs at $t = t_b$ in the n th cycle, when the scale factor reaches its minimum $a_{\min}^{(n)}$. We expand the scale factor in a Taylor series about $t = t_b$:

$$a(t) \approx a_{\min}^{(n)} \left[1 + \frac{1}{2} \alpha (t - t_b)^2 \right], \quad (88)$$

where α is a positive constant determined by the dynamics near the bounce. Differentiating, we obtain:

$$\dot{a}(t) \approx a_{\min}^{(n)} \alpha (t - t_b). \quad (89)$$

Thus, the Hubble parameter near the bounce is:

$$H(t) = \frac{\dot{a}}{a} \approx \alpha (t - t_b), \quad (90)$$

and consequently:

$$\dot{H} \approx \alpha. \quad (91)$$

3. Iterative evolution of the minimal scale factor

To capture the change in the minimal scale factor from one cycle to the next, consider the baryon density at the bounce. At $t = t_b^{(n)}$ the baryon density is:

$$\rho_b^{(n)} = \rho_{b0} e^{\beta\phi^{(n)}} \left(a_{\min}^{(n)} \right)^{-3}, \quad (92)$$

where we define:

$$\phi^{(n)} \equiv \phi \left(t_b^{(n)} \right). \quad (93)$$

Assuming that the baryon density at the bounce remains approximately constant from cycle to cycle:

$$\rho_b^{(n+1)} \approx \rho_b^{(n)}, \quad (94)$$

we take the logarithm of (92):

$$\ln \rho_b^{(n)} = \ln \rho_{b0} + \beta \phi^{(n)} - 3 \ln a_{\min}^{(n)}. \quad (95)$$

Similarly, at the $(n+1)$ th bounce:

$$\ln \rho_b^{(n+1)} = \ln \rho_{b0} + \beta \phi^{(n+1)} - 3 \ln a_{\min}^{(n+1)}. \quad (96)$$

Subtracting (95) from (96) and using (94), we obtain:

$$\beta \left(\phi^{(n+1)} - \phi^{(n)} \right) - 3 \left(\ln a_{\min}^{(n+1)} - \ln a_{\min}^{(n)} \right) \approx 0. \quad (97)$$

Defining:

$$\Delta\phi = \phi^{(n+1)} - \phi^{(n)} \quad (98)$$

and:

$$\Delta \ln a_{\min} = \ln \frac{a_{\min}^{(n+1)}}{a_{\min}^{(n)}}, \quad (99)$$

(97) becomes:

$$\beta\Delta\phi - 3\Delta\ln a_{\min} \approx 0. \quad (100)$$

Solving for $\Delta\ln a_{\min}$ we obtain:

$$\ln \frac{a_{\min}^{(n+1)}}{a_{\min}^{(n)}} \approx \frac{\beta}{3}\Delta\phi. \quad (101)$$

For convenience, we introduce a positive constant γ (with $\gamma = 1/3$ in this simple derivation) and, if necessary, a minus sign to reflect the precise effect of the scalar evolution on the bounce amplitude. In general, we may write:

$$\ln \frac{a_{\min}^{(n+1)}}{a_{\min}^{(n)}} \approx -\gamma\beta\Delta\phi, \quad (102)$$

where the sign of $\Delta\phi$ (i.e., whether ϕ increases or decreases from bounce to bounce) determines if the cycle amplitude is damped or amplified.

4. Thermodynamic considerations

In addition to the geometric evolution described above, thermodynamic considerations (more details in Sec. XIII) impose further constraints on cyclic evolution from the perspective of the second law of thermodynamics. In standard cosmology the first law is written as:

$$d(\rho V) + pdV = TdS, \quad (103)$$

where $V = a^3$ is the spatial volume, ρ and p denote the energy density and pressure of the cosmic fluid, T is the temperature, and S is the entropy. When a non-minimal (exponential) coupling is present, the baryonic sector is modified (cf. (11)), and the Gibbs relation generalizes to (see, e.g., [125]):

$$TdS = d(\rho V) + pdV - \mu d(f(\phi)N_b), \quad (104)$$

where N_b is the baryon number and μ is the associated chemical potential. Differentiating with respect to time, one obtains the entropy production rate:

$$\frac{dS}{dt} = \frac{1}{T} \left[V\dot{\rho} + (\rho + p)\dot{V} - \mu \frac{d}{dt}(f(\phi)N_b) \right]. \quad (105)$$

During each cycle the minimal scale factor a_{\min} changes according to (102), which in turn affects the cosmic volume $V = a^3$. This variation leads to a change in the energy content of the baryonic fluid. For example, assuming that the dominant contribution to the entropy comes from the baryonic fluid (for which $p_b \approx 0$), we have:

$$\frac{d}{dt}(\rho_b V) = \frac{d}{dt}(\rho_{b0} e^{\beta\phi}) = \rho_{b0} \beta \dot{\phi} e^{\beta\phi}. \quad (106)$$

Integrating (105) over one cycle yields a net change in entropy, ΔS . In order for the generalized second law of

thermodynamics to hold, the total entropy (including the horizon entropy in an expanding universe) must satisfy:

$$\Delta S \geq 0. \quad (107)$$

Since the iterative relation (102) implies a change in the volume and, consequently, the energy and entropy content of the baryonic sector, the condition:

$$|\gamma\beta\Delta\phi| \ll 1 \quad (108)$$

not only ensures nearly cyclic evolution in the geometric sense but also guarantees that the entropy production per cycle is sufficiently small and positive, in agreement with the generalized second law (see, e.g., [73, 76, 77, 126]).

VIII. FIFTH FORCE AND SCREENING TESTS

A. Einstein frame set-up

All baryons couple to the scalar through the conformal factor (2)⁸. The Klein–Gordon equation becomes:

$$\ddot{\phi} + 3H\dot{\phi} + V'(\phi) = -\beta\rho e^{\beta\phi}, \quad (109)$$

so dynamics in a medium of density ρ are governed by the **effective potential**:

$$V_{eff}(\phi, \rho) = \mathcal{V}(\phi) + \rho e^{\beta\phi}. \quad (110)$$

If a minimum exists:

$$V'_{eff}(\phi_{\min}) = 0, \quad (111)$$

small oscillations have the **density-dependent mass** of the form:

$$m_{eff}^2(\rho) = V''(\phi_{\min}) + \beta^2 \rho e^{\beta\phi_{\min}}. \quad (112)$$

The resulting fifth-force potential is the following:

$$V_5(r) = -\frac{GM_1 M_2}{r} \left[1 + 2\beta^2 e^{-m_{eff}r} \right], \quad (113)$$

so $m_{eff}r \gg 1$ realizes *chameleon screening*. In the unscreened limit ($m_{eff} \rightarrow 0$) comparison with Brans–Dicke theory gives:

$$\beta^2 = \frac{1}{2\omega_{BD} + 3}, \quad (114)$$

a useful conversion when quoting PPN bounds.

⁸ Throughout this section ρ denotes the *local rest-mass density* in the Einstein frame; it should *not* be confused with the background quantity $\rho_b(a, \phi) = e^{\beta\phi} \rho_{b0} a^{-3}$. When quoting laboratory limits, we take the representative density $\rho_{lab} \simeq 10^3 \text{ kg m}^{-3}$.

B. Screening analysis for the SF potentials

1. Axions/ALPs

Near $\phi = 0$:

$$\phi_{\min} \simeq -\frac{\beta\rho}{\Lambda_c^4}, \quad (115)$$

therefore:

$$m_{\text{eff}}^2 \simeq \Lambda_c^4 + \beta^2\rho \quad (116)$$

and consequently:

$$m_{\text{eff}} \propto \rho^{1/2} \quad (117)$$

So the chameleon screening operates [115, 127]. Cassini time-delay data give the constraints in the range of [128]:

$$|\beta| \lesssim 10^{-3}. \quad (118)$$

2. Cyclic ekpyrotic

Because $V'(\phi)$ never balances the $-\beta\rho e^{\beta\phi}$ term, no ϕ_{\min} exists and $m_{\text{eff}} \approx 0$. The bound [99, 128]:

$$\gamma_{\text{PPN}} - 1 < 2.3 \times 10^{-5} \quad (119)$$

translates via (114) into:

$$|\beta| \lesssim 2.5 \times 10^{-3}. \quad (120)$$

3. Exponential/Ekpyrotic with Λ

Solving $V'_{\text{eff}} = 0$ gives:

$$\phi_{\min} = \frac{\ln\left(\frac{\beta}{cV_0}\rho\right)}{c + \beta}, \quad (121)$$

which implies:

$$m_{\text{eff}}^2 = \beta(c + \beta)\rho e^{\beta\phi_{\min}} \quad (122)$$

requiring $\rho \gg cV_0/\beta$ for screening. For $V_0^{1/4} \gtrsim 10^{-3}$ eV this fails in the lab, so the limit (120) applies.

4. Quintessence

For $|\lambda\phi|, |\beta\phi| \ll 1$ and $n > 1$:

$$\phi_{\min} \simeq -\left(\frac{\beta}{nV_0\lambda^n\rho}\right)^{1/(n-1)} \quad (123)$$

and:

$$m_{\text{eff}}^2 \simeq n(n-1)V_0\lambda^n\phi_{\min}^{n-2} + \beta^2\rho, \quad (124)$$

giving:

$$m_{\text{eff}} \propto \rho^{n/(2n-2)} > \rho^{1/2}. \quad (125)$$

The stronger screening relaxes torsion-balance limits to [100]:

$$|\beta| \lesssim 10^{-2} \quad \wedge \quad n \geq 2. \quad (126)$$

5. SFDM

In such a model one could define:

$$m^2 \equiv V_0\lambda^2. \quad (127)$$

Linearizing for $|\beta\phi| \ll 1$ gives the minimum and the effective mass of the form:

$$\phi_{\min} \simeq -\frac{\beta}{m^2}\rho \quad (128)$$

$$m_{\text{eff}}^2 \simeq m^2 \left(1 + \frac{\beta^2}{m^2}\rho\right). \quad (129)$$

For ultra-light DM ($m \sim 10^{-22}$ eV) and $\rho_{\text{lab}}, m_{\text{eff}}^{-1} \gtrsim 10^6$ km, so the force is unscreened. Eöt-Wash data imply [98]:

$$|\beta| \lesssim 10^{-4} - 10^{-2}. \quad (130)$$

C. Synthesis of constraints

The preceding analysis signifies that the parameter β is constrained in the following manner:

$$|\beta|_{\text{PPN}} \lesssim 2 \times 10^{-3} \quad (131a)$$

$$|\beta|_{\text{lab}} \lesssim 10^{-4} - 10^{-2} \quad (131b)$$

$$|\beta|_{\text{CMB/LSS}} \lesssim 5 \times 10^{-2}. \quad (131c)$$

Chameleon-compatible potentials (axions/ALPs and quintessence) satisfy local bounds even for $|\beta| \sim 10^{-2}$, whereas *unscreened* models (cyclic-ekpyrotic, exponential/ekpyrotic with Λ and ultra light SFDM) must obey the tighter limits (120) and (130). Therefore, these fifth force diagnostics provide an independent viability filter that complements the dynamical analysis of the subsequent sections.

IX. PGWS WITH NON-BUNCH-DAVIES VACUUM WITHIN NMC MODELS

A. Tensor mode equation

With conformal time τ the perturbed line element is:

$$ds^2 = a^2(\tau)[-d\tau^2 + (\delta_{ij} + h_{ij})dx^i dx^j]. \quad (132)$$

Because $f(\phi)$ multiplies only the matter Lagrangian, the transverse-traceless modes satisfy:

$$h_k'' + 2\mathcal{H} h_k' + k^2 h_k = 0. \quad (133)$$

Introducing $u_k \equiv a h_k$ gives the *Mukhanov-Sasaki* form:

$$u_k'' + \left(k^2 - \frac{a''}{a}\right) u_k = 0. \quad (134)$$

B. Power-law backgrounds and Hankel solutions

For a single power-law epoch one could assume that:

$$a(\tau) = a_0 |\tau|^p \quad \wedge \quad p = \frac{2}{1 + 3\omega_{\text{eff}}}, \quad (135)$$

with:

$$p = \frac{2}{1 + 3\omega_{\text{eff}}} \quad (136)$$

and:

$$\frac{a''}{a} = \frac{p(p-1)}{\tau^2} \quad (137)$$

with:

$$\nu^2 = \frac{1}{4} + p(p-1). \quad (138)$$

Then the exact solution is given by:

$$u_k(\tau) = \sqrt{-\tau} \left[\alpha_k H_\nu^{(1)}(-k\tau) + \beta_k H_\nu^{(2)}(-k\tau) \right] \quad (139)$$

with the Bogoliubov normalization:

$$|\alpha_k|^2 - |\beta_k|^2 = 1. \quad (140)$$

Bunch-Davies (BD) initial data correspond to $\alpha_k = 1$ and $\beta_k = 0$.

C. Bounce matching and transfer matrix

For the analytic \mathcal{C}^1 bounce:

$$a(\tau) = a_B \left[1 + \left(\frac{\tau}{\tau_B} \right)^2 \right]^{p/2} \quad \wedge \quad p > 0, \quad (141)$$

the asymptotic Hankel modes are connected through the *transfer matrix* \mathcal{M}_k :

$$\mathcal{M}_k \equiv \begin{pmatrix} \mathcal{A}_k & \mathcal{B}_k \\ \mathcal{B}_k^* & \mathcal{A}_k^* \end{pmatrix} \quad (142)$$

by the relation:

$$\begin{pmatrix} \alpha_k^{(+)} \\ \beta_k^{(+)} \end{pmatrix} = \mathcal{M}_k \begin{pmatrix} \alpha_k^{(-)} \\ \beta_k^{(-)} \end{pmatrix}, \quad (143)$$

with $\vartheta_k \equiv k\tau_B$ and:

$$\mathcal{A}_k = e^{i\vartheta_k} \left[1 + \frac{i}{2} \vartheta_k^{2p+1} \Gamma(-2p-1) \right], \quad (144a)$$

$$\mathcal{B}_k = i e^{i\vartheta_k} \vartheta_k^{2p+1} \Gamma(-2p-1) + \mathcal{O}(\vartheta_k^{4p+2}), \quad (144b)$$

which fulfills:

$$|\mathcal{A}_k|^2 - |\mathcal{B}_k|^2 = 1 \quad (145)$$

up to $\mathcal{O}(\vartheta_k^{4p+2})$.

For a *slow-roll inflation* ($p \simeq -1$) the same equations (143)–(144) follow by analytic continuation in p through the poles of $\Gamma(-2p-1)$, reproducing the familiar oscillatory corrections to a nearly scale-invariant background.

D. Tensor power spectrum

On super-horizon scales ($|k\tau| \ll 1$) the dimensionless spectrum $P_T \equiv (2k^3/\pi^2)|h_k|^2$ is:

$$P_T(k) = \frac{2^{2\nu} \Gamma^2(\nu)}{\pi^3} |\alpha_k - \beta_k|^2 \left(\frac{k}{aH} \right)^{3-2\nu}, \quad (146)$$

and BD initial data before the bounce give

$$\begin{aligned} P_T(k) &= P_T^{(\text{BD})}(k) \left[1 + 2|\mathcal{B}_k|^2 - 2\Re(\mathcal{A}_k \mathcal{B}_k^*) \right] \\ &\simeq P_T^{(\text{BD})}(k) \left[1 + \Gamma^2(-2p-1) (k\tau_B)^{4p+2} + \dots \right], \end{aligned} \quad (147)$$

valid for $k\tau_B \lesssim 1$.

E. Spectral regimes and observational signatures

1. Tilt and amplitude

An ekpyrotic contraction ($\omega \gg 1$, $p \ll 1$) yields the standard blue tilt $n_T \simeq 2$ plus the smooth step of Eq. (147). In slow-roll inflation ($p \simeq -1$) the analytic continuation of $\Gamma(-2p-1)$ produces a sub-percent oscillatory modulation on top of $n_T \simeq 0$.

2. Dependence on the NMC coupling

While Eq. (133) itself is β -independent, both p and τ_B inherit a β dependence from the modified Friedmann equations, schematically $H_B \propto \beta^2$ (Sec. IX G).

3. Minimal coupling comparison

Minimal ekpyrotic models share $n_T = 2$ but lack the intrinsic break (147); by contrast $\mathcal{B}_k \propto k^{2p+1}$ in the present NMC scenario causes an oscillation amplitude that *grows* towards high k .

F. Extensions and open directions

1. Parity violation

A Chern–Simons term $\theta(\phi)R\tilde{R}$ [129] makes \mathcal{M}_k helicity-dependent, producing net circular polarization [130, 131].

2. Resonant amplification

If the equation of state temporarily satisfies $\omega < -\frac{1}{3}$ inside the bounce, $\nu \rightarrow \nu + i\xi$ and the step is promoted to a narrow resonance [132].

3. Loop-quantum corrections

Replacing $k^2 \rightarrow k^2(1 + \ell_B^2 k^2)$ suppress \mathcal{B}_k as $e^{-\ell_B^2 k^2}$ [133].

4. Non-Gaussianity

The same α_k, β_k control the tensor bispectrum; with $\mathcal{B}_k \neq 0$ the squeezed limit is enhanced by $\propto |\mathcal{B}_k|$ [109].

G. Numerical estimations

1. Back-reaction bounds on excited states

The excited energy density:

$$\rho_{\text{exc}} = \int d \ln k \frac{|\mathcal{B}_k|^2 k^4}{2\pi^2 a^4} \quad (148)$$

must obey $\rho_{\text{exc}} < \rho_{\text{tot}}$ [134, 135].

A conservative estimate:

$$|\mathcal{B}_k|^2 \lesssim \left(\frac{H_B}{M_{\text{Pl}}} \right)^2 \quad (149)$$

forces:

$$\tau_B \gtrsim 10^3 H_B^{-1} \quad (150)$$

for $p \simeq 0.05$, comfortably satisfied by the numerical examples used below.

2. Mapping the NMC to the bounce scale

Solving the joint Jordan–Einstein system to linear order in β yields:

$$H_B \simeq \frac{\beta^2}{6} M_{\text{Pl}} \quad (151)$$

and therefore:

$$\tau_B^{-1} \simeq p H_B, \quad (152)$$

providing the scaling adopted in Sec. IX E [136, 137].

3. Explicit amplitude forecasts

Combining equations (146)–(147) with the LISA [138, 139] power-law sensitivity [140] shows that for $p = 0.05$ and $\beta = 0.8$:

$$\Omega_{\text{GW}} h^2 \approx 4 \times 10^{-13} \quad (153)$$

at $f \simeq 0.7$ Hz, two orders of magnitude above the mission baseline and therefore *testable* in early LISA data.

4. Anisotropy growth through the bounce

Because the shear term scales as a^{-6} , it can dominate unless the ekpyrotic fluid red-shifts faster. For the exponential NMC potential one has $\rho_\phi \propto a^{-3(1+\omega)}$; requiring $\omega > 1$, automatically satisfied for all β relevant here, maintains anisotropies subdominant [141, 142].

5. Beyond leading-order matching

The closed-form \mathcal{M}_k of (143) ignores the k -dependence of the effective sound speed that arises once metric loops are included [143]. Extending the matching to $\mathcal{O}(k^4)$ would sharpen the shape of the break and is left for future work.

H. Outlook

We have derived a closed-form transfer matrix \mathcal{M}_k valid for all $p > 0$ and presented a compact master formula (146) for the primordial tensor spectrum with arbitrary Bogoliubov coefficients. The combination produces a blue, scale-dependent break whose location and amplitude are fixed by the two background parameters (p, τ_B) , themselves set by the NMC parameter β . Current PTA data already constrain $|\beta| \lesssim 1$ for break frequencies $10^{-18} - 10^{-16}$ Hz, while LISA/DECIGO can reach $|\beta| \lesssim 0.3$ in the $10^{-2} - 1$ Hz range. Remaining open issues, explicit back-reaction bounds, anisotropy control, and higher-order matching, are identified in Sec. IX G and provide clear targets for future theoretical work and upcoming GWs observations.

X. DETAILED PHASE SPACE EVOLUTIONS

In this section, we synthesize the information from the fixed-point tables (Tables I–XIV) and discuss in more detail how the universe can evolve through different cosmic

epochs within each of the non-minimally coupled (NMC) scalar field models studied. The tables list various critical (fixed) points that arise in the dynamical system description (Sec. V), along with their stability properties. In cosmological terms, these equilibrium solutions correspond to distinct evolutionary phases or asymptotic states (e.g. radiation era, matter era, stiff matter domination, dark energy domination, cyclic bounce points, etc.). Below, we highlight how typical trajectories in phase space may pass from one fixed point to another, illuminating the possible scenarios for the universe's history.

A. ALP/axion-like models (Tables I-II)

1. Overview of fixed points

The ALPs model features a potential $\mathcal{V}(\phi) = \Lambda_c^4(1 - \cos\phi)$, together with an exponential non-minimal coupling $f(\phi) = e^{\beta\phi}$. Tables I-II identify several critical points. Notable points include:

- \mathcal{A} : a *radiation-dominated* solution with $\Omega_r = 1$ and $\Omega_\phi = 0$, typically appearing as a saddle.
- \mathcal{B} , \mathcal{D} : *stiff matter-like* solutions, where $x^2 = 1$ (i.e. kinetic energy dominates). These can be unstable or saddle-like depending on the exact eigenvalues and whether β exceeds certain thresholds.
- \mathcal{C} : a *dark energy* solution ($\Omega_\phi = 1$, $\omega_\phi = -1$), which can be stable (an attractor) and thus describe late-time cosmic acceleration (Fig. 1).
- \mathcal{F} : a β -dependent *matter-like* solution where $\Omega_\phi \approx 2\beta^2/3$ and $\omega_{eff} = 2\beta^2/3$. This can appear as a saddle or be transient if $\beta \neq 0$.

2. Possible cosmic evolution

A typical cosmological trajectory for small or moderate $|\beta|$ might proceed as follows:

- At very early times, the universe is effectively at (or near) the radiation point \mathcal{A} . Because \mathcal{A} is a saddle, trajectories eventually leave radiation domination.
- As the expansion cools the universe, the effective mass of the scalar field changes. The system can transit through a kinetic-dominated (stiff matter) epoch (\mathcal{B} or \mathcal{D}) but only briefly (again, typically a saddle or unstable node).
- The field then either moves into a matter-like era (\mathcal{F}) if β -effects are significant enough, *or* it bypasses that if β is small, ending up near the dark energy attractor \mathcal{C} . The point \mathcal{C} is stable and describes the late-time cosmic acceleration with $\omega_\phi \approx -1$.

In this way, the final stage of cosmic evolution is typically the stable \mathcal{C} (or \mathcal{E} in certain parameter ranges), giving an accelerated expansion that mimics a cosmological constant-like epoch. If $|\beta|$ is very large, additional subtleties arise, most notably, fifth force constraints or a significant departure from the standard matter era.

B. Cyclic ekpyrotic models (Tables III-V)

1. Overview of fixed points

For the potential $\mathcal{V}(\phi) = \mathcal{V}_0(e^{b\phi} - e^{-c\phi})$, repeated bounces can be obtained if the scalar passes between the $-e^{-c\phi}$ -dominated regime (contracting/bounce phase) and the $e^{b\phi}$ -dominated regime (expanding phase). Among the critical points identified:

- $\mathcal{A}, \mathcal{B}, \mathcal{C}$: *radiation-dominated* fixed points (all with $\Omega_r = 1$ and $\Omega_\phi = 0$), usually saddles, differing by the way b , c , and β factor into λ_ϕ .
- \mathcal{D} : a *dark energy*-type solution with $\Omega_\phi = 1$, $\omega_\phi = -1$, stable or saddle according to the combinations of parameters (b, c, β) .
- \mathcal{E}, \mathcal{F} : *stiff matter* solutions with $x = \pm 1$, usually appearing as unstable or saddle epochs.
- $\mathcal{G}, \mathcal{H}, \mathcal{I}, \mathcal{J}$: these are more involved solutions in which β explicitly appears; they can be matter-like or partially radiation-like solutions, some of which can be stable for certain parameter windows, while others remain saddle points. Some are also crucial for describing how the universe transitions near bounce phases or between expansions and contractions.

2. Possible cosmic evolution

Because the *cyclic* scenario attempts to have repeated expansions and contractions, the universe might exhibit the following cycle:

- Start in an expanding phase, possibly near one of the radiation-dominated fixed points, e.g. \mathcal{A} .
- Move through a stiff or matter-like phase as $e^{b\phi}$ dominates. Depending on β , baryon density might be partially “screened” or “enhanced,” which changes how the scale factor evolves toward a maximum or recollapse.
- The field transitions to a contracting stage governed by $-e^{-c\phi}$; near the bounce, certain nontrivial fixed points (like \mathcal{D} in some expansions) might appear in the extended phase space.

- (iv) After the bounce, the universe re-enters an expanding cycle. If $|\beta|$ is small, subsequent cycles can look nearly identical, repeating the loop. If $|\beta|$ is sizable, the amplitude of each cycle (a_{\min}) can shift, eventually leading to a single bounce (rather than an infinite cycle) or a different stable attractor.

In short, the presence of β can make certain bounce-adjacent fixed points stable or unstable, altering the cycle. For many parameter choices, repeated cycles remain possible. However, if β is large, the universe might fail to repeat after a finite number of bounces, eventually landing in a stable expanding phase dominated by either stiff ϕ -kinetic energy or by a dark energy-like attractor.

C. Ekpyrotic/exponential SF with Λ (Tables VI-VIII)

1. Overview of fixed points

This potential:

$$\mathcal{V}(\phi) = 2\Lambda \pm \mathcal{V}_0 e^{-c\phi}, \quad (154)$$

allows for (i) a negative-exponential, ekpyrotic-like regime if the sign is $-$, or (ii) an inflationary-like regime if $+$ is chosen and Λ dominates. Key fixed points include:

- $\mathcal{A}, \mathcal{B}, \mathcal{C}$: again, radiation-like solutions (with $\Omega_r = 1$) that appear as saddles.
- \mathcal{D} : a *dark energy* (de Sitter) solution with $y = 1, x = 0, \omega_{eff} = -1$. Its stability depends on whether β and c preserve or spoil the negativity of certain eigenvalues.
- \mathcal{E}, \mathcal{F} : *stiff matter* points with $x^2 = 1$. They are typically either unstable or saddles.
- $\mathcal{G}, \mathcal{H}, \mathcal{I}, \mathcal{J}$: additional solutions with partial radiation or matter features, some β -dependent. They can be important in describing transitions near the bounce or the exit from it.

2. Possible cosmic evolution

A typical path in the N -time (e-fold) phase space could look like:

- (i) The universe first sits near a radiation saddle (\mathcal{A} or \mathcal{B}) at very early times.
- (ii) If the negative exponential piece is relevant, an ekpyrotic contraction can occur, passing near a stiff solution (\mathcal{E} or \mathcal{F}) or a bounce-like point. Then the positive Λ eventually takes over.

- (iii) The final stage is the stable de Sitter-type solution (\mathcal{D}), with $\omega_\phi \rightarrow -1$. If the sign is $+$ and $\Lambda > 0$, the system can pass directly to inflation-like expansions. In contrast, if β is sufficiently large, the baryon coupling modifies the scale factor's approach to Λ -domination, possibly delaying or hastening the transition.

Hence one often sees a bounce (if $-$ sign and $|\beta|$ do not impede it), followed by long-term acceleration at \mathcal{D} . If the potential shape or β is chosen differently, the system may remain stuck in a matter- or stiff matter-like solution.

D. Quintessence-type models (Tables IX-XI)

1. Overview of fixed points

For a generic quintessence potential, e.g. $\sinh^n(\lambda\phi)$, we observe standard categories of fixed points:

- \mathcal{A}, \mathcal{B} : *radiation* points with $\Omega_r \approx 1, \Omega_\phi \approx 0$, or small variations thereof, typically saddles.
- \mathcal{C} : a *dark energy* attractor with $\omega_\phi = -1$ and $\Omega_\phi = 1$. Usually stable if n and λ lie in suitable ranges (see, Fig. 2).
- \mathcal{D} : a *stiff* solution ($x^2 = 1$), relevant for early or transitional epochs, typically not stable.
- \mathcal{E}, \mathcal{F} : solutions with partial matter-like or radiation-like behavior. For example, \mathcal{E} can have $\Omega_r \neq 0$ if β is nonzero.

2. Possible cosmic evolution

A representative expansion history might be:

- (i) Start near radiation (\mathcal{A} or \mathcal{B}) if the universe is initially hot.
- (ii) Move into a matter-like regime (possibly \mathcal{F}), or pass briefly through a kinetic era (\mathcal{D}).
- (iii) Eventually, for large cosmic times, the path approaches the dark energy attractor \mathcal{C} . In standard (uncoupled) quintessence, this is well known to produce late-time cosmic acceleration. The non-minimal coupling modifies the growth of ϕ so that the universe can shift the exact redshift of DE onset. If $\beta > 0$ is moderate, the scalar can “steal” energy from baryons, thereby producing earlier acceleration. If $\beta < 0$, the field's vacuum energy might remain subdominant longer, delaying acceleration.

Numerical solutions confirm these typical transitions unless $|\beta|$ is large enough to drastically alter the matter era or violate local constraints [99].

E. SFDM models (Tables XII-XIV)

1. Overview of fixed points

In the SFDM scenario, $\mathcal{V}(\phi) = \mathcal{V}_0 [\cosh(\lambda\phi) - 1]$, and for small ϕ , the field behaves like a massive scalar, $\omega_\phi \approx 0$. The tables show points:

- \mathcal{A}, \mathcal{B} : radiation-dominated solutions, saddles.
- \mathcal{C} : a *dark energy* point with $\omega_\phi = -1$ and $\Omega_\phi = 1$, stable in certain domains of (λ, β) .
- \mathcal{D} : a stiff/kinetic solution again with $x^2 = 1$.
- \mathcal{E}, \mathcal{F} : possible matter-like or β -dependent solutions. For instance, if β is small and ϕ remains near zero for a while, the universe can mimic cold dark matter before it transitions to $\omega_\phi \rightarrow -1$ at late times.

2. Possible cosmic evolution

A typical SFDM universe could unfold thus:

- (i) Initially dominated by radiation, near \mathcal{A} or \mathcal{B} .
- (ii) As temperature drops, the scalar's mass term $m^2\phi^2/2$ drives oscillations around $\phi = 0$, effectively giving $\rho_\phi \propto a^{-3}$, so the universe *behaves* like CDM. In the tables, this stage often corresponds to a path crossing near \mathcal{F} or a matter-like line, but not necessarily a stable fixed point unless β specifically makes it so.
- (iii) Finally, for large ϕ , $\cosh(\lambda\phi) - 1$ saturates, driving $\omega_\phi \rightarrow -1$. The universe thus enters the dark energy-like solution \mathcal{C} , which can be stable.

The non-minimal coupling modifies how quickly this transition from $\omega_\phi \approx 0$ to $\omega_\phi \approx -1$ happens, possibly shifting structure-formation epochs or the late-time acceleration scale. For $|\beta| \gtrsim 1$, the field exchanges energy with baryons strongly; local screening constraints must then be satisfied.

F. General lessons and phase space flow

From the above discussions tied to the tables:

- (1) *Radiation points* ($\Omega_r \approx 1$) almost always serve as saddles that approximate the early universe.
- (2) *stiff matter or kinetic-dominated points* show up frequently, can be transient or unstable, but are relevant near bounces or in very early expansions.
- (3) *dark energy points* (with $\omega_\phi \approx -1$) often act as stable attractors, governing the late-time fate of the universe in many scenarios, unless a truly cyclic solution forbids the final acceleration.

- (4) *Matter-like solutions* appear when $\beta \neq 0$ because the exponential coupling redefines the effective density in baryons or the scalar. Typically, these are saddles or short-lived intermediate stages, but they can be relevant for observational signatures (e.g. alleviating the H_0 or σ_8 tensions, if the coupling is tuned).

In bouncing or cyclic contexts (ekpyrotic models), multiple fixed points can appear that characterize expansions, bounces, and recollapses. The viability of repeated cycles depends on whether these points remain stable or get destabilized by β -driven matter-scalar energy transfer. In quintessence- or SFDM-type models, standard radiation and matter epochs are recovered for small $|\beta|$, while moderate or large $|\beta|$ can significantly alter the duration and timing of these eras.

Overall, the detailed phase-space flows, encoded in the eigenvalues, existence conditions, and stabilities summarized in the tables, demonstrate the wide spectrum of possible cosmic evolutions. They range from single-bounce universes to genuinely cyclic expansions, or from standard matter-to-dark energy trajectories to scenarios with substantial modifications of the effective matter era. In each case, the interplay between the scalar potential shape (ekpyrotic, ALP-like, quintessence, SFDM) and the non-minimal coupling β is what determines the specific path across the fixed points.

XI. COSMOLOGICAL TENSIONS AND THE ROLE OF NMC SF

Recent measurements in cosmology, such as the so-called H_0 tension between *Planck* data and local supernovae distance-ladder measurements, or the σ_8 tension between CMB-inferred clustering amplitude and weak-lensing surveys, suggest that new physics beyond the simplest Λ -CDM may be at play [35, 36].

A non-minimal coupling $f(\phi) = e^{\beta\phi}$ can modify the expansion rate during late times in a way that might reconcile high values of H_0 with CMB data [36, 144]. For instance, if ϕ exchanges energy with baryons, the background expansion can speed up near $z \sim 0$.

However, the same effect can degrade fits to the BAO or weak lensing unless β is carefully chosen. Some chameleon-based models or scalar-tensor theories with suitably tuned potentials can indeed *alleviate* the H_0 tension by a small margin, although fully resolving it might require more complicated interactions.

Weak-lensing surveys (e.g. KiDS, DES, HSC) prefer lower σ_8 or lower S_8 relative to *Planck* Λ -CDM fits [145]. A chameleon-like mediated fifth force can enhance structure growth at certain scales, but also produce environment-dependent suppression if screening is significant.

A. Addressing the Hubble and S_8 tensions

In non-minimally coupled cosmological models the Friedmann equation takes the form:

$$3H^2(z) = \rho_r(z) + \rho_b(z) + \rho_\phi(z), \quad (155)$$

with the baryon density modified by the coupling function $f(\phi) = \exp(\beta\phi)$ as:

$$\rho_b(z) = \rho_{b0} e^{\beta\phi(z)} (1+z)^3. \quad (156)$$

A simple ansatz for the evolution of the scalar field is to assume:

$$\phi(z) = \phi_0 + \alpha \ln(1+z), \quad (157)$$

so that:

$$e^{\beta\phi(z)} = e^{\beta\phi_0} (1+z)^{\alpha\beta}. \quad (158)$$

Thus, the effective baryon density becomes:

$$\rho_b(z) = \rho_{b0} e^{\beta\phi_0} (1+z)^{3+\alpha\beta}. \quad (159)$$

In the minimal-coupling case one has the standard scaling $\rho_b^{MC}(z) = \rho_{b0} (1+z)^3$; here the effective exponent is:

$$n_{\text{eff}} \equiv 3 + \alpha\beta. \quad (160)$$

If the product $\alpha\beta$ is negative (i.e. if the field decreases as the universe expands), then matter will dilute faster than in Λ -CDM.

1. Implications for the Hubble Tension:

The Hubble constant inferred from the CMB depends on the expansion history. A faster dilution of matter reduces the effective Ω_m at low and intermediate redshifts. For example, assume that in the NMC model we have:

$$\alpha\beta = -0.1. \quad (161)$$

Then at $z = 1$ one obtains:

$$\frac{(1+z)^{n_{\text{eff}}}}{(1+z)^3} = 2^{-1/10} \approx 0.93, \quad (162)$$

i.e. a reduction of about 7% in the baryon density relative to the minimal coupling case. When fitting the CMB angular-diameter distance, a lower effective matter density can be compensated by a higher Hubble constant. Detailed numerical studies (see, e.g., [36]) indicate that a few percent reduction in Ω_m can shift H_0 upward by 5–10%, potentially reconciling the CMB-inferred value (e.g. $\sim 67 \text{ km s}^{-1} \text{ Mpc}^{-1}$) with local measurements (e.g. $\sim 73 \text{ km s}^{-1} \text{ Mpc}^{-1}$).

2. Implications for the S_8 tension

The parameter:

$$S_8 \equiv \sigma_8 \sqrt{\frac{\Omega_m}{0.3}}, \quad (163)$$

measures the amplitude of matter fluctuations relative to the matter density. In the NMC scenario the effective matter density is given by:

$$\Omega_m^{\text{eff}} = \Omega_{b0} e^{\beta\phi_0} + \Omega_{c0} e^{\beta\phi_0}. \quad (164)$$

For instance, if we choose $\beta\phi_0 = -0.05$ so that $e^{\beta\phi_0} \approx 0.95$, the effective matter density is reduced by about 5% relative to the minimal case. Moreover, the altered expansion history tends to suppress the growth of perturbations, thereby lowering σ_8 . If in the minimal model one obtains $\sigma_8^{MC} \simeq 0.83$, a 10% reduction may yield $\sigma_8^{NMC} \simeq 0.75$. Consequently, one finds:

$$S_8^{NMC} = 0.75 \sqrt{\frac{0.285}{0.3}} \simeq 0.75 \times 0.975 \approx 0.73, \quad (165)$$

which is in better agreement with weak-lensing surveys (which typically favor $S_8 \sim 0.75\text{--}0.78$).

While a full resolution of the H_0 and S_8 tensions requires a numerical integration of the full set of modified background and perturbation equations, these analytical estimates illustrate that an exponential NMC can provide the necessary modifications to the expansion history and growth of structure. Future work will involve detailed parameter scans and confrontation with current data.

XII. NEW ASPECTS OF NMC IN ULDM MODELS

A. Introduction

Ultra-light dark matter (ULDM) models—including fuzzy dark matter (FDM), self-interacting fuzzy dark matter (SIFDM), and superfluid dark matter—describe a dark matter component composed of bosons with masses in the range $10^{-24} \text{ eV} \lesssim m \lesssim 1 \text{ eV}$ (see, e.g., [19, 20, 22]). On galactic scales, ULDM can form a Bose–Einstein condensate (BEC) or superfluid state, leading to wave-like behavior that may address some small-scale challenges of the cold dark matter paradigm.

In the models discussed in this article, the scalar field ϕ is NMC via an exponential function (2), so that the matter Lagrangian depends on the rescaled metric $\tilde{g}_{\mu\nu} = f^2(\phi) g_{\mu\nu}$. Consequently, the effective matter density becomes:

$$\rho_m(a, \phi) = \rho_{m0} a^{-3} e^{\beta\phi}, \quad (166)$$

and the scalar field equation picks up a source term:

$$\ddot{\phi} + 3H\dot{\phi} + \mathcal{V}'(\phi) = -\beta e^{\beta\phi} \rho_m. \quad (167)$$

This chapter derives several analytical relations that demonstrate how the non-minimal coupling modifies key physical quantities in ULDM models—such as the effective Jeans length, sound speed, and solitonic core properties—and discusses potential new phenomenological aspects relative to the minimally coupled (MC) case.

B. Modified Jeans scale and speed of sound

For ULDM, the small-scale behavior is characterized by the competition between gravity and quantum pressure. In the standard (MC) case the dynamics of the condensate are governed by the Schrödinger-Poisson system:

$$i\hbar \frac{\partial \psi}{\partial t} = -\frac{\hbar^2}{2m} \nabla^2 \psi + m\Phi\psi, \quad (168)$$

$$\nabla^2 \Phi = 4\pi G |\psi|^2, \quad (169)$$

where ψ is the wavefunction of the condensate and $\rho = |\psi|^2$.

The quantum (or effective) pressure leads to a Jeans scale given approximately by (see, e.g., [19]):

$$\lambda_J^{MC} \sim \frac{2\pi}{m} \left(\frac{\hbar^2}{G\rho_m} \right)^{1/4}. \quad (170)$$

In the NMC scenario the effective matter density is rescaled by $e^{\beta\phi}$ (166). Therefore, the Jeans scale becomes:

$$\lambda_J^{NMC} \sim \frac{2\pi}{m} \left(\frac{\hbar^2}{G\rho_m e^{\beta\phi}} \right)^{1/4} = \lambda_J^{MC} e^{-\beta\phi/4}. \quad (171)$$

Thus, for $\beta > 0$ the effective Jeans length is reduced, which implies that structures (and the corresponding solitonic cores) can form on slightly smaller scales than in the MC case. Conversely, for $\beta < 0$ the Jeans scale is increased.

In addition, the speed of sound of the condensate in the non-relativistic limit is determined by the effective pressure. In the MC case the sound speed is approximately:

$$c_s^2 \sim \frac{k^2}{4m^2}, \quad (172)$$

where k is a characteristic wavenumber. In the NMC case, the effective pressure acquires corrections from the energy transfer between the scalar field and the matter fluid. Denoting these corrections by Δp , one may write an effective speed of sound as:

$$c_{s,NMC}^2 \approx c_s^2 + \frac{\partial \Delta p}{\partial \rho_m}. \quad (173)$$

In a first-order approximation, if we assume that $\Delta p \propto \beta \phi \rho_m / H$, the modification to the sound speed is proportional to β and the rate of change of ϕ .

C. Solitonic core formation and the NMC

Ultra-light dark matter models predict that wave interference effects and quantum pressure support a central solitonic core in dark matter halos (see, e.g., [146]). In the MC case, the core profile is determined by a balance between the gradient energy and gravitational potential. A common approximate soliton density profile is given by:

$$\rho_{sol}(r) \simeq \rho_0 \left[1 + \left(\frac{r}{r_c^{MC}} \right)^2 \right]^{-8}, \quad (174)$$

where r_c^{MC} is the core radius in the minimally coupled case.

In the NMC scenario the chameleon-like mechanism introduces two important modifications:

1. The effective matter density is rescaled by $e^{\beta\phi}$ (cf. (166)), which in turn modifies the gravitational potential in the Poisson equation.
2. The scalar field equation itself contains an extra source term (167), which drives a secular evolution of ϕ . This alters the balance between gravitational attraction and quantum pressure.

We may model the effect on the soliton core radius in a phenomenological way as:

$$r_c^{NMC} \simeq r_c^{MC} [1 + \eta\beta\langle\phi\rangle], \quad (175)$$

where η is a dimensionless parameter whose precise value can be determined through numerical simulations, and $\langle\phi\rangle$ is the average scalar field value in the halo region. Therefore, the NMC mechanism can either reduce or enhance the core radius, thereby modifying the central density profile of DM halos. Such changes may be observable in high-resolution rotation curves of dwarf galaxies and in gravitational lensing profiles.

XIII. THERMODYNAMICS AND QUANTUM GRAVITY CONSTRAINTS IN NMC COSMOLOGICAL MODELS

Non-minimally coupled (NMC) scalar-field cosmologies offer a rich phenomenology in which energy is exchanged between the scalar field and the matter (or radiation) sectors. The presence of the coupling modifies the standard thermodynamic evolution and induces irreversible (non-equilibrium) effects. Moreover, when one incorporates gravitational (horizon) thermodynamics, new constraints emerge that bear on quantum gravity considerations.

A. Equilibrium thermodynamics and the modified Gibbs relation

In standard cosmological thermodynamics the first law is expressed as:

$$d(\rho V) + p dV = T dS, \quad (176)$$

where $V = a^3$ is the comoving volume, ρ the energy density, p the pressure, T the temperature, and S the entropy (see, e.g., [147]). When a non-minimal coupling is present, the particle number is rescaled. Defining the effective baryon number as:

$$N_{\text{eff}} = f(\phi) N_b, \quad (177)$$

the Gibbs relation generalizes to:

$$T dS = d(\rho V) + p dV - \mu d(f(\phi) N_b), \quad (178)$$

where μ denotes the chemical potential associated with the baryon number N_b (see, e.g., [73, 76, 77, 126]). In the case of FLRW universe, the total internal energy is defined as:

$$U = \rho V \quad (179)$$

$$dU = V d\rho + \rho dV. \quad (180)$$

Thus, (178) becomes:

$$T dS = V d\rho + (\rho + p) dV - \mu d(f(\phi) N_b). \quad (181)$$

Dividing by an infinitesimal time dt yields the entropy production rate:

$$\frac{dS}{dt} = \frac{1}{T} \left[\dot{\rho} V + (\rho + p) \dot{V} - \mu \frac{d}{dt} (f(\phi) N_b) \right]. \quad (182)$$

In the absence of the NMC ($f(\phi) = 1$) with conserved N_b this expression reduces to the standard adiabatic case.

B. Non-equilibrium processes and causal dissipative dynamics

When the scalar field ϕ exchanges energy rapidly with the matter sector, a non-equilibrium treatment is warranted. In such cases the continuity equation for non-relativistic matter is modified to:

$$\dot{\rho}_m + 3H \rho_m = \beta \dot{\phi} \rho_m. \quad (183)$$

The source term, proportional to $\beta \dot{\phi} \rho_m$, indicates that the scalar field “pumps” or “extracts” energy from the matter sector and introduces an irreversible component.

This additional energy exchange is often recast as an effective bulk viscous pressure. Writing the total effective pressure as:

$$p_{\text{eff}} = p + \Pi, \quad (184)$$

one compares the modified conservation law with the standard form:

$$\dot{\rho}_m + 3H(\rho_m + p_m + \Pi) = 0. \quad (185)$$

For pressureless matter ($p_m = 0$) the comparison (cf. [148]) shows that:

$$3H \Pi_{\text{NMC}} = -\beta \dot{\phi} \rho_m, \quad (186)$$

so that:

$$\Pi_{\text{NMC}} = -\frac{\beta \dot{\phi}}{3H} \rho_m. \quad (187)$$

1. The Eckart approach

In the classical (instantaneous) *Eckart* formulation of relativistic dissipative fluids [148] the bulk viscous pressure is given by:

$$\Pi_{\text{Eckart}} = -\zeta \theta, \quad (188)$$

where ζ is the bulk viscosity coefficient and the expansion scalar is given by:

$$\theta = 3H. \quad (189)$$

If intrinsic viscous effects (parameterized by ζ) are negligible compared to the effect of the non-minimal coupling, then the effective pressure is dominated by Π_{NMC} in Eq. (187).

2. Israel-Stewart causal thermodynamics

A more refined treatment of dissipative processes employs the *Israel-Stewart* causal framework [149–151], which introduces a finite relaxation time τ . In this approach the evolution of the viscous pressure is governed by the relation:

$$\tau \dot{\Pi} + \Pi = -\zeta \theta - \frac{1}{2} \tau \Pi \left(3H + \frac{\dot{\tau}}{\tau} - \frac{\dot{\zeta}}{\zeta} - \frac{\dot{T}}{T} \right). \quad (190)$$

To account for the non-minimal coupling, one adds the source term Π_{NMC} from Eq. (187) so that:

$$\tau \dot{\Pi} + \Pi = -\zeta \theta + \Pi_{\text{NMC}} - \frac{1}{2} \tau \Pi \left(3H + \frac{\dot{\tau}}{\tau} - \frac{\dot{\zeta}}{\zeta} - \frac{\dot{T}}{T} \right). \quad (191)$$

For small but finite τ an approximate solution may be written by neglecting $\dot{\Pi}$ and assuming that the quantity:

$$\Gamma \equiv 3H + \frac{\dot{\tau}}{\tau} - \frac{\dot{\zeta}}{\zeta} - \frac{\dot{T}}{T} \quad (192)$$

remains roughly constant. Then:

$$\Pi \approx \frac{-\zeta \theta + \Pi_{\text{NMC}}}{1 + \frac{1}{2} \tau \Gamma}. \quad (193)$$

In the limit with $\tau \rightarrow 0$ the causal delay vanishes, and one recovers the instantaneous Eckart relation.

a. Example Assume that the baryonic energy density evolves as:

$$\rho_m = \rho_{m0} a^{-3} e^{\beta\phi}, \quad (194)$$

and that the scalar field obeys a scaling law:

$$\dot{\phi} \sim \phi_0 H \quad (\phi_0 = \text{const.}). \quad (195)$$

Then, (187) gives:

$$\Pi_{\text{NMC}} = -\frac{\beta\phi_0}{3} \rho_m. \quad (196)$$

Substituting this into Eq. (193) yields:

$$\Pi \approx \frac{-\zeta\theta - \frac{\beta\phi_0}{3}\rho_m}{1 + \frac{1}{2}\tau\Gamma}. \quad (197)$$

For negligible intrinsic viscosity (small ζ) the effective pressure is then dominated by the NMC term modulated by a causal delay factor:

$$\Pi \approx -\frac{\beta\phi_0}{3} \rho_m \left(1 - \frac{1}{2}\tau\Gamma\right) \quad (198)$$

up to the first order in τ .

C. Horizon thermodynamics and the generalized second law

An alternative perspective on cosmological thermodynamics is provided by horizon (gravitational) entropy. In the de Sitter-like or late-time accelerating regimes the cosmological horizon is characterized by:

$$T_{\text{GH}} = \frac{H}{2\pi} \quad (199)$$

and:

$$S_{\text{GH}} = \frac{\pi}{H^2} \quad (200)$$

as originally derived in [74, 75]. One defines the total entropy as:

$$S_{\text{tot}} = S_{m+r+\phi} + S_{\text{GH}}, \quad (201)$$

where $S_{m+r+\phi}$ denotes the combined matter, radiation, and SF entropy. The generalized second law (GSL) requires:

$$\frac{dS_{\text{tot}}}{dt} \geq 0. \quad (202)$$

In bouncing or cyclic models the evolution of S_{GH} may be non-monotonic (decreasing during contraction and increasing during accelerated expansion), but the presence of irreversible entropy production via the NMC coupling, as encapsulated by (182) (and an equivalent open system formulation in [125]), ensures that the overall entropy does not decrease.

D. Quantum gravity constraints and thermodynamic bounds

Quantum gravity considerations (in particular, holographic principle [152, 153] and the Bekenstein bound [154, 155]) limit the amount of entropy that can be stored within a given region. In the context of NMC models the total matter entropy produced over one cycle is roughly proportional to:

$$\Delta S \propto \beta \Delta\phi, \quad (203)$$

with $\Delta\phi$ denoting the field excursion. If $\Delta\phi$ exceeds a value of $\mathcal{O}(1) M_{\text{Pl}}$, then the accumulated entropy may approach or exceed the holographic bound. Such thermodynamic bounds are closely linked to recent Swampland conjectures and quantum gravity constraints (see, e.g., [62, 153, 156, 157]), thereby providing an upper limit on the allowed field excursion in viable cosmological models.

E. Summary

In summary, this unified framework demonstrates that:

- The equilibrium thermodynamics of NMC models is captured by a generalized Gibbs relation (178) in which the effective baryon number, rescaled by the coupling function, gives rise to additional work terms.
- Non-equilibrium (irreversible) effects are naturally incorporated through an effective bulk viscous pressure. The instantaneous response is described by the Eckart formulation (188)–(187)), while a more realistic causal evolution is provided by the Israel–Stewart framework ((191) and (193)).
- Horizon thermodynamics introduces an independent gravitational entropy (Eq. (199)) whose evolution, when combined with matter entropy (Eq. (201)), ensures that the generalized second law (202) is satisfied even during non-singular bounces.
- Finally, quantum gravity arguments, via holographic and Bekenstein bounds, impose a thermodynamic limitation on the total field excursion, thereby linking $\Delta\phi$ to $\mathcal{O}(1) M_{\text{Pl}}$ and providing a concrete connection to Swampland constraints.

XIV. ENERGY CONDITIONS, BOUNCE DYNAMICS, AND SWAMPLAND CONSTRAINTS IN NMC COSMOLOGIES

In this section, we present an integrated framework combining a detailed analysis of classical and effective energy conditions [158], a derivation of non-singular bounce dynamics triggered by NMC, and the constraints imposed by recent Swampland conjectures. We show that

an exponential non-minimal coupling not only induces a brief, controlled violation of energy conditions (thus enabling bounce phenomena) but also ensures that the scalar field dynamics remains compatible with bounds from quantum gravity.

A. Energy conditions and NMC

1. Classical Energy Conditions

In standard General Relativity the Einstein field equations read:

$$G_{\mu\nu} = \kappa^2 T_{\mu\nu}, \quad (204)$$

with $G_{\mu\nu}$ the Einstein tensor and $T_{\mu\nu}$ the stress-energy tensor. The classical energy conditions are imposed on $T_{\mu\nu}$ to guarantee physically reasonable matter:

- **Weak Energy Condition (WEC):**

$$T_{\mu\nu} u^\mu u^\nu \geq 0 \quad \forall u^\mu \text{ (timelike, with } u^\mu u_\mu = -1), \quad (205)$$

ensuring each observer measures non-negative local energy density.

- **Null Energy Condition (NEC):**

$$T_{\mu\nu} k^\mu k^\nu \geq 0 \quad \forall k^\mu \text{ (null, with } k^\mu k_\mu = 0), \quad (206)$$

which is central to singularity theorems [159–161] and bounce scenarios.

- **Dominant Energy Condition (DEC):**

$$T_{\mu\nu} u^\mu u^\nu \geq 0, \quad T_{\mu\nu} u^\nu \text{ being timelike or null}, \quad (207)$$

to preclude super-luminal energy propagation.

- **Strong Energy Condition (SEC):**

$$\left(T_{\mu\nu} - \frac{1}{2} T g_{\mu\nu}\right) u^\mu u^\nu \geq 0, \quad (208)$$

implying geodesic convergence under certain circumstances — even though accelerated expansion phases may violate the SEC [160, 162].

2. Effective stress-energy tensor with NMC

In the NMC framework the scalar field ϕ couples to the matter sector via an exponential factor. Consequently, the baryonic energy density evolves as:

$$\rho_b(a, \phi) = \rho_{b0} a^{-3}(\tau) e^{\beta\phi(\tau)}, \quad (209)$$

and the total effective stress-energy tensor is defined as:

$$T_{\mu\nu}^{(\text{eff})} = T_{\mu\nu}^{(m)} + T_{\mu\nu}^{(\phi)} + \Delta T_{\mu\nu}^{(\text{coupl})}. \quad (210)$$

where:

$$T_{\mu\nu}^{(\phi)} \equiv \nabla_\mu \phi \nabla_\nu \phi - \frac{1}{2} g_{\mu\nu} \left[(\nabla\phi)^2 + \mathcal{V}(\phi) \right] \quad (211)$$

and⁹:

$$\begin{aligned} \Delta T_{\mu\nu}^{(\text{coupl})} &\equiv 2\beta \left[\nabla_\mu \nabla_\nu \phi - g_{\mu\nu} \square \phi \right] \\ &\quad + 2\beta^2 \left[\nabla_\mu \phi \nabla_\nu \phi - g_{\mu\nu} (\nabla\phi)^2 \right] \end{aligned} \quad (212)$$

The presence of $e^{\beta\phi}$ may induce episodes of effective negative pressure, and thus violations of the NEC or SEC, in controlled, short-lived intervals [163].

3. Approximate NEC violation and the bounce mechanism

For a spatially flat FLRW background, a non-singular bounce is characterized by $H(\tau_b) = 0$ and $\dot{H}(\tau_b) > 0$. The Friedmann equations are

$$3H^2 = \rho_{\text{tot}}, \quad (213a)$$

$$2\dot{H} + 3H^2 = -(\rho_{\text{tot}} + 3p_{\text{tot}}). \quad (213b)$$

In a classical setting $\rho_{\text{tot}} + p_{\text{tot}} \geq 0$; however, with NMC the continuity equation for baryons becomes:

$$\dot{\rho}_b + 3H \rho_b = \beta \dot{\phi} \rho_b, \quad (214)$$

which may be interpreted as introducing an effective pressure:

$$p_{\text{eff}}^{(b)} = -\frac{\beta \dot{\phi}}{3H} \rho_b. \quad (215)$$

Expanding the scale factor and scalar field near the bounce time τ_b as

$$a(\tau) \approx a_b \left[1 + \frac{1}{2} \alpha (\tau - \tau_b)^2 + \dots \right], \quad (216a)$$

$$\phi(\tau) \approx \phi_b + \phi'_1 (\tau - \tau_b) + \dots, \quad (216b)$$

one obtains an effective bulk viscosity term:

$$\Pi_{\text{NMC}}(\tau) \approx -\frac{\beta \phi'_1}{3\alpha (\tau - \tau_b)} \rho_b(\tau_b) e^{-\frac{3}{2} \alpha (\tau - \tau_b)^2 + \beta \phi'_1 (\tau - \tau_b)}. \quad (217)$$

While Π_{NMC} diverges as $(\tau - \tau_b)^{-1}$, the divergence is integrable, thereby ensuring a transient violation of $\rho + p \geq 0$ that is sufficient to yield $\dot{H} > 0$ at the bounce [163].

⁹ The exact derivation of $\Delta T_{\mu\nu}^{(\text{coupl})}$ can be found in Appendix A

4. Thermodynamic interpretation and quantum energy inequalities

The standard Gibbs relation is modified in the presence of NMC to:

$$T dS = d(\rho V) + p dV - \mu d[f(\phi) N_b]. \quad (218)$$

Here, the extra $-\mu d[f(\phi) N_b]$ term plays the role of a bulk viscosity, characterized by:

$$\Pi_{\text{NMC}} = -\frac{\beta \dot{\phi}}{3H} \rho_b. \quad (219)$$

This viscous contribution links the temporary energy condition violation with irreversible matter entropy production. On the quantum side, negative energy densities are constrained by the so called *Quantum Energy Inequalities* (QEIs)¹⁰ of the schematic form [165]:

$$\Delta E = \int_{-\infty}^{\infty} \langle T_{tt}(t) \rangle \sigma(t) dt \gtrsim -\frac{C}{\tau^4}, \quad (220)$$

with C a constant of order unity and $\sigma(t)$ a smooth sampling function. The short-lived nature of the NEC violation as in (217) is thus fully compatible with such quantum bounds.

B. Swampland conjectures and field excursion constraints

1. Overview of Swampland Conjectures

Recent advances in string theory and quantum gravity suggest that only a subset of effective low-energy theories can be embedded in a comprehensive UV framework. Three key conjectures are:

1. Swampland Distance Conjecture (SDC):

$$\Delta\phi \lesssim \mathcal{O}(1) M_{\text{Pl}}, \quad (221)$$

implying that large field excursions trigger an infinite tower of light states.

2. de Sitter Conjecture (dSC):

$$M_{\text{Pl}} \frac{|V'|}{V} \gtrsim c_1 \quad \vee \quad M_{\text{Pl}}^2 \frac{V''}{V} \lesssim -c_2, \quad (222)$$

which rules out (meta-)stable de Sitter vacua in string theory.

3. Trans-Planckian Censorship Conjecture (TCC):

$$\frac{a(t_f)}{a(t_i)} < \frac{M_{\text{Pl}}}{H(t_f)}, \quad (223)$$

ensuring that sub-Planckian quantum modes do not evolve to super-Hubble scales.

2. Application to specific scalar field potentials

Within the NMC framework the scalar field dynamics are subject to these Swampland bounds. We now discuss several representative potentials:

a. Axions/ALPs: For the generalized potential of the form:

$$\mathcal{V}(\phi) = \Lambda_c^4 \left[1 - \cos\left(\frac{\phi}{f}\right) \right], \quad (224)$$

if the decay constant satisfies $f \ll M_{\text{Pl}}$, then the periodicity naturally restricts the field excursion ($\Delta\phi < 2\pi f$), in line with (221). In contrast, natural inflation models that require $f \gtrsim M_{\text{Pl}}$ face potential tension with the SDC and dSC unless NMC effects provide extra damping.

b. Exponential/Ekpyrotic/Cyclic: Models employing potentials of the form:

$$\mathcal{V}(\phi) = V_0 (e^{b\phi} - e^{-c\phi}) \quad \vee \quad \mathcal{V}(\phi) = 2\Lambda - V_0 e^{-c\phi}, \quad (225)$$

typically use a steep negative exponential during contraction so that $M_{\text{Pl}} |V'|/|V| \sim \mathcal{O}(1)$. In these scenarios the NMC coupling further restricts the field excursion, ensuring that the bounce occurs before $\Delta\phi$ exceeds the SDC bound.

c. Quintessence and SFDM: For quintessence models with potentials:

$$\mathcal{V}(\phi) = V_0 [\sinh(\lambda\phi)]^n, \quad (226)$$

the challenge is to simultaneously achieve an effective slow-roll phase (with small $|V'/V|$) and to satisfy the dSC. In the NMC framework the modified scalar equation of motion:

$$\ddot{\phi} + 3H\dot{\phi} + V'(\phi) = -\beta \rho_m, \quad (227)$$

introduces extra damping that helps keep the overall field excursion $\Delta\phi$ sub-Planckian. Similarly, in SFDM models with:

$$\mathcal{V}(\phi) = V_0 [\cosh(\lambda\phi) - 1], \quad (228)$$

the field oscillates about $\phi = 0$, naturally confining the evolution within the SDC limits.

3. Cosmological implications of bounded field excursions

The Swampland constraints, particularly the SDC, imply:

$$\Delta\phi \lesssim \mathcal{O}(1) M_{\text{Pl}}. \quad (229)$$

This limitation has several significant consequences:

- 1. Finite cyclic evolution:** In cyclic or bouncing cosmologies, the small (per cycle) field excursion prevents cumulative drift, ensuring that each bounce is triggered in a controlled region of field space.

¹⁰ The first example of QEI was presented in [164].

2. **Bounded entropy production:** Since irreversible entropy production is proportional to $\beta \Delta\phi$, a cap on $\Delta\phi$ naturally limits the injected entropy per cycle.
3. **Controlled bounce dynamics:** The bounce condition (roughly when $\dot{\phi}^2 \gtrsim |\mathcal{V}(\phi)|$) is reached within a finite excursion, precluding the field from entering regions where an infinite tower of light states would compromise the effective theory.
4. **Avoidance of no-go theorems:** Compared to standard large-field inflation models with super-Planckian excursions (as dictated by the Lyth bound [166]), the NMC framework facilitates slow-roll or bounce solutions with $\Delta\phi \lesssim \mathcal{O}(1) M_{Pl}$, in agreement with the Swampland program.

C. Discussion

The discussion above establishes a deep interconnection between macroscopic cosmological dynamics and underlying quantum gravity constraints:

- An exponential non-minimal coupling $f(\phi) = e^{\beta\phi}$ modifies the effective stress-energy tensor such that a transient, integrable violation of the NEC triggers a non-singular bounce.
- The modified Gibbs relation, via the extra $d[f(\phi)N_b]$ term, links the temporary negative-pressure phase to irreversible entropy production—a connection that provides a thermodynamic arrow of time.
- Simultaneously, Swampland conjectures (SDC, dSC, TCC) enforce stringent bounds on the field excursion and the steepness of potentials. NMC effects, by damping the scalar field evolution, naturally ensure that $\Delta\phi$ remains sub-Planckian, even for models requiring steep potentials.
- Analyses of specific potentials (axion/ALP, exponential/ekpyrotic, quintessence, and SFDM) demonstrate that the resulting dynamics satisfy both observational requirements and the underlying quantum gravity constraints.

Thus, the integrated framework presented here not only provides an alternative to standard inflationary scenarios but also embeds cosmic bounce dynamics and late-time acceleration within a UV-complete effective field theory framework.

XV. EXTENDED ENERGY CONDITIONS TESTS FOR NMC MODELS

In this section we generalize the *point-wise* energy conditions to their *averaged* and *semi-classical* counterparts,

and derive explicit analytic criteria for the NMC Einstein-frame effective stress-energy tensor:

$$T_{\mu\nu}^{(\text{eff})} = T_{\mu\nu}^{(\phi)} + e^{-2\beta\phi} T_{\mu\nu}^{(m)} + 2\beta \left(\nabla_\mu \nabla_\nu \phi - g_{\mu\nu} \square\phi \right) + 2\beta^2 \left(\nabla_\mu \phi \nabla_\nu \phi - g_{\mu\nu} (\nabla\phi)^2 \right), \quad (230)$$

and identify the phenomenological consequences for early-time inflation, non-singular bounces and cyclic scenarios.

A. Averaged energy conditions

For any complete causal geodesic with tangent ℓ^μ ($\ell^2 = 0$) or u^μ ($u^2 = -1$) we define the *averaged* null/weak/strong energy densities [158, 167] as:

$$\mathcal{A}_N \equiv \int_{-\infty}^{+\infty} d\lambda T_{\mu\nu}^{(\text{eff})} \ell^\mu \ell^\nu \quad (231a)$$

$$\mathcal{A}_W \equiv \int_{-\infty}^{+\infty} d\tau T_{\mu\nu}^{(\text{eff})} u^\mu u^\nu \quad (231b)$$

$$\mathcal{A}_S \equiv \int_{-\infty}^{+\infty} d\tau \left[T_{\mu\nu}^{(\text{eff})} - \frac{1}{2} g_{\mu\nu} T^{(\text{eff})} \right] u^\mu u^\nu \quad (231c)$$

where λ (τ) is an affine (proper) parameter. Using (230) and the FLRW line element in *conformal* time τ one finds

$$\mathcal{A}_N = \int_{-\infty}^{+\infty} a^{-2}(\tau) d\tau \left[\rho + p - 2\beta\phi' \rho_b + 2\beta^2 \rho_b e^{\beta\phi} \right]. \quad (232)$$

Analogous expressions hold for \mathcal{A}_W and \mathcal{A}_S . From (232) we infer:

- (a) *Inflation.* In slow-roll ($\dot{\phi}^2 \ll V$) one has $\rho + p \simeq 0$, and if $\beta\phi' > 0$ the term $-2\beta\phi' \rho_b$ can keep $\mathcal{A}_N \geq 0$, so that the *averaged* NEC remains satisfied even if the *local* NEC is violated.
- (b) *Ekpyrotic/bounce phase.* Near the bounce ($H = 0$, $\dot{H} > 0$) the kinetic energy dominates, $\rho + p \simeq \dot{\phi}^2 > 0$. Nevertheless, the $+2\beta^2 \rho_b e^{\beta\phi}$ term can drive $\mathcal{A}_N < 0$, yielding a controlled ANEC violation immune to standard quantum-inequality bounds.
- (c) *Cyclic scenarios.* Over a full ekpyrotic/bounce expansion cycle one finds $\oint a^{-2} d\tau \rho \simeq 0$ and the two β -induced terms cancel to $\mathcal{O}(\beta)$, so $\oint \mathcal{A}_N \simeq 0$, restoring the global ANEC across cycles.

B. Semi-classical (quantum) energy conditions

The semi-classical regime is governed by *quantum energy inequalities* (QEI) and the *quantum null energy*

condition (QNEC) [165, 168]. For any smooth sampling function $\sigma(\tau)$ one has ¹¹:

$$\int_{-\infty}^{+\infty} d\tau \sigma^2(\tau) \langle T_{\mu\nu}^{(\text{eff})} u^\mu u^\nu \rangle \geq -\frac{C}{\tau_\sigma^4}, \quad (233)$$

where τ_σ is the characteristic width of σ .

Specializing to a comoving observer in FLRW (now in *cosmic* time t) gives the semi-classical weak energy condition:

$$\langle \rho_{\text{eff}} \rangle_\sigma \gtrsim -\frac{C}{a^4 \tau_\sigma^4} + \beta^2 \langle \rho_b e^{\beta\phi} \rangle_\sigma, \quad (234)$$

so that the positive β^2 contribution provides a natural buffer. Analogously, the QNEC on a null generator of the apparent horizon reads:

$$\frac{2\pi}{\hbar} \langle T_{\mu\nu}^{(\text{eff})} \ell^\mu \ell^\nu \rangle \geq \frac{\partial^2 S_{\text{out}}}{\partial \lambda^2}, \quad (235)$$

with S_{out} denoting the *von Neumann entropy* [169, 170] outside the cut. Inserting (230) into (235) yields a new, *coupling-assisted* lower bound:

$$\frac{\partial^2 S_{\text{out}}}{\partial \lambda^2} \leq \frac{2\pi}{\hbar} (\rho + p) - \frac{4\pi}{\hbar} [\beta \dot{\phi} \rho_b - \beta^2 \rho_b e^{\beta\phi}]. \quad (236)$$

Hence, even when $\rho + p \simeq 0$ (slow-roll), the second term is sufficiently negative to satisfy the QNEC, while at a bounce the sign flips and no conflict arises with (236).

C. Differential relation

Combining the averaged NEC (232) with the QNEC (236), and using $\dot{\rho}_b = -3H\rho_b + \beta \dot{\phi} \rho_b$, one finds the following compact constraint:

$$\frac{d}{dt} [a^2(\rho + p)] = 2\beta^2 \dot{\phi} a^2 \rho_b e^{\beta\phi} - \frac{\hbar}{\pi a^2} \frac{\partial^2 S_{\text{out}}}{\partial \lambda^2}. \quad (237)$$

This identity links macroscopic (averaged) NEC violation to quantum- information flow across null horizons. In particular:

- **Inflation:** With $\dot{\phi} < 0$ and $H > 0$, the left-hand side decreases in time ($\propto d[a^2(\rho + p)]/dt < 0$), enabling graceful exit, while the entropy term is suppressed by the (approximate) de Sitter temperature.
- **Bounce:** At $H = 0$ the LHS is positive (since $\dot{H} > 0$) and is balanced by the positive first term on the RHS (for $\beta > 0$), supplying precisely the NEC-breaking needed for a non-singular bounce.
- **Cyclic models:** Integrating (237) over one cycle, $\oint dt \partial_\lambda^2 S_{\text{out}} = 0$, so entropy is extremized (but not necessarily minimized) at successive bounces [53].

D. Implications and observational outlook

- *Inflationary spectra.* The β -dependent damping of $\rho + p$ softens the tensor tilt n_T , allowing a mildly blue tilt ($n_T \lesssim 0.3$) without violating ANEC—testable by next-generation CMB B-mode experiments.
- *Bounce signatures.* Equation (232) predicts a step-like suppression of the scalar power at $k \sim a_B H_B$ with amplitude $\Delta\mathcal{P}/\mathcal{P} \simeq 2\beta^2 \rho_b / (3H^2)$, yielding $\mathcal{O}(10\%)$ features for $\beta \sim 0.05$, within reach of LITE-BIRD.
- *Cyclic thermodynamics.* The new relation (237) guarantees that bulk-viscous entropy from matter-scalar exchange remains consistent with the QEI bound (233), resolving the entropy-accumulation issue of earlier cyclic proposals [171].

Summary

The averaged and semi-classical energy conditions provide model-independent diagnostics for NMC cosmologies. In the Einstein frame, the exponential coupling adds two positive-definite terms ($\propto \beta \phi'$ and $\propto \beta^2$) to the effective stress tensor (230), which (1) protect slow-roll inflation from quantum inequalities, (2) supply NEC-breaking for a smooth bounce, and (3) ensure entropy consistency over cycles. Equation (237) encapsulates these properties.

XVI. BARYOGENESIS IN NMC COSMOLOGIES

In this section we analyze the generation of the baryon asymmetry of the universe (BAU), quantified by the *baryon-to-photon ratio* [172, 173]:

$$\eta_B \equiv \frac{n_b}{n_\gamma} = \frac{n_b - n_{\bar{b}}}{n_\gamma} = 6.04(12) \times 10^{-10}, \quad (238)$$

in the context of the considered NMC scalar field cosmological models. After a brief introduction to the general requirements for successful baryogenesis, we show how each of the Sakharov's conditions [174] may be realized in the Einstein frame NMC framework, derive expressions for the resulting asymmetry (including back-reaction and freeze-out shift), and compare with the standard mechanisms.

A. Brief overview and Sakharov conditions

Any successful baryogenesis scenario must satisfy the three Sakharov conditions [174]:

¹¹ In 4D spacetime the sharp constant for a massless scalar is $C = 3/(32\pi^2)$.

1. *Baryon number violation* ($\Delta B \neq 0$);
2. *C and CP violation*;
3. *Departure from thermal equilibrium*.

In conventional treatments (e.g. GUT- or electroweak-baryogenesis [94, 175]), these arise from heavy particle decays or sphaleron¹² transitions. In NMC cosmologies new ingredients, most notably the time-varying coupling $f(\phi) = e^{\beta\phi}$, provide additional sources of *CP* and effective chemical potentials, as we now detail.

B. Baryon number violation

NMC itself does not directly induce *B*-violating operators, so one assumes the presence of either:

- **GUT-scale decays:** heavy *X*-bosons with $\mathcal{L} \supset y_X X \bar{q} q$, or
- **Electroweak sphalerons:** active for $T \gtrsim 100$ GeV.

The Boltzmann equation for the baryon number density n_B in an expanding universe reads:

$$\dot{n}_B + 3Hn_B = -\Gamma_B(T)(n_B - n_B^{\text{eq}}) + S_B(t), \quad (239)$$

where Γ_B is the *B*-violating rate and S_B an effective *source* term arising from *CP*-violating chemical potentials (see below).

C. C and CP violation via the time-varying coupling

In NMC models the conformal factor (2) depends on time through $\phi(t)$. By analogy with the so called “*spontaneous baryogenesis*” [177], one may write an effective Lagrangian coupling:

$$\mathcal{L}_{\text{int}} = -\frac{1}{M_*^2} \partial_\mu f(\phi) J_B^\mu = -\frac{\beta}{M_*^2} \dot{\phi} J_B^0 + \dots, \quad (240)$$

where J_B^μ is the baryon current and M_* a cutoff scale. In thermal equilibrium this term induces an *effective chemical potential*:

$$\mu_B^{\text{eff}} = \frac{\beta \dot{\phi}}{M_*^2}, \quad (241)$$

which biases baryon-number-violating processes to produce a net *B*-asymmetry. The *CP* violation is automatic, since $\dot{\phi} \neq 0$ spontaneously breaks time-reversal invariance, hence *CPT* on the cosmological background.

¹² *Sphaleron* is a static solution to the electroweak field equations. Geometrically, it can be considered as a saddle point of the electroweak potential in an infinite-dimensional field space. An etymological examination of the name reveals its origins in the ancient Greek word “*sphaleros*” which means “*ready to fall*” or “*unstable*” [176].

D. Departure from equilibrium

In the NMC framework the continuity equation for matter acquires a source:

$$\dot{\rho}_m + 3H\rho_m = +\beta \dot{\phi} \rho_m, \quad (242)$$

so that the background evolution itself departs from standard adiabaticity. More precisely, if processes freeze out at temperature T_D when:

$$\Gamma_B(T_D) \simeq H_{\text{eff}}(T_D), \quad (243)$$

then the freeze-out condition is modified by the additional term on the right-hand side. Solving:

$$\Gamma_B(T_D) = H(T_D) \left(1 + \delta_D\right), \quad (244)$$

where:

$$\delta_D \equiv \frac{\beta \dot{\phi}(T_D)}{3H(T_D)}, \quad (245)$$

one finds up to the first order:

$$T_D \simeq T_D^{(0)} \left(1 - \frac{1}{n} \delta_D\right), \quad (246)$$

where $T_D^{(0)}$ is the standard freeze-out temperature and n the power-law index in $\Gamma_B \propto T^n$.

E. Back-reaction on SF

The baryon-generating interaction (240) feeds back into the ϕ equation of motion:

$$\ddot{\phi} + 3H\dot{\phi} + V'(\phi) = \frac{\beta}{M_*^2} \langle J_B^0 \rangle \simeq \frac{\beta}{M_*^2} n_B. \quad (247)$$

Using our estimate $n_B/s \sim 10^{-10}$ one finds the source term $\beta n_B/M_*^2$ to be many orders of magnitude below $V'(\phi)$ for typical $M_* \gtrsim 10^{15}$ GeV, hence safely negligible during baryogenesis. However, in low-scale or late-time scenarios (e.g. quintessence-driven BAU) this back-reaction could in principle slow the roll of ϕ or leave imprints on its perturbations.

F. Analytic estimate of the BAU

In the sudden (instantaneous) freeze-out approximation [178, 179]:

$$\left. \frac{n_B}{s} \right|_{T=T_D} \simeq \frac{15}{4\pi^2 g_*} \frac{g_{*s}(T_0)}{g_{*s}(T_D)} \frac{\mu_B^{\text{eff}}}{T_D} \simeq \frac{15}{4\pi^2 g_*} \frac{1}{100} \frac{\beta \dot{\phi}(T_D)}{M_*^2 T_D}, \quad (248)$$

and including the shift (246) gives a small correction of order δ_D/n . Matching the observed $n_B/s \sim 10^{-10}$ again points to $\beta \sim \mathcal{O}(1)$, $T_D \sim 10^{10}$ GeV, $M_* \sim 10^{16}$ GeV as a natural benchmark.

G. Comparison with standard scenarios

- **GUT–baryogenesis:** relies on out-of-equilibrium decays of X -bosons at $T \sim 10^{15-16}$ GeV, with CP violation in Yukawa couplings. In NMC models the departure from equilibrium is partially provided by $\dot{\phi} \neq 0$, relaxing the required super-heavy scales.
- **Electroweak baryogenesis:** uses a first-order phase transition at $T \sim 100$ GeV and CP -violating bubble walls. NMC can supplement the out-of-equilibrium condition via (242), potentially easing the strong first-order requirement.
- **Leptogenesis:** the BAU arises from a lepton asymmetry via seesaw neutrino decays. An NMC-driven chemical potential $\mu_L \sim \beta\dot{\phi}/M_*^2$ can similarly bias L -violating decays, with sphalerons converting $L \rightarrow B$.

H. Observational and phenomenological constraints

Current limits on primordial isocurvature from Planck tighten any extra scalar-induced chemical potential to (no detected CDM isocurvature [180]):

$$\left. \frac{\beta\dot{\phi}}{M_*^2} \right|_{T \sim T_{CMB}} \lesssim 10^{-5}, \quad (249)$$

while laboratory and astrophysical bounds on CPT -violation constrain any time-varying $\dot{\phi}$ coupling to baryons (from spin-precession experiments [181]) at the level of:

$$\left. \frac{\beta\dot{\phi}}{M_*^2} \right|_{t_0} \lesssim 10^{-23} \text{ GeV}. \quad (250)$$

Together these imply either $M_* \gtrsim 10^{15}$ GeV for $\beta \sim 1$, or $\beta \ll 1$ if lower cutoffs are considered in dark-sector models.

I. Implications and outlook

The mechanism of “spontaneous baryogenesis” in NMC cosmologies leverages the same coupling $f(\phi) = e^{\beta\phi}$ that modifies the background and perturbation evolution (Secs. II–III), providing:

1. A *novel source of CP violation*, automatic in any rolling- ϕ epoch.
2. A *built-in departure from equilibrium*, via the modified continuity (242).
3. A *natural link* between dark-sector dynamics and high-scale baryogenesis.

4. Flagged *non-equilibrium regimes* where $\dot{\phi}$ varies non-adiabatically (e.g. near features in $\mathcal{V}(\phi)$), potentially driving $\delta_D \rightarrow \mathcal{O}(1)$.

Future work should embed this within concrete particle-physics completions (e.g. coupling to right-handed neutrinos) and explore potential observational signatures (e.g. correlated isocurvature modes or CPT -violating imprints).

XVII. THERMODYNAMIC UNIQUENESS OF THE BIG BANG: PENROSE ANALYSIS AND NMC COSMOLOGY

The thermodynamic state of the universe at its origin has long been a subject of deep investigation. In a series of seminal works, Penrose argued that the Big Bang must have been a state of exceptionally low gravitational entropy. His reasoning, detailed in [54–56, 161, 182], is based on the observation that, although matter in thermal equilibrium can possess enormous entropy, the gravitational field remains in a very low-entropy state if its free (radiative) component, quantified by the *Weyl curvature tensor*, nearly vanishes. This idea is encapsulated in what is now known as the *Weyl Curvature Hypothesis* (WCH) [161].

A. Penrose’s gravitational entropy and the Weyl curvature hypothesis

In Penrose’s picture the gravitational entropy is associated with the free gravitational field. A heuristic measure is given by [182]:

$$S_{\text{grav}} \sim \int d^3x \sqrt{h} \sqrt{C_{\mu\nu\rho\sigma} C^{\mu\nu\rho\sigma}}, \quad (251)$$

where h is the determinant of the spatial metric and $C_{\mu\nu\rho\sigma}$ is the *Weyl curvature tensor*¹³ [160]:

$$\begin{aligned} C_{\mu\nu\rho\sigma} \equiv & R_{\mu\nu\rho\sigma} + \frac{2}{(n-2)} (g_{\mu[\sigma} R_{\rho]\nu} + g_{\nu[\rho} R_{\sigma]\mu}) \\ & + \frac{2}{(n-1)(n-2)} R g_{\mu[\rho} g_{\sigma]\nu}, \end{aligned} \quad (252)$$

which is manifestly traceless. Penrose argued that at the Big Bang the Weyl curvature was essentially zero:

$$S_{\text{grav}} \approx 0, \quad (253)$$

thus setting the stage for an extremely low-entropy initial gravitational state. The vanishing of the Weyl tensor implies that, although the matter sector is in an

¹³ General definition in the n -dimensional spacetime.

extremely high-entropy thermal state, the gravitational field is highly ordered - a special boundary condition that Penrose postulates is necessary to account for the enormous overall increase in entropy observed during cosmic evolution.

1. Scaling of the Weyl invariant

In bouncing and cyclic ekpyrotic models, the universe undergoes a contraction phase dominated by a component with a very large effective equation-of-state parameter $\omega \gg 1$. In anisotropic cosmologies, such as the Bianchi type I model, the shear scalar σ^2 (a measure of anisotropy) typically scales as:

$$\sigma^2 \propto a^{-6}. \quad (254)$$

For an ekpyrotic field, the energy density scales steeply as:

$$\rho \propto a^{-3(1+\omega)}. \quad (255)$$

Defining the dimensionless ratio:

$$\epsilon \equiv \frac{\sigma^2}{\rho}, \quad (256)$$

its scaling becomes:

$$\epsilon \propto a^{-6+3(1+\omega)} = a^{3(\omega-1)}. \quad (257)$$

Since the Weyl invariant is expected to depend on both the anisotropic shear and the dominant energy density, one can argue (see e.g., [47]) that:

$$C_{\mu\nu\rho\sigma} C^{\mu\nu\rho\sigma} \propto \left(\frac{\sigma^2}{\rho}\right)^2 \rho^2 \propto a^{-6(1+\omega)}. \quad (258)$$

Thus, during contraction in an ekpyrotic phase, the Weyl invariant decays extremely rapidly. For example, if the universe contracts by a factor e^{-N} during a phase with $\omega \sim 10$, then even a modest N (e.g., $N \sim 5$) implies:

$$C_{\mu\nu\rho\sigma} C^{\mu\nu\rho\sigma} \propto e^{-6 \times 5 \times (1+10)} \approx e^{-330} \ll 10^{-100}, \quad (259)$$

which is effectively zero. This *dynamical suppression* of gravitational entropy is key to achieving the special low-entropy condition that Penrose uses to explain the arrow of time.

B. Modified Gibbs relation and irreversible processes

In the NMC models considered in this work the scalar field ϕ is coupled to the matter sector via an exponential function (2) that modifies the effective matter density. For instance, the baryonic energy density now scales as:

$$\rho_b(a, \phi) = \rho_{b0} a^{-3} e^{\beta\phi}, \quad (260)$$

in contrast to the usual a^{-3} behavior.

C. Entropy evolution

A novel perspective emerges when one considers the differential evolution of both gravitational and matter entropy. Defining the total entropy as:

$$S_{\text{tot}} = S_{\text{grav}} + S_{\text{matter}}, \quad (261)$$

we can write:

$$\frac{dS_{\text{tot}}}{dt} = \frac{dS_{\text{grav}}}{dt} + \frac{dS_{\text{matter}}}{dt}. \quad (262)$$

Assuming that the gravitational entropy is essentially measured by the Weyl invariant as in (251), and employing the scaling given in (258), we posit that:

$$S_{\text{grav}} \propto a^3 \sqrt{C_{\mu\nu\rho\sigma} C^{\mu\nu\rho\sigma}} \propto a^{3-3(1+\omega)} = a^{-3\omega}, \quad (263)$$

so that, using the Hubble law $\dot{a} = H a$, the time derivative becomes:

$$\frac{dS_{\text{grav}}}{dt} = -3\omega H S_{\text{grav}}. \quad (264)$$

Here, during an ekpyrotic contraction with $\omega \gg 1$ and $H < 0$, the gravitational entropy is exponentially suppressed.

For the matter sector, differentiating the generalized Gibbs relation (218) provides:

$$\frac{dS_{\text{matter}}}{dt} = \frac{1}{T} \left[V \dot{\rho} + (\rho + p) \dot{V} - \mu \frac{d}{dt} (f(\phi) N_b) \right]. \quad (265)$$

Thus, the coupled differential equation governing the total entropy evolution is:

$$\frac{dS_{\text{tot}}}{dt} = \frac{1}{T} \left[V \dot{\rho} + (\rho + p) \dot{V} - \mu \frac{d}{dt} (f(\phi) N_b) \right] - 3\omega H S_{\text{grav}}. \quad (266)$$

Equation (266) reveals that while gravitational entropy is rapidly suppressed during contraction, irreversible thermodynamic processes in the matter sector (driven by the non-minimal coupling) ensure a continuous increase in matter entropy. This formulation quantitatively supports the concept of a cycle-to-cycle dynamical resetting of gravitational entropy alongside an accumulating matter entropy, a mechanism that has been recently discussed in the literature [171, 183].

D. Combined gravitational and matter entropy in cyclic models

A novel perspective emerges when we consider both Penrose's low gravitational entropy and the irreversible matter entropy produced in NMC cosmology. In cyclic ekpyrotic models, the universe undergoes repeated phases of contraction and expansion. During the ekpyrotic contraction the effective equation-of-state satisfies

$\omega \gg 1$, so that the Weyl curvature invariant decays steeply according to:

$$C_{\mu\nu\rho\sigma}C^{\mu\nu\rho\sigma} \propto a^{-6(1+w)}. \quad (267)$$

Thus, even a modest contraction can effectively reduce the gravitational entropy (as measured by (251) to zero at each bounce. Simultaneously, the irreversible processes in the matter sector, enhanced by the direct coupling $f(\phi) = e^{\beta\phi}$, lead to a cumulative increase in matter entropy. Defining the total entropy as:

$$S_{\text{tot}} = S_{\text{grav}} + S_{\text{matter}}, \quad (268)$$

a dual mechanism emerges: the gravitational entropy is dynamically reset to a near-zero value at every bounce, while the matter entropy increases monotonically. This separation explains the emergence of the macroscopic arrow of time without requiring a singular, fine-tuned low-entropy initial condition.

1. Quantitative estimate

Suppose that during an ekpyrotic contraction phase the scale factor decreases by a factor e^{-N} . Then, by (267):

$$C_{\mu\nu\rho\sigma}C^{\mu\nu\rho\sigma} \propto e^{-6N(1+w)}. \quad (269)$$

For example, with $\omega \sim 10$ and $N \sim 5$, the Weyl invariant is suppressed by roughly:

$$e^{-6 \times 5 \times 11} \approx e^{-330} \ll 10^{-100}, \quad (270)$$

which is effectively zero. Concurrently, if irreversible processes produce a matter entropy change ΔS over a cycle estimated by:

$$\Delta S \sim \frac{1}{T} \left[-\mu \Delta(f(\phi)N_b) \right], \quad (271)$$

then over many cycles the total matter entropy increases while the gravitational entropy is repeatedly reset. This quantitative picture, though schematic, provides a unified explanation for the observed arrow of time.

E. Penrose analysis vs. NMC approaches

Both Penrose's gravitational entropy analysis and the NMC approach address the entropy problem from complementary viewpoints:

- **Gravitational vs. matter entropy:** Penrose argues that the gravitational field started in a low-entropy state as the Weyl curvature nearly vanished at the Big Bang ($S_{\text{grav}} \approx 0$; see (253). In NMC cosmology, however, the focus shifts to the matter sector where the coupling $f(\phi) = e^{\beta\phi}$ modifies the effective baryon density (260) and leads to irreversible entropy production (266).

- **Static initial condition vs. dynamical resetting:** In Penrose's view the initial low gravitational entropy is imposed as a unique boundary condition. By contrast, in cyclic ekpyrotic models, the extremely high effective equation-of-state during contraction dynamically suppress the Weyl curvature (via (267)), effectively resetting the gravitational entropy at each bounce.
- **Irreversibility:** Penrose's analysis centers on a special initial state. In NMC models, the inclusion of irreversible processes (via the generalized Gibbs relation in (178) and the associated bulk viscosity in (187) results in a continuous increase in matter entropy that, when combined with the periodic resetting of gravitational entropy, produces the observed arrow of time.

F. Implications for the arrow of time and cosmic evolution

The integration of Penrose's gravitational entropy analysis with the irreversible thermodynamics of NMC cosmology leads to a dual perspective:

1. **Dynamical resetting:** In cyclic and ekpyrotic models the contraction phase (with $\omega \gg 1$) suppress the Weyl curvature sharply (cf. (267)), thereby resetting the gravitational entropy to near-zero at each bounce.
2. **Continuous matter entropy production:** Simultaneously, the direct coupling between the scalar field and matter (via $f(\phi) = e^{\beta\phi}$) ensures that matter entropy increases irreversibly over time.
3. **Emergence of the arrow of time:** The combination of a periodically low gravitational entropy and a monotonically increasing matter entropy naturally establishes a macroscopic arrow of time, with the initial state emerging as a dynamical property rather than a fixed boundary condition.

G. Perspectives and future directions

In conclusion, while Penrose's thermodynamic arguments [54–56, 161, 182] emphasize that the Big Bang began with nearly zero gravitational entropy, the non-minimally coupled cosmological models presented here provide a dynamic mechanism to achieve such a state. The ekpyrotic contraction phase, characterized by an extremely high EoS parameter ω , drives the Weyl curvature invariant to decay steeply (as in (267)), thereby dynamically resetting the gravitational sector at each bounce. Concurrently, the explicit coupling $f(\phi) = e^{\beta\phi}$ leads to irreversible matter entropy production (via (178)

and (182)). The interplay between these two processes, gravitational reset and increased matter entropy, is encapsulated in the novel differential formulations provided (see (264) and (266)) and further constrained by the holographic entropy bounds (199). These insights not only reinforce the thermodynamic uniqueness of the Big Bang, but also offer promising avenues for future research, including detailed numerical simulations aimed at uncovering observable signatures in the cosmic microwave background and large-scale structure [171, 183].

XVIII. CONCLUSIONS AND PERSPECTIVES

Conclusions

This work presents a unified Einstein-frame analysis of a non-minimally coupled scalar sector in which all visible-sector fields experience the conformal factor $f(\phi) = e^{\beta\phi}$. Exact background equations, the full linear perturbation system, a five-dimensional autonomous dynamical set, and a systematic fixed-point classification have been obtained for five representative potentials: axions/ALPs, cyclic ekpyrotic, exponential/ekpyrotic with a cosmological constant, quintessence, and SFDM. The main results can be summarized as follows.

First, the coupling rescales the baryon density to $\rho_b \propto a^{-3}e^{\beta\phi}$, alters the kinetic term in the Klein-Gordon equation and adds β -dependent sources in every perturbation channel. A compact set of dimensionless variables reduces the background to an autonomous form whose critical points encode the full cosmological phase space; their existence and eigenvalue structure are listed in Tables I–XIV. For each potential at least one early-radiation saddle, one transient stiff state, and one late-time attractor were found, the latter being either a dark-energy fixed point with $\omega_{eff} \simeq -1$ or a matter-like node that depends on β .

Second, β -induced corrections remain compatible with laboratory fifth-force searches provided $|\beta| \lesssim 10^{-2}$ in unscreened models and $|\beta| \lesssim 5 \times 10^{-2}$ when the potential admits chameleon screening, in agreement with torsion-balance, Cassini and MICROSCOPE limits [98, 99, 101]. Within these ranges the modified growth history can soften the current H_0 and S_8 tensions by diluting baryons faster than a^{-3} and by lowering the effective clustering amplitude, while simultaneously leaving CMB anisotropies almost unchanged.

Third, an analytic transfer matrix for primordial tensor modes was derived. In ekpyrotic and cyclic scenarios it predicts a blue spectrum with a step-like break whose scale k_* is fixed by $\tau_B \propto \beta^{-2}$. For $\beta = 0.8$ the associated signal peaks around $f \simeq 0.7$ Hz with $\Omega_{GW}h^2 \sim 4 \times 10^{-13}$, placing it well inside the planned LISA band [68]. Smaller values of β push the step to the PTA window, where existing NANOGrav data already impose $|\beta| \lesssim 1$.

Fourth, the coupling supplies an effective bulk viscosity $\Pi_{NMC} = -\beta\dot{\phi}\rho_b/(3H)$ that can violate the null energy

condition for a period shorter than the inverse Hubble time, thereby realizing a smooth, ghost-free bounce while respecting quantum-energy inequalities. During the ekpyrotic contraction that precedes the bounce the Weyl invariant decays as $a^{-6(1+\omega)}$, dynamically enforcing Penrose’s low-entropy initial condition without fine-tuning.

Fifth, a rolling ϕ generates the chemical potential $\mu_B = \beta\dot{\phi}/M_*^2$. Taking $M_* \gtrsim 10^{15}\sqrt{\beta}$ GeV and $\beta \sim 10^{-1}$ yields $n_B/s \simeq 6 \times 10^{-10}$ at temperatures near 10^{10} GeV. Because the back-reaction term $\beta n_B/M_*^2$ is then negligible in the Klein-Gordon equation, baryogenesis and cosmological evolution remain self-consistent.

Finally, the scalar excursions in every viable scenario satisfy $\Delta\phi \lesssim \mathcal{O}(1)M_{Pl}$, automatically obeying the Swampland distance conjecture, while the potentials either respect the original de Sitter bound or evade it through the ekpyrotic phase. Energy condition diagnostics show that averaged and quantum versions of the null condition are never violated for longer than allowed by quantum information theorems.

Future directions

Observationally, the model predicts a step or oscillation in the stochastic gravitational wave background, a mild scale dependence in the growth index, and a small early-ISW imprint in the CMB. These can be tested with coming LISA, PTA, Euclid and CMB-S4 data. On the theoretical side, matching non-linear structure formation to the modified perturbation equations and embedding the exponential coupling in an UV-complete string construction are immediate priorities. A dedicated Monte-Carlo analysis, including the full set of dynamical variables in a Boltzmann solver, will be required to quantify the joint likelihood of β and the potential parameters. Progress along these lines will determine whether the exponential non-minimal coupling can provide a coherent, data-driven alternative to Λ -CDM model and to single-field inflation.

ACKNOWLEDGMENTS

The author would like to thank *Roksana Szwarc*, *Eleonora Di Valentino*, *William Giarè*, *Carsten van de Bruck* and *Dong Ha Lee* for their accurate observations and comments on the article. In addition, the author dedicates the article to *Roksana Szwarc*, his parents: *Bożena* and *Krzysztof*, his sister *Dominika*, and last but not least: *Antonio*, *Bob*, *Bob II*, *Groovy*, *Milena* and *Stuart*.

This article is based upon work from COST Action CA21136 – “Addressing observational tensions in cosmology with systematics and fundamental physics (CosmoVerse)”, supported by COST (European Cooperation in Science and Technology).

This article is based upon work from COST Action COSMIC WISPerS CA21106, supported by COST (European Cooperation in Science and Technology).

Appendix A: Derivation of the coupling terms in the effective energy-momentum tensor for the SF

In our model the matter fields couple to the metric via the conformally transformed metric:

$$\tilde{g}_{\mu\nu} = f^2(\phi)g_{\mu\nu} \quad \wedge \quad f(\phi) = e^{\beta\phi}. \quad (\text{A1})$$

Thus the matter action depends on ϕ via:

$$S_m[f^2(\phi)g_{\mu\nu}, \chi]. \quad (\text{A2})$$

In this appendix we derive explicitly the additional coupling terms that appear in the effective stress-energy tensor when the total action:

$$S[g_{\mu\nu}, \phi, \chi] = \frac{1}{2\kappa^2} \int d^4x \sqrt{-g} \left\{ R - g^{\mu\nu} \partial_\mu \phi \partial_\nu \phi - \mathcal{V}(\phi) \right\} + S_m[f^2(\phi)g_{\mu\nu}, \chi] \quad (\text{A3})$$

is varied with respect to the metric $g_{\mu\nu}$.

a. Variation of the matter action Since the matter fields see the metric $\tilde{g}_{\mu\nu} = f^2(\phi)g_{\mu\nu}$, the variation of the matter action yields:

$$\delta S_m = \frac{1}{2} \int d^4x \sqrt{-\tilde{g}} \tilde{T}^{\mu\nu} \delta \tilde{g}_{\mu\nu}, \quad (\text{A4})$$

where:

$$\tilde{T}^{\mu\nu} \equiv -\frac{2}{\sqrt{-\tilde{g}}} \frac{\delta S_m}{\delta \tilde{g}_{\mu\nu}}. \quad (\text{A5})$$

Noting that:

$$\delta \tilde{g}_{\mu\nu} = f^2(\phi) \delta g_{\mu\nu} \quad (\text{A6})$$

and using the relation:

$$\sqrt{-\tilde{g}} = f^4(\phi) \sqrt{-g}, \quad (\text{A7})$$

we deduce that:

$$\delta S_m = \frac{1}{2} \int d^4x \sqrt{-g} f^6(\phi) \tilde{T}^{\mu\nu} \delta g_{\mu\nu}. \quad (\text{A8})$$

This variation implies that the contribution of matter to the Einstein equations appears rescaled by powers of $f(\phi)$.

b. Variation from the conformal transformation Under the conformal rescaling:

$$\tilde{g}_{\mu\nu} = f^2(\phi)g_{\mu\nu}, \quad (\text{A9})$$

the Ricci scalar transforms as [136, 184]:

$$\tilde{R} = f^{-2}(\phi) \left[R - 6 \square \ln f(\phi) - 6 (\nabla \ln f(\phi))^2 \right]. \quad (\text{A10})$$

When the gravitational part of the action is expressed in terms of the original metric $g_{\mu\nu}$ and the scalar field ϕ , additional terms arise from the derivatives of $f(\phi)$. One can show that the resulting Einstein equations can be written as:

$$G_{\mu\nu} = T_{\mu\nu}^{(\phi)} + \frac{1}{f^2(\phi)} T_{\mu\nu}^{(m)} + \frac{2}{f(\phi)} \left[\nabla_\mu \nabla_\nu f(\phi) - g_{\mu\nu} \square f(\phi) \right], \quad (\text{A11})$$

where:

$$T_{\mu\nu}^{(\phi)} = \nabla_\mu \phi \nabla_\nu \phi - \frac{1}{2} g_{\mu\nu} \left[(\nabla \phi)^2 + \mathcal{V}(\phi) \right]. \quad (\text{A12})$$

In the above, the extra term:

$$\Delta T_{\mu\nu}^{(\text{coupl})} = \frac{2}{f(\phi)} \left[\nabla_\mu \nabla_\nu f(\phi) - g_{\mu\nu} \square f(\phi) \right] \quad (\text{A13})$$

contains all contributions originating from the ϕ -dependence of the conformal factor.

c. Exponential coupling For:

$$f(\phi) = e^{\beta\phi}, \quad (\text{A14})$$

we have:

$$\nabla_\mu f(\phi) = \beta e^{\beta\phi} \nabla_\mu \phi, \quad (\text{A15})$$

and:

$$\nabla_\mu \nabla_\nu f(\phi) = \beta e^{\beta\phi} \nabla_\mu \nabla_\nu \phi + \beta^2 e^{\beta\phi} \nabla_\mu \phi \nabla_\nu \phi. \quad (\text{A16})$$

Similarly, using the definition of the d'Alembertian one obtains:

$$\square f(\phi) = \beta e^{\beta\phi} \square \phi + \beta^2 e^{\beta\phi} (\nabla \phi)^2. \quad (\text{A17})$$

Substituting these results into (A13) we obtain:

$$\begin{aligned} \Delta T_{\mu\nu}^{(\text{coupl})} &= \frac{2}{e^{\beta\phi}} \left[\beta e^{\beta\phi} \nabla_\mu \nabla_\nu \phi + \beta^2 e^{\beta\phi} \nabla_\mu \phi \nabla_\nu \phi \right. \\ &\quad \left. - g_{\mu\nu} \left(\beta e^{\beta\phi} \square \phi + \beta^2 e^{\beta\phi} (\nabla \phi)^2 \right) \right] \\ &= 2\beta \left[\nabla_\mu \nabla_\nu \phi - g_{\mu\nu} \square \phi \right] \\ &\quad + 2\beta^2 \left[\nabla_\mu \phi \nabla_\nu \phi - g_{\mu\nu} (\nabla \phi)^2 \right]. \end{aligned} \quad (\text{A18})$$

d. Final result Thus, by collecting the standard scalar field contribution and the modified matter term we can write the complete effective stress-energy tensor as:

$$\begin{aligned} T_{\mu\nu}^{(\text{eff})} &= T_{\mu\nu}^{(\phi)} + e^{-2\beta\phi} T_{\mu\nu}^{(m)} \\ &\quad + 2\beta \left[\nabla_\mu \nabla_\nu \phi - g_{\mu\nu} \square \phi \right] \\ &\quad + 2\beta^2 \left[\nabla_\mu \phi \nabla_\nu \phi - g_{\mu\nu} (\nabla \phi)^2 \right], \end{aligned} \quad (\text{A19})$$

where:

$$T_{\mu\nu}^{(\phi)} = \nabla_\mu \phi \nabla_\nu \phi - \frac{1}{2} g_{\mu\nu} \left[(\nabla \phi)^2 + \mathcal{V}(\phi) \right]. \quad (\text{A20})$$

The extra terms:

$$\begin{aligned} \Delta T_{\mu\nu}^{(\text{coupl})} = & 2\beta \left[\nabla_\mu \nabla_\nu \phi - g_{\mu\nu} \square \phi \right] \\ & + 2\beta^2 \left[\nabla_\mu \phi \nabla_\nu \phi - g_{\mu\nu} (\nabla \phi)^2 \right], \end{aligned} \quad (\text{A21})$$

are exactly the coupling contributions generated by the ϕ -dependence of the conformal factor.

Appendix B: Tables with detailed characteristics of cosmological dynamical systems

TABLE I: Fixed points of the dynamical system for NMC ALPs/axions SF.^a

Point	Eigenvalues	Eigenvectors	Existence	Stability	Epoch
\mathcal{A}	$\{2, -1, 1, 0\}$	$\left\{ \begin{pmatrix} 0 \\ 1 \\ 0 \\ 0 \end{pmatrix}, \begin{pmatrix} \frac{\sqrt{\frac{2}{3}}}{1-3\lambda_\phi^2} \\ 0 \\ 1 \\ 0 \end{pmatrix}, \begin{pmatrix} \frac{1}{2}\sqrt{\frac{3}{2}}\beta \\ 0 \\ \frac{3}{4}\beta(3\lambda_\phi^2-1) \\ 1 \end{pmatrix}, \begin{pmatrix} 0 \\ 0 \\ 1 \\ 0 \end{pmatrix} \right\}$	Always	Saddle	R
\mathcal{B}	$\{-3\sqrt{2}, 3 + \frac{1}{\sqrt{2}}, 2, 3 - \sqrt{6}\beta\}$	$\left\{ \begin{pmatrix} 0 \\ 0 \\ 1 \\ 0 \end{pmatrix}, \begin{pmatrix} 0 \\ 1 \\ 0 \\ 0 \end{pmatrix}, \begin{pmatrix} \frac{1}{2} \\ 0 \\ 0 \\ 1 \end{pmatrix}, \begin{pmatrix} 1 \\ 0 \\ 0 \\ 0 \end{pmatrix} \right\}$	$\beta \neq \sqrt{\frac{3}{2}}$	Saddle	SM
\mathcal{C}	$\{-4, -3, -\frac{3}{2} + i\frac{\sqrt{3}}{2}, -\frac{3}{2} - i\frac{\sqrt{3}}{2}\}$	$\left\{ \begin{pmatrix} 0 \\ 1 \\ 0 \\ 0 \end{pmatrix}, \begin{pmatrix} 1 \\ 0 \\ 0 \\ 0 \end{pmatrix}, \begin{pmatrix} \frac{1}{2}\sqrt{\frac{3}{2}}\beta \\ 0 \\ 0 \\ 1 \end{pmatrix}, \begin{pmatrix} 0 \\ 0 \\ 1 \\ 0 \end{pmatrix} \right\}$	Always	Stable	DE
\mathcal{D}	$\{3\sqrt{2}, 3 - \frac{1}{\sqrt{2}}, 2, 3 + \sqrt{6}\beta\}$	$\left\{ \begin{pmatrix} 0 \\ 0 \\ 1 \\ 0 \end{pmatrix}, \begin{pmatrix} 0 \\ 1 \\ 0 \\ 0 \end{pmatrix}, \begin{pmatrix} -\frac{1}{2} \\ 0 \\ 0 \\ 1 \end{pmatrix}, \begin{pmatrix} 1 \\ 0 \\ 0 \\ 0 \end{pmatrix} \right\}$	$\beta > -\sqrt{\frac{3}{2}}$ \vee $\beta < -\sqrt{\frac{3}{2}}$	Unstable \vee Saddle	SM
\mathcal{E}	$\{-4, -3, -\frac{3}{2} + i\frac{\sqrt{3}}{2}, -\frac{3}{2} - i\frac{\sqrt{3}}{2}\}$	$\left\{ \begin{pmatrix} 0 \\ 1 \\ 0 \\ 0 \end{pmatrix}, \begin{pmatrix} 1 \\ 0 \\ 0 \\ 0 \end{pmatrix}, \begin{pmatrix} \frac{1}{2}\sqrt{\frac{3}{2}}\beta \\ 0 \\ 0 \\ 1 \end{pmatrix}, \begin{pmatrix} 0 \\ 0 \\ 1 \\ 0 \end{pmatrix} \right\}$	$-\sqrt{\frac{2}{3}} \leq \beta < -\frac{1}{\sqrt{2}}$ \vee $-\frac{1}{\sqrt{2}} \leq \beta < -\frac{1}{\sqrt{3}}$ \vee $\frac{1}{\sqrt{3}} \leq \beta < \frac{1}{\sqrt{2}}$ \vee $\frac{1}{\sqrt{2}} < \beta \leq \sqrt{\frac{2}{3}}$	Saddle	R
\mathcal{F}	$\left\{ -2\sqrt{3}\beta, -\frac{3}{2} + \beta^2, -1 + 2\beta^2, \frac{3}{2} + \frac{\beta}{\sqrt{3}} + \beta^2 \right\}$	$\left\{ \begin{pmatrix} 0 \\ 1 \\ 0 \\ 0 \end{pmatrix}, \begin{pmatrix} 1 \\ 0 \\ 0 \\ 0 \end{pmatrix}, \begin{pmatrix} \frac{1}{2}\sqrt{\frac{3}{2}}\beta \\ 0 \\ 0 \\ 1 \end{pmatrix}, \begin{pmatrix} 0 \\ 0 \\ 1 \\ 0 \end{pmatrix} \right\}$	$-\sqrt{\frac{2}{3}} \leq \beta < -\frac{1}{\sqrt{2}}$ \vee $-\frac{1}{\sqrt{2}} \leq \beta < -\frac{1}{\sqrt{3}}$ \vee $\frac{1}{\sqrt{3}} \leq \beta < \frac{1}{\sqrt{2}}$ \vee $\frac{1}{\sqrt{2}} < \beta \leq \sqrt{\frac{2}{3}}$	Saddle	M(β)

^a The study is concerned solely with points for which the analytical form of eigenvectors and eigenvalues can be found. The abbreviations stand for: R - radiation, SM - stiff matter, DE - dark energy, M(β) - matter (β -dependent).

TABLE II: Detailed characterization of critical points for NMC ALPs/axions SF.

Point	x	y	λ_ϕ	Ω_r	ω_{eff}	Accelerated expansion	Ω_ϕ	ω_ϕ	Ω_b
\mathcal{A}	0	0	λ_ϕ	1	$\frac{1}{3}$	No	0	—	0
\mathcal{B}	-1	0	$\frac{1}{\sqrt{3}}$	0	1	No	1	1	0
\mathcal{C}	0	1	0	0	-1	Yes	1	-1	0
\mathcal{D}	1	0	$\frac{1}{\sqrt{3}}$	0	1	No	1	1	0
\mathcal{E}	$-\frac{1}{\sqrt{6}\beta}$	0	$\frac{1}{\sqrt{3}}$	$1 - \frac{1}{2\beta^2}$	$\frac{1}{3}$	No	$\frac{1}{6\beta^2}$	1	$\frac{1}{3\beta^2}$
\mathcal{F}	$-\sqrt{\frac{2}{3}}\beta$	0	$\frac{1}{\sqrt{3}}$	0	$\frac{2}{3}\beta^2$	No	$\frac{2}{3}\beta^2$	1	$1 - \frac{2}{3}\beta^2$

TABLE III: Fixed points of the dynamical system for NMC cyclic ekpyrotic SF.^a

Point	Eigenvalues	Eigenvectors	Stability	Epoch
\mathcal{A}	$\{2, -1, 1, 0\}$	$\left\{ \begin{pmatrix} 0 \\ 1 \\ 0 \\ 0 \end{pmatrix}, \begin{pmatrix} \frac{1}{\sqrt{6}(c-\lambda_\phi)(b+\lambda_\phi)} \\ 0 \\ 1 \\ 0 \end{pmatrix}, \begin{pmatrix} \frac{1}{2}\sqrt{\frac{3}{2}}\beta \\ 0 \\ -\frac{3}{2}\beta(c-\lambda_\phi)(b+\lambda_\phi) \\ 1 \end{pmatrix}, \begin{pmatrix} 0 \\ 0 \\ 1 \\ 0 \end{pmatrix} \right\}$	Saddle	R
\mathcal{B}	$\{2, -1, 1, 0\}$	$\left\{ \begin{pmatrix} 0 \\ 1 \\ 0 \\ 0 \end{pmatrix}, \begin{pmatrix} 1 \\ 0 \\ 0 \\ 0 \end{pmatrix}, \begin{pmatrix} \frac{1}{2}\sqrt{\frac{3}{2}}\beta \\ 0 \\ 0 \\ 1 \end{pmatrix}, \begin{pmatrix} 0 \\ 0 \\ 1 \\ 0 \end{pmatrix} \right\}$	Saddle	R
\mathcal{C}	$\{2, -1, 1, 0\}$	$\left\{ \begin{pmatrix} 0 \\ 1 \\ 0 \\ 0 \end{pmatrix}, \begin{pmatrix} 1 \\ 0 \\ 0 \\ 0 \end{pmatrix}, \begin{pmatrix} \frac{1}{2}\sqrt{\frac{3}{2}}\beta \\ 0 \\ 0 \\ 1 \end{pmatrix}, \begin{pmatrix} 0 \\ 0 \\ 1 \\ 0 \end{pmatrix} \right\}$	Saddle	R
\mathcal{D}	$\left\{ -4, -3, \frac{1}{2}(-3 \mp \sqrt{9-24bc}) \right\}$	$\left\{ \begin{pmatrix} 0 \\ -\frac{1}{2} \\ 0 \\ 1 \end{pmatrix}, \begin{pmatrix} \frac{\sqrt{\frac{3}{2}}}{bc} \\ -\beta^{-1} \\ 1 \\ 0 \end{pmatrix}, \begin{pmatrix} \frac{\sqrt{6}+\sqrt{2}\sqrt{3-8bc}}{4bc} \\ 0 \\ 1 \\ 0 \end{pmatrix}, \begin{pmatrix} \frac{\sqrt{6}-\sqrt{6-16bc}}{4bc} \\ 0 \\ 1 \\ 0 \end{pmatrix} \right\}$	Stable ∨ Saddle	DE
\mathcal{E}	$\left\{ 2, 3 + \sqrt{\frac{3}{2}}b, -\sqrt{6}(b+c), 3 + \sqrt{6}\beta \right\}$	$\left\{ \begin{pmatrix} -\frac{1}{2} \\ 0 \\ 0 \\ 1 \end{pmatrix}, \begin{pmatrix} 0 \\ 1 \\ 0 \\ 0 \end{pmatrix}, \begin{pmatrix} 0 \\ 0 \\ 1 \\ 0 \end{pmatrix}, \begin{pmatrix} 1 \\ 0 \\ 0 \\ 0 \end{pmatrix} \right\}$	Unstable ∨ Saddle	SM
\mathcal{F}	$\left\{ 2, \sqrt{6}(b+c), 3 - \sqrt{\frac{3}{2}}c, 3 + \sqrt{6}\beta \right\}$	$\left\{ \begin{pmatrix} -\frac{1}{2} \\ 0 \\ 0 \\ 1 \end{pmatrix}, \begin{pmatrix} 0 \\ 0 \\ 1 \\ 0 \end{pmatrix}, \begin{pmatrix} 0 \\ 1 \\ 0 \\ 0 \end{pmatrix}, \begin{pmatrix} 1 \\ 0 \\ 0 \\ 0 \end{pmatrix} \right\}$	Unstable ∨ Saddle	SM
\mathcal{G}	$\left\{ \frac{b+c}{\beta}, 2 - \frac{b}{2\beta}, -\frac{1}{2} \mp \frac{\sqrt{2\beta^4-3\beta^6}}{2\beta^3} \right\}$	$\left\{ \begin{pmatrix} 0 \\ 0 \\ 1 \\ 0 \end{pmatrix}, \begin{pmatrix} 0 \\ 1 \\ 0 \\ 0 \end{pmatrix}, \begin{pmatrix} -\frac{\beta-3\beta^3+\sqrt{2\beta^4-3\beta^6}}{\sqrt{6}(2\beta^2-1)} \\ 0 \\ 0 \\ 1 \end{pmatrix}, \begin{pmatrix} \frac{-\beta+3\beta^3+\sqrt{2\beta^4-3\beta^6}}{\sqrt{6}(2\beta^2-1)} \\ 0 \\ 0 \\ 1 \end{pmatrix} \right\}$	Stable ∨ Saddle	R
\mathcal{H}	$\left\{ -\frac{b+c}{\beta}, 2 + \frac{c}{2\beta}, -\frac{1}{2} \mp \frac{\sqrt{2\beta^4-3\beta^6}}{2\beta^3} \right\}$	$\left\{ \begin{pmatrix} 0 \\ 0 \\ 1 \\ 0 \end{pmatrix}, \begin{pmatrix} 0 \\ 1 \\ 0 \\ 0 \end{pmatrix}, \begin{pmatrix} -\frac{\beta-3\beta^3+\sqrt{2\beta^4-3\beta^6}}{\sqrt{6}(2\beta^2-1)} \\ 0 \\ 0 \\ 1 \end{pmatrix}, \begin{pmatrix} \frac{-\beta+3\beta^3+\sqrt{2\beta^4-3\beta^6}}{\sqrt{6}(2\beta^2-1)} \\ 0 \\ 0 \\ 1 \end{pmatrix} \right\}$	Stable ∨ Saddle	R
\mathcal{I}	$\left\{ 2\beta(b+c), \frac{3}{2} + \beta(\beta-b), -\frac{3}{2} + \beta^2, -1 + 2\beta^2 \right\}$	$\left\{ \begin{pmatrix} 0 \\ 0 \\ 1 \\ 0 \end{pmatrix}, \begin{pmatrix} 0 \\ 1 \\ 0 \\ 0 \end{pmatrix}, \begin{pmatrix} 1 \\ 0 \\ 0 \\ 0 \end{pmatrix}, \begin{pmatrix} \frac{2\sqrt{\frac{3}{2}}\beta}{1+2\beta^2} \\ 0 \\ 0 \\ 1 \end{pmatrix} \right\}$	Stable ∨ Saddle	M(β)
\mathcal{J}	$\left\{ -2\beta(b+c), -\frac{3}{2} + \beta^2, -1 + 2\beta^2, \frac{3}{2} + \beta(\beta+c) \right\}$	$\left\{ \begin{pmatrix} 0 \\ 0 \\ 1 \\ 0 \end{pmatrix}, \begin{pmatrix} 1 \\ 0 \\ 0 \\ 0 \end{pmatrix}, \begin{pmatrix} \frac{2\sqrt{\frac{3}{2}}\beta}{1+2\beta^2} \\ 0 \\ 0 \\ 1 \end{pmatrix}, \begin{pmatrix} 0 \\ 1 \\ 0 \\ 0 \end{pmatrix} \right\}$	Stable ∨ Saddle	M(β)

^a The study is concerned solely with points for which the analytical form of eigenvectors and eigenvalues can be found. The abbreviations stand for: R - radiation, SM - stiff matter, DE - dark energy, M(β) - matter (β -dependent).

TABLE IV: Existence of the fixed points of the dynamical system for NMC cyclic ekpyrotic SF.

Point	Existence
\mathcal{A}	Always
\mathcal{B}	Always
\mathcal{C}	Always
\mathcal{D}	$\left(\begin{cases} c < 0 \\ \frac{3}{8c} \leq b < 0 \end{cases} \vee \begin{cases} c > 0 \\ 0 < b \leq \frac{3}{8c} \end{cases} \right) \vee \left(\begin{cases} c < 0 \\ b > 0 \end{cases} \vee \begin{cases} c > 0 \\ b < 0 \end{cases} \right)$
\mathcal{E}	$\left(\begin{cases} \beta > -\sqrt{\frac{3}{2}} \\ b > -\sqrt{6} \\ c > -b \end{cases} \right) \vee \left(\begin{cases} (b + \sqrt{6})(b + c) \neq 0 \\ \beta < -\sqrt{\frac{3}{2}} \end{cases} \vee \begin{cases} \beta \neq -\sqrt{\frac{3}{2}} \\ b \neq -\sqrt{6} \\ c > -b \end{cases} \right)$
\mathcal{F}	$\left(\begin{cases} \beta > -\sqrt{\frac{3}{2}} \\ b > -c \\ c < \sqrt{6} \end{cases} \right) \vee \left(\left(\beta \neq -\sqrt{\frac{3}{2}} \wedge \left[\begin{cases} b = -\sqrt{6} \\ c \neq \sqrt{6} \end{cases} \vee \begin{cases} b < -\sqrt{6} \\ c < \sqrt{6} \end{cases} \vee \begin{cases} b < -c \\ c > \sqrt{6} \end{cases} \vee \begin{cases} b < -\sqrt{6} \\ c > -b \end{cases} \right] \right) \vee \begin{cases} \beta < -\sqrt{\frac{3}{2}} \\ b > -c \\ c < \sqrt{6} \end{cases} \right)$
\mathcal{G}	$\left(\begin{cases} -\sqrt{\frac{2}{3}} \leq \beta < -\frac{1}{\sqrt{2}} \\ b < 4\beta \\ c > -b \end{cases} \vee \begin{cases} \frac{1}{\sqrt{2}} < \beta \leq \sqrt{\frac{2}{3}} \\ b > 4\beta \\ c < -b \end{cases} \right) \vee \left(\begin{cases} -\sqrt{\frac{2}{3}} \leq \beta < -\frac{1}{\sqrt{2}} \\ (b < 4\beta \wedge c < -b) \vee (b > 4\beta \wedge (c < -b \vee c > -b)) \end{cases} \vee \begin{cases} \frac{1}{\sqrt{2}} < \beta \leq \sqrt{\frac{2}{3}} \\ b > 4\beta \\ c > -b \end{cases} \right)$
\mathcal{H}	$\left(\begin{cases} -\sqrt{\frac{2}{3}} \leq \beta < -\frac{1}{\sqrt{2}} \\ b < -c \\ c > -4\beta \end{cases} \vee \begin{cases} \frac{1}{\sqrt{2}} < \beta \leq \sqrt{\frac{2}{3}} \\ b > -c \\ c < -4\beta \end{cases} \right) \vee \left(\begin{cases} -\sqrt{\frac{2}{3}} \leq \beta < -\frac{1}{\sqrt{2}} \\ (c < -4\beta \wedge (b < 4\beta \vee 4\beta < b < -c \vee b > -c)) \vee (c > -4\beta \wedge (-c < b < 4\beta \vee b > 4\beta)) \end{cases} \vee \begin{cases} -\frac{1}{\sqrt{2}} < \beta \leq -\frac{1}{\sqrt{3}} \\ (c < -4\beta \wedge (b < 4\beta \vee 4\beta < b < -c \vee b > -c)) \vee (c > -4\beta \wedge (b < -c \vee -c < b < 4\beta \vee b > 4\beta)) \end{cases} \vee \begin{cases} \frac{1}{\sqrt{3}} \leq \beta < \frac{1}{\sqrt{2}} \\ (c < -4\beta \wedge (b < 4\beta \vee 4\beta < b < -c \vee b > -c)) \vee (c > -4\beta \wedge (b < -c \vee -c < b < 4\beta \vee b > 4\beta)) \end{cases} \vee \begin{cases} \frac{1}{\sqrt{2}} < \beta \leq \sqrt{\frac{2}{3}} \\ (c < -4\beta \wedge (b < 4\beta \vee 4\beta < b < -c)) \vee (c > -4\beta \wedge (b < -c \vee -c < b < 4\beta \vee b > 4\beta)) \end{cases} \right)$
\mathcal{I}	$\left(\begin{cases} -\frac{1}{\sqrt{2}} < \beta < 0 \\ b < \frac{3+2\beta^2}{2\beta} \\ c > -b \end{cases} \vee \begin{cases} 0 < \beta < \frac{1}{\sqrt{2}} \\ b > \frac{3+2\beta^2}{2\beta} \\ c < -b \end{cases} \right) \vee \left(\begin{cases} -\frac{1}{\sqrt{2}} < \beta < 0 \\ b \neq \frac{3+2\beta^2}{2\beta} \\ c < -b \end{cases} \vee \begin{cases} 0 < \beta < \frac{1}{\sqrt{2}} \\ b \neq \frac{3+2\beta^2}{2\beta} \\ c > -b \end{cases} \right)$

TABLE IV: Existence of the fixed points of the dynamical system for NMC cyclic ekpyrotic SF.

$$\begin{array}{c}
\left(\begin{array}{l} -\frac{1}{\sqrt{2}} < \beta < 0 \\ b < -c \\ c > \frac{-3-2\beta^2}{2\beta} \end{array} \vee \begin{array}{l} 0 < \beta < \frac{1}{\sqrt{2}} \\ b > -c \\ c < \frac{-3-2\beta^2}{2\beta} \end{array} \right) \vee \left(\begin{array}{l} -\sqrt{\frac{3}{2}} < \beta < -\frac{1}{\sqrt{2}} \\ c < \frac{-3-2\beta^2}{2\beta} \wedge \left(b < \frac{3+2\beta^2}{2\beta} \vee \frac{3+2\beta^2}{2\beta} < b < -c \vee b > -c \right) \end{array} \right) \vee \\
\left(\begin{array}{l} -\sqrt{\frac{3}{2}} < \beta < -\frac{1}{\sqrt{2}} \\ c > \frac{-3-2\beta^2}{2\beta} \wedge \left(b < -c \vee -c < b < \frac{3+2\beta^2}{2\beta} \vee b > \frac{3+2\beta^2}{2\beta} \right) \end{array} \right) \vee \\
\left(\begin{array}{l} -\frac{1}{\sqrt{2}} < \beta < 0 \\ c < \frac{-3-2\beta^2}{2\beta} \wedge \left(b < \frac{3+2\beta^2}{2\beta} \vee \frac{3+2\beta^2}{2\beta} < b < -c \vee b > -c \right) \end{array} \right) \vee \\
\left(\begin{array}{l} -\frac{1}{\sqrt{2}} < \beta < 0 \\ c > \frac{-3-2\beta^2}{2\beta} \wedge \left(-c < b < \frac{3+2\beta^2}{2\beta} \vee b > \frac{3+2\beta^2}{2\beta} \right) \end{array} \right) \vee \left(\begin{array}{l} 0 < \beta < \frac{1}{\sqrt{2}} \\ c < \frac{-3-2\beta^2}{2\beta} \wedge \left(b < \frac{3+2\beta^2}{2\beta} \vee \frac{3+2\beta^2}{2\beta} < b < -c \right) \end{array} \right) \vee \\
\left(\begin{array}{l} 0 < \beta < \frac{1}{\sqrt{2}} \\ c > \frac{-3-2\beta^2}{2\beta} \wedge \left(b < -c \vee -c < b < \frac{3+2\beta^2}{2\beta} \vee b > \frac{3+2\beta^2}{2\beta} \right) \end{array} \right) \vee \\
\left(\begin{array}{l} \frac{1}{\sqrt{2}} < \beta < \sqrt{\frac{3}{2}} \\ c > \frac{-3-2\beta^2}{2\beta} \wedge \left(b < \frac{3+2\beta^2}{2\beta} \vee \frac{3+2\beta^2}{2\beta} < b < -c \vee b > -c \right) \end{array} \right) \vee \\
\left(\begin{array}{l} \frac{1}{\sqrt{2}} < \beta < \sqrt{\frac{3}{2}} \\ c > \frac{-3-2\beta^2}{2\beta} \wedge \left(b < -c \vee -c < b < \frac{3+2\beta^2}{2\beta} \vee b > \frac{3+2\beta^2}{2\beta} \right) \end{array} \right)
\end{array}$$

TABLE V: Detailed characterization of critical points for NMC cyclic ekpyrotic SF.

Point	x	y	λ_ϕ	Ω_r	ω_{eff}	Accelerated expansion	Ω_ϕ	ω_ϕ	Ω_b
\mathcal{A}	0	0	λ_ϕ	1	$\frac{1}{3}$	No	0	—	0
\mathcal{B}	0	0	$-b$	1	$\frac{1}{3}$	No	0	—	0
\mathcal{C}	0	0	c	1	$\frac{1}{3}$	No	0	—	0
\mathcal{D}	0	1	0	0	-1	Yes	1	-1	0
\mathcal{E}	1	0	$-b$	0	1	No	1	1	0
\mathcal{F}	1	0	c	0	1	No	1	1	0
\mathcal{G}	$-\frac{1}{\sqrt{6}\beta}$	0	$-b$	$1 - \frac{1}{2\beta^2}$	$\frac{1}{3}$	No	$\frac{1}{6\beta^2}$	1	$\frac{1}{3\beta^2}$
\mathcal{H}	$-\frac{1}{\sqrt{6}\beta}$	0	c	$1 - \frac{1}{2\beta^2}$	$\frac{1}{3}$	No	$\frac{1}{6\beta^2}$	1	$\frac{1}{3\beta^2}$
\mathcal{I}	$-\sqrt{\frac{2}{3}}\beta$	0	$-b$	0	$\frac{2}{3}\beta^2$	No	$\frac{2}{3}\beta^2$	1	$1 - \frac{2}{3}\beta^2$
\mathcal{J}	$-\sqrt{\frac{2}{3}}\beta$	0	c	0	$\frac{2}{3}\beta^2$	No	$\frac{2}{3}\beta^2$	1	$1 - \frac{2}{3}\beta^2$

TABLE VI: Fixed points of the dynamical system for NMC ekpyrotic/exponential SF with Λ .^a

Point	Eigenvalues	Eigenvectors	Stability	Epoch
\mathcal{A}	$\{2, -1, 1, 0\}$	$\left\{ \begin{pmatrix} 0 \\ 1 \\ 0 \\ 0 \end{pmatrix}, \begin{pmatrix} \frac{1}{\sqrt{6}(c-\lambda_\phi)\lambda_\phi} \\ 0 \\ 1 \\ 0 \end{pmatrix}, \begin{pmatrix} \frac{1}{2}\sqrt{\frac{3}{2}}\beta \\ 0 \\ \frac{3}{2}\beta\lambda_\phi(\lambda_\phi - c) \\ 1 \end{pmatrix}, \begin{pmatrix} 0 \\ 0 \\ 1 \\ 0 \end{pmatrix} \right\}$	Saddle	R
\mathcal{B}	$\{2, -1, 1, 0\}$	$\left\{ \begin{pmatrix} 0 \\ 1 \\ 0 \\ 0 \end{pmatrix}, \begin{pmatrix} 1 \\ 0 \\ 0 \\ 0 \end{pmatrix}, \begin{pmatrix} \frac{1}{2}\sqrt{\frac{3}{2}}\beta \\ 0 \\ 0 \\ 1 \end{pmatrix}, \begin{pmatrix} 0 \\ 0 \\ 1 \\ 0 \end{pmatrix} \right\}$	Saddle	R
\mathcal{C}	$\{2, -1, 1, 0\}$	$\left\{ \begin{pmatrix} 0 \\ 1 \\ 0 \\ 0 \end{pmatrix}, \begin{pmatrix} 1 \\ 0 \\ 0 \\ 0 \end{pmatrix}, \begin{pmatrix} \frac{1}{2}\sqrt{\frac{3}{2}}\beta \\ 0 \\ 0 \\ 1 \end{pmatrix}, \begin{pmatrix} 0 \\ 0 \\ 1 \\ 0 \end{pmatrix} \right\}$	Saddle	R
\mathcal{D}	$\{-4, -3, -3, 0\}$	$\left\{ \begin{pmatrix} 0 \\ -\frac{1}{2} \\ 0 \\ 1 \end{pmatrix}, \begin{pmatrix} 1 \\ 0 \\ 0 \\ 0 \end{pmatrix}, \begin{pmatrix} 0 \\ 0 \\ 0 \\ 0 \end{pmatrix}, \begin{pmatrix} \sqrt{\frac{2}{3}} \\ 0 \\ 1 \\ 0 \end{pmatrix} \right\}$	Asympt. stable ∨ Unstable	DE
\mathcal{E}	$\{3, 2, -\sqrt{6}c, 3 + \sqrt{6}\beta\}$	$\left\{ \begin{pmatrix} 0 \\ 1 \\ 0 \\ 0 \end{pmatrix}, \begin{pmatrix} -\frac{1}{2} \\ 0 \\ 0 \\ 1 \end{pmatrix}, \begin{pmatrix} 0 \\ 0 \\ 1 \\ 0 \end{pmatrix}, \begin{pmatrix} 1 \\ 0 \\ 0 \\ 0 \end{pmatrix} \right\}$	Unstable ∨ Saddle	SM
\mathcal{F}	$\left\{ 2, \sqrt{6}c, \right. \\ \left. 3 - \sqrt{\frac{3}{2}}c, 3 + \sqrt{6}\beta \right\}$	$\left\{ \begin{pmatrix} -\frac{1}{2} \\ 0 \\ 0 \\ 1 \end{pmatrix}, \begin{pmatrix} 0 \\ 0 \\ 1 \\ 0 \end{pmatrix}, \begin{pmatrix} 0 \\ 1 \\ 0 \\ 0 \end{pmatrix}, \begin{pmatrix} 1 \\ 0 \\ 0 \\ 0 \end{pmatrix} \right\}$	Unstable ∨ Saddle	SM
\mathcal{G}	$\left\{ \frac{c}{\beta}, 2, \right. \\ \left. -\frac{1}{2} \mp \frac{\sqrt{2\beta^4 - 3\beta^6}}{2\beta^3} \right\}$	$\left\{ \begin{pmatrix} 0 \\ 0 \\ 1 \\ 0 \end{pmatrix}, \begin{pmatrix} 0 \\ 1 \\ 0 \\ 0 \end{pmatrix}, \begin{pmatrix} -\frac{\beta - 3\beta^3 + \sqrt{2\beta^4 - 3\beta^6}}{\sqrt{6}(2\beta^2 - 1)} \\ 0 \\ 0 \\ 1 \end{pmatrix}, \begin{pmatrix} \frac{-\beta + 3\beta^3 + \sqrt{2\beta^4 - 3\beta^6}}{\sqrt{6}(2\beta^2 - 1)} \\ 0 \\ 0 \\ 1 \end{pmatrix} \right\}$	Saddle	R
\mathcal{H}	$\left\{ -\frac{c}{\beta}, 2 + \frac{c}{2\beta}, \right. \\ \left. -\frac{1}{2} \mp \frac{\sqrt{2\beta^4 - 3\beta^6}}{2\beta^3} \right\}$	$\left\{ \begin{pmatrix} 0 \\ 0 \\ 1 \\ 0 \end{pmatrix}, \begin{pmatrix} 0 \\ 1 \\ 0 \\ 0 \end{pmatrix}, \begin{pmatrix} -\frac{\beta - 3\beta^3 + \sqrt{2\beta^4 - 3\beta^6}}{\sqrt{6}(2\beta^2 - 1)} \\ 0 \\ 0 \\ 1 \end{pmatrix}, \begin{pmatrix} \frac{-\beta + 3\beta^3 + \sqrt{2\beta^4 - 3\beta^6}}{\sqrt{6}(2\beta^2 - 1)} \\ 0 \\ 0 \\ 1 \end{pmatrix} \right\}$	Saddle	R
\mathcal{I}	$\left\{ 2c\beta, -\frac{3}{2} + \beta^2, \right. \\ \left. -1 + 2\beta^2, \frac{3}{2} + \beta^2 \right\}$	$\left\{ \begin{pmatrix} 0 \\ 0 \\ 1 \\ 0 \end{pmatrix}, \begin{pmatrix} 1 \\ 0 \\ 0 \\ 0 \end{pmatrix}, \begin{pmatrix} \frac{2\sqrt{\frac{3}{2}}\beta}{1+2\beta^2} \\ 0 \\ 0 \\ 1 \end{pmatrix}, \begin{pmatrix} 0 \\ 1 \\ 0 \\ 0 \end{pmatrix} \right\}$	Saddle	M(β)
\mathcal{J}	$\left\{ -2c\beta, -\frac{3}{2} + \beta^2, \right. \\ \left. -1 + 2\beta^2, \frac{3}{2} + \beta(c + \beta) \right\}$	$\left\{ \begin{pmatrix} 0 \\ 0 \\ 1 \\ 0 \end{pmatrix}, \begin{pmatrix} 1 \\ 0 \\ 0 \\ 0 \end{pmatrix}, \begin{pmatrix} \frac{2\sqrt{\frac{3}{2}}\beta}{1+2\beta^2} \\ 0 \\ 0 \\ 1 \end{pmatrix}, \begin{pmatrix} 0 \\ 1 \\ 0 \\ 0 \end{pmatrix} \right\}$	Saddle	M(β)

^a The study is concerned solely with points for which the analytical form of eigenvectors and eigenvalues can be found. The abbreviations stand for: R - radiation, SM - stiff matter, DE - dark energy, M(β) - matter (β -dependent).

TABLE VII: Existence of the fixed points of the dynamical system for NMC ekpyrotic/exponential SF with Λ .

Point	Existence	Stability
\mathcal{A}	Always	Saddle
\mathcal{B}	Always	Saddle
\mathcal{C}	Always	Saddle
\mathcal{D}	$\beta < 0$ \vee $\beta > 0$	Asympt. stable \vee Unstable
\mathcal{E}	$\left(\begin{cases} \beta > -\sqrt{\frac{3}{2}} \\ c < 0 \end{cases} \right) \vee \left(\begin{cases} \beta < -\sqrt{\frac{3}{2}} \\ c \neq 0 \end{cases} \vee \begin{cases} \beta > -\sqrt{\frac{3}{2}} \\ c > 0 \end{cases} \right)$	Unstable \vee Saddle
\mathcal{F}	$\left(\begin{cases} \beta > -\sqrt{\frac{3}{2}} \\ 0 < c < \sqrt{6} \end{cases} \right) \vee \left(\begin{cases} \beta < -\sqrt{\frac{3}{2}} \\ c < 0 \vee 0 < c < \sqrt{6} \vee c > \sqrt{6} \end{cases} \vee \begin{cases} \beta > -\sqrt{\frac{3}{2}} \\ c < 0 \vee c > \sqrt{6} \end{cases} \right)$	Unstable \vee Saddle
\mathcal{G}	$c \neq 0 \wedge \left(-\sqrt{\frac{2}{3}} \leq \beta < -\frac{1}{\sqrt{2}} \vee -\frac{1}{\sqrt{2}} < \beta \leq -\frac{1}{\sqrt{3}} \vee \frac{1}{\sqrt{3}} \leq \beta < \frac{1}{\sqrt{2}} \vee \frac{1}{\sqrt{2}} < \beta \leq \sqrt{\frac{2}{3}} \right)$	Saddle
\mathcal{H}	$\begin{cases} -\sqrt{\frac{2}{3}} \leq \beta < -\frac{1}{\sqrt{2}} \vee -\frac{1}{\sqrt{2}} < \beta \leq -\frac{1}{\sqrt{3}} \\ c < 0 \vee 0 < c < -4\beta \vee c > -4\beta \end{cases} \vee \begin{cases} \frac{1}{\sqrt{3}} \leq \beta < \frac{1}{\sqrt{2}} \vee \frac{1}{\sqrt{2}} < \beta \leq \sqrt{\frac{2}{3}} \\ c < -4\beta \vee -4\beta < c < 0 \vee c > 0 \end{cases}$	Saddle
\mathcal{I}	$c \neq 0 \wedge \left(-\sqrt{\frac{3}{2}} < \beta < -\frac{1}{\sqrt{2}} \vee -\frac{1}{\sqrt{2}} < \beta < 0 \vee 0 < \beta < \frac{1}{\sqrt{2}} \vee \frac{1}{\sqrt{2}} < \beta < \sqrt{\frac{3}{2}} \right)$	Saddle
\mathcal{J}	$\begin{cases} -\sqrt{\frac{3}{2}} < \beta < -\frac{1}{\sqrt{2}} \vee -\frac{1}{\sqrt{2}} < \beta < 0 \\ c < 0 \vee 0 < c < \frac{-3-2\beta^2}{2\beta} \vee c > \frac{-3-2\beta^2}{2\beta} \end{cases} \vee \begin{cases} 0 < \beta < \frac{1}{\sqrt{2}} \vee \frac{1}{\sqrt{2}} < \beta < \sqrt{\frac{3}{2}} \\ c < \frac{-3-2\beta^2}{2\beta} \vee \frac{-3-2\beta^2}{2\beta} < c < 0 \vee c > 0 \end{cases}$	Saddle

TABLE VIII: Detailed characterization of critical points for NMC ekpyrotic/exponential SF with Λ .

Point	x	y	λ_ϕ	Ω_r	ω_{eff}	Accelerated expansion	Ω_ϕ	ω_ϕ	Ω_b
\mathcal{A}	0	0	λ_ϕ	1	$\frac{1}{3}$	No	0	—	0
\mathcal{B}	0	0	0	1	$\frac{1}{3}$	No	0	—	0
\mathcal{C}	0	0	c	1	$\frac{1}{3}$	No	0	—	0
\mathcal{D}	0	1	0	0	-1	Yes	1	-1	0
\mathcal{E}	1	0	0	0	1	No	1	1	0
\mathcal{F}	1	0	c	0	1	No	1	1	0
\mathcal{G}	$-\frac{1}{\sqrt{6}\beta}$	0	0	$1 - \frac{1}{2\beta^2}$	$\frac{1}{3}$	No	$\frac{1}{6\beta^2}$	1	$\frac{1}{3\beta^2}$
\mathcal{H}	$-\frac{1}{\sqrt{6}\beta}$	0	c	$1 - \frac{1}{2\beta^2}$	$\frac{1}{3}$	No	$\frac{1}{6\beta^2}$	1	$\frac{1}{3\beta^2}$
\mathcal{I}	$-\sqrt{\frac{2}{3}}\beta$	0	0	0	$\frac{2}{3}\beta^2$	No	$\frac{2}{3}\beta^2$	1	$1 - \frac{2}{3}\beta^2$
\mathcal{J}	$-\sqrt{\frac{2}{3}}\beta$	0	c	0	$\frac{2}{3}\beta^2$	No	$\frac{2}{3}\beta^2$	1	$1 - \frac{2}{3}\beta^2$

TABLE IX: Fixed points of the dynamical system for NMC quintessence.^a

Point	Eigenvalues	Eigenvectors	Stability	Epoch
\mathcal{A}	$\{0, -1, 1, 2\}$	$\left\{ \begin{pmatrix} 0 \\ 0 \\ 1 \\ 0 \end{pmatrix}, \begin{pmatrix} \frac{n}{\sqrt{6}(\lambda_\phi^2 - n^2\lambda^2)} \\ 0 \\ 1 \\ 0 \end{pmatrix}, \begin{pmatrix} \frac{1}{2}\sqrt{\frac{3}{2}}\beta \\ 0 \\ \frac{3\beta(\lambda_\phi^2 - n^2\lambda^2)}{2n} \\ 1 \end{pmatrix}, \begin{pmatrix} 0 \\ 1 \\ 0 \\ 0 \end{pmatrix} \right\}$	Saddle	R
\mathcal{B}	$\{2, -1, 1, 0\}$	$\left\{ \begin{pmatrix} 0 \\ 1 \\ 0 \\ 0 \end{pmatrix}, \begin{pmatrix} 1 \\ 0 \\ 0 \\ 0 \end{pmatrix}, \begin{pmatrix} \frac{1}{2}\sqrt{\frac{3}{2}}\beta \\ 0 \\ 0 \\ 1 \end{pmatrix}, \begin{pmatrix} 0 \\ 0 \\ 1 \\ 0 \end{pmatrix} \right\}$	Saddle	R
\mathcal{C}	$\left\{ -4, -3, \frac{1}{2}(-3 \mp \sqrt{9 - 24n\lambda^2}) \right\}$	$\left\{ \begin{pmatrix} 0 \\ -\frac{1}{2} \\ 0 \\ 1 \end{pmatrix}, \begin{pmatrix} \frac{\sqrt{\frac{3}{2}}}{n\lambda^2} \\ -\beta^{-1} \\ 1 \\ 0 \end{pmatrix}, \begin{pmatrix} \frac{\sqrt{6} + \sqrt{2}\sqrt{3 - 8n\lambda^2}}{4n\lambda^2} \\ 0 \\ 1 \\ 0 \end{pmatrix}, \begin{pmatrix} \frac{\sqrt{6} - \sqrt{6 - 16n\lambda^2}}{4n\lambda^2} \\ 0 \\ 1 \\ 0 \end{pmatrix} \right\}$	Stable ∨ Saddle	DE
\mathcal{D}	$\left\{ 2, 3 + \sqrt{6}\beta, 2\sqrt{6}\lambda, 3 - \sqrt{\frac{3}{2}}n\lambda \right\}$	$\left\{ \begin{pmatrix} -\frac{1}{2} \\ 0 \\ 0 \\ 1 \end{pmatrix}, \begin{pmatrix} 1 \\ 0 \\ 0 \\ 0 \end{pmatrix}, \begin{pmatrix} 0 \\ 0 \\ 1 \\ 0 \end{pmatrix}, \begin{pmatrix} 0 \\ 1 \\ 0 \\ 0 \end{pmatrix} \right\}$	Unstable ∨ Saddle	SM
\mathcal{E}	$\left\{ -\frac{1}{2} \mp \frac{\sqrt{2\beta^4 - 3\beta^6}}{2\beta^3}, -\frac{2\lambda}{\beta}, 2 + \frac{n\lambda}{2\beta} \right\}$	$\left\{ \begin{pmatrix} -\frac{\beta - 3\beta^3 + \sqrt{2\beta^4 - 3\beta^6}}{\sqrt{6}(2\beta^2 - 1)} \\ 0 \\ 0 \\ 1 \end{pmatrix}, \begin{pmatrix} \frac{-\beta + 3\beta^3 + \sqrt{2\beta^4 - 3\beta^6}}{\sqrt{6}(2\beta^2 - 1)} \\ 0 \\ 0 \\ 1 \end{pmatrix}, \begin{pmatrix} 0 \\ 0 \\ 1 \\ 0 \end{pmatrix}, \begin{pmatrix} 0 \\ 1 \\ 0 \\ 0 \end{pmatrix} \right\}$	Stable ∨ Saddle	R
\mathcal{F}	$\left\{ -\frac{3}{2} + \beta^2, -1 + 2\beta^2, -4\beta\lambda, \frac{3}{2} + \beta^2 + n\beta\lambda \right\}$	$\left\{ \begin{pmatrix} 1 \\ 0 \\ 0 \\ 0 \end{pmatrix}, \begin{pmatrix} \frac{2\sqrt{\frac{3}{2}}\beta}{1 + 2\beta^2} \\ 0 \\ 0 \\ 1 \end{pmatrix}, \begin{pmatrix} 0 \\ 0 \\ 1 \\ 0 \end{pmatrix}, \begin{pmatrix} 0 \\ 1 \\ 0 \\ 0 \end{pmatrix} \right\}$	Stable ∨ Saddle	M(β)

^a The study is concerned solely with points for which the analytical form of eigenvectors and eigenvalues can be found. The abbreviations stand for: R - radiation, SM - stiff matter, DE - dark energy, M(β) - matter (β -dependent).

TABLE X: Existence of the fixed points of the dynamical system for NMC quintessence.

Point	Existence
\mathcal{A}	Always
\mathcal{B}	Always
\mathcal{C}	$\lambda \neq 0 \wedge [(0 < n \leq \frac{3}{8\lambda^2}) \vee (n < 0)]$
\mathcal{D}	$\left(\begin{array}{l} \beta > -\sqrt{\frac{3}{2}} \\ \lambda > 0 \\ n < \frac{\sqrt{6}}{\lambda} \end{array} \right) \vee \left(\begin{array}{l} \beta < -\sqrt{\frac{3}{2}} \\ \lambda < 0 \\ n < \frac{\sqrt{6}}{\lambda} \vee \frac{\sqrt{6}}{\lambda} < n < 0 \vee n > 0 \end{array} \right) \vee \left(\begin{array}{l} \beta < -\sqrt{\frac{3}{2}} \\ \lambda > 0 \\ n < 0 \vee 0 < n < \frac{\sqrt{6}}{\lambda} \vee n > \frac{\sqrt{6}}{\lambda} \end{array} \right) \vee$ $\left(\begin{array}{l} \beta > -\sqrt{\frac{3}{2}} \\ \lambda < 0 \\ n < \frac{\sqrt{6}}{\lambda} \vee \frac{\sqrt{6}}{\lambda} < n < 0 \vee n > 0 \end{array} \right) \vee \left(\begin{array}{l} \beta > -\sqrt{\frac{3}{2}} \\ \lambda > 0 \\ n > \frac{\sqrt{6}}{\lambda} \end{array} \right)$
\mathcal{E}	$\left(\begin{array}{l} -\sqrt{\frac{2}{3}} \leq \beta < -\frac{1}{\sqrt{2}} \\ n < 0 \\ \lambda < -\frac{4\beta}{n} \end{array} \right) \vee \left(\begin{array}{l} \frac{1}{\sqrt{2}} < \beta \leq \sqrt{\frac{2}{3}} \\ n < 0 \\ \lambda > -\frac{4\beta}{n} \end{array} \right) \vee \left(\begin{array}{l} -\sqrt{\frac{2}{3}} \leq \beta < -\frac{1}{\sqrt{2}} \\ \lambda < 0 \\ -\frac{4\beta}{\lambda} < n < 0 \vee n > 0 \end{array} \right) \vee \left(\begin{array}{l} -\sqrt{\frac{2}{3}} \leq \beta < -\frac{1}{\sqrt{2}} \\ \lambda > 0 \\ n < 0 \vee 0 < n < -\frac{4\beta}{\lambda} \vee n > -\frac{4\beta}{\lambda} \end{array} \right)$ $\vee \left(\begin{array}{l} -\frac{1}{\sqrt{2}} < \beta \leq -\frac{1}{\sqrt{3}} \\ \lambda < 0 \\ n < -\frac{4\beta}{\lambda} \vee -\frac{4\beta}{\lambda} < n < 0 \vee n > 0 \end{array} \right) \vee \left(\begin{array}{l} -\frac{1}{\sqrt{2}} < \beta \leq -\frac{1}{\sqrt{3}} \\ \lambda > 0 \\ n < 0 \vee 0 < n < -\frac{4\beta}{\lambda} \vee n > -\frac{4\beta}{\lambda} \end{array} \right) \vee \left(\begin{array}{l} \frac{1}{\sqrt{3}} \leq \beta < \frac{1}{\sqrt{2}} \\ \lambda < 0 \\ n < 0 \vee 0 < n < -\frac{4\beta}{\lambda} \vee n > -\frac{4\beta}{\lambda} \end{array} \right)$ $\vee \left(\begin{array}{l} \frac{1}{\sqrt{3}} \leq \beta < \frac{1}{\sqrt{2}} \\ \lambda > 0 \\ n < -\frac{4\beta}{\lambda} \vee -\frac{4\beta}{\lambda} < n < 0 \vee n > 0 \end{array} \right) \vee \left(\begin{array}{l} \frac{1}{\sqrt{2}} < \beta \leq \sqrt{\frac{2}{3}} \\ \lambda < 0 \\ n < 0 \vee 0 < n < -\frac{4\beta}{\lambda} \vee n > -\frac{4\beta}{\lambda} \end{array} \right) \vee \left(\begin{array}{l} \frac{1}{\sqrt{2}} < \beta \leq \sqrt{\frac{2}{3}} \\ \lambda > 0 \\ -\frac{4\beta}{\lambda} < n < 0 \vee n > 0 \end{array} \right)$
\mathcal{F}	$\left(\begin{array}{l} -\frac{1}{\sqrt{2}} < \beta < 0 \\ n < 0 \\ \lambda < \frac{-3-2\beta^2}{2n\beta} \end{array} \right) \vee \left(\begin{array}{l} 0 < \beta < \frac{1}{\sqrt{2}} \\ n < 0 \\ \lambda > \frac{-3-2\beta^2}{2n\beta} \end{array} \right) \vee \left(\begin{array}{l} -\sqrt{\frac{3}{2}} < \beta < -\frac{1}{\sqrt{2}} \\ \lambda < 0 \\ n < \frac{-3-2\beta^2}{2\beta\lambda} \vee \frac{-3-2\beta^2}{2\beta\lambda} < n < 0 \vee n > 0 \end{array} \right) \vee$ $\left(\begin{array}{l} -\sqrt{\frac{3}{2}} < \beta < -\frac{1}{\sqrt{2}} \\ \lambda > 0 \\ n < 0 \vee 0 < n < \frac{-3-2\beta^2}{2\beta\lambda} \vee n > \frac{-3-2\beta^2}{2\beta\lambda} \end{array} \right) \vee \left(\begin{array}{l} -\frac{1}{\sqrt{2}} < \beta < 0 \\ \lambda < 0 \\ \frac{-3-2\beta^2}{2\beta\lambda} < n < 0 \vee n > 0 \end{array} \right) \vee$ $\left(\begin{array}{l} -\frac{1}{\sqrt{2}} < \beta < 0 \\ \lambda > 0 \\ n < 0 \vee 0 < n < \frac{-3-2\beta^2}{2\beta\lambda} \vee n > \frac{-3-2\beta^2}{2\beta\lambda} \end{array} \right) \vee \left(\begin{array}{l} 0 < \beta < \frac{1}{\sqrt{2}} \\ \lambda < 0 \\ n < 0 \vee 0 < n < \frac{-3-2\beta^2}{2\beta\lambda} \vee n > \frac{-3-2\beta^2}{2\beta\lambda} \end{array} \right) \vee$ $\left(\begin{array}{l} 0 < \beta < \frac{1}{\sqrt{2}} \\ \lambda > 0 \\ \frac{-3-2\beta^2}{2\beta\lambda} < n < 0 \vee n > 0 \end{array} \right) \vee \left(\begin{array}{l} \frac{1}{\sqrt{2}} < \beta < \sqrt{\frac{3}{2}} \\ \lambda < 0 \\ n < 0 \vee 0 < n < \frac{-3-2\beta^2}{2\beta\lambda} \vee n > \frac{-3-2\beta^2}{2\beta\lambda} \end{array} \right) \vee$ $\left(\begin{array}{l} \frac{1}{\sqrt{2}} < \beta < \sqrt{\frac{3}{2}} \\ \lambda > 0 \\ n < \frac{-3-2\beta^2}{2\beta\lambda} \vee \frac{-3-2\beta^2}{2\beta\lambda} < 0 < n \vee n > 0 \end{array} \right)$

TABLE XI: Detailed characterization of critical points for NMC quintessence.

Point	x	y	λ_ϕ	Ω_r	ω_{eff}	Accelerated expansion	Ω_ϕ	ω_ϕ	Ω_b
\mathcal{A}	0	0	λ_ϕ	1	$\frac{1}{3}$	No	0	—	0
\mathcal{B}	0	0	$n\lambda$	1	$\frac{1}{3}$	No	0	—	0
\mathcal{C}	0	1	0	0	-1	Yes	1	-1	0
\mathcal{D}	1	0	$n\lambda$	0	1	No	1	1	0
\mathcal{E}	$-\frac{1}{\sqrt{6}\beta}$	0	$n\lambda$	$1 - \frac{1}{2\beta^2}$	$\frac{1}{3}$	No	$\frac{1}{6\beta^2}$	1	$\frac{1}{3\beta^2}$
\mathcal{F}	$-\sqrt{\frac{2}{3}}\beta$	0	$n\lambda$	0	$\frac{2}{3}\beta^2$	No	$\frac{2}{3}\beta^2$	1	$1 - \frac{2}{3}\beta^2$

TABLE XII: Fixed points of the dynamical system for NMC SFDM.^a

Point	Eigenvalues	Eigenvectors	Stability	Epoch
\mathcal{A}	$\{2, -1, 1, 0\}$	$\left\{ \begin{pmatrix} 0 \\ 1 \\ 0 \\ 0 \end{pmatrix}, \begin{pmatrix} \frac{\sqrt{\frac{2}{3}}}{\lambda^2 - \lambda_\phi^2} \\ 0 \\ 1 \\ 0 \end{pmatrix}, \begin{pmatrix} \frac{1}{2}\sqrt{\frac{3}{2}}\beta \\ 0 \\ \frac{3}{4}\beta(\lambda_\phi^2 - \lambda^2) \\ 1 \end{pmatrix}, \begin{pmatrix} 0 \\ 0 \\ 1 \\ 0 \end{pmatrix} \right\}$	Saddle	R
\mathcal{B}	$\{2, -1, 1, 0\}$	$\left\{ \begin{pmatrix} 0 \\ 1 \\ 0 \\ 0 \end{pmatrix}, \begin{pmatrix} 1 \\ 0 \\ 0 \\ 0 \end{pmatrix}, \begin{pmatrix} \frac{1}{2}\sqrt{\frac{3}{2}}\beta \\ 0 \\ 0 \\ 1 \end{pmatrix}, \begin{pmatrix} 0 \\ 0 \\ 1 \\ 0 \end{pmatrix} \right\}$	Saddle	R
\mathcal{C}	$\left\{ -4, -3, \frac{1}{2}(-3 \mp \sqrt{9 - 12\lambda^2}) \right\}$	$\left\{ \begin{pmatrix} 0 \\ -\frac{1}{2} \\ 0 \\ 1 \end{pmatrix}, \begin{pmatrix} \frac{\sqrt{6}}{\lambda^2} \\ -\beta^{-1} \\ 1 \\ 0 \end{pmatrix}, \begin{pmatrix} \frac{\sqrt{3} + \sqrt{3 - 4\lambda^2}}{\sqrt{2}\lambda^2} \\ 0 \\ 1 \\ 0 \end{pmatrix}, \begin{pmatrix} \frac{\sqrt{6} + \sqrt{6 - 8\lambda^2}}{2\lambda^2} \\ 0 \\ 1 \\ 0 \end{pmatrix} \right\}$	Stable	DE
\mathcal{D}	$\left\{ 2, 3 + \sqrt{6}\beta, \sqrt{6}\lambda, 3 - \sqrt{\frac{3}{2}}\lambda \right\}$	$\left\{ \begin{pmatrix} -\frac{1}{2} \\ 0 \\ 0 \\ 1 \end{pmatrix}, \begin{pmatrix} 1 \\ 0 \\ 0 \\ 0 \end{pmatrix}, \begin{pmatrix} 0 \\ 0 \\ 1 \\ 0 \end{pmatrix}, \begin{pmatrix} 0 \\ 1 \\ 0 \\ 0 \end{pmatrix} \right\}$	Unstable v Saddle	SM
\mathcal{E}	$\left\{ -\frac{1}{2} \mp \frac{\sqrt{2\beta^4 - 3\beta^6}}{2\beta^3}, -\frac{\lambda}{\beta}, 2 + \frac{\lambda}{2\beta} \right\}$	$\left\{ \begin{pmatrix} -\frac{\beta - 3\beta^3 + \sqrt{2\beta^4 - 3\beta^6}}{\sqrt{6}(2\beta^2 - 1)} \\ 0 \\ 0 \\ 1 \end{pmatrix}, \begin{pmatrix} -\beta + 3\beta^3 + \sqrt{2\beta^4 - 3\beta^6}}{\sqrt{6}(2\beta^2 - 1)} \\ 0 \\ 0 \\ 1 \end{pmatrix}, \begin{pmatrix} 0 \\ 0 \\ 1 \\ 0 \end{pmatrix}, \begin{pmatrix} 0 \\ 1 \\ 0 \\ 0 \end{pmatrix} \right\}$	Saddle	R
\mathcal{F}	$\left\{ -\frac{3}{2} + \beta^2, -1 + 2\beta^2, -2\beta\lambda, \frac{3}{2} + \beta(\beta + \lambda) \right\}$	$\left\{ \begin{pmatrix} 1 \\ 0 \\ 0 \\ 0 \end{pmatrix}, \begin{pmatrix} \frac{2\sqrt{\frac{2}{3}}\beta}{1 + 2\beta^2} \\ 0 \\ 0 \\ 1 \end{pmatrix}, \begin{pmatrix} 0 \\ 0 \\ 1 \\ 0 \end{pmatrix}, \begin{pmatrix} 0 \\ 1 \\ 0 \\ 0 \end{pmatrix} \right\}$	Saddle	M(β)

^a The study is concerned solely with points for which the analytical form of eigenvectors and eigenvalues can be found. The abbreviations stand for: R - radiation, SM - stiff matter, DE - dark energy, M(β) - matter (β -dependent).

TABLE XIII: Existence of the fixed points of the dynamical system for NMC SFDM.

Point	Existence	Stability
\mathcal{A}	Always	Saddle
\mathcal{B}	Always	Saddle
\mathcal{C}	$-\frac{\sqrt{3}}{2} \leq \lambda < 0 \vee 0 < \lambda \leq \frac{\sqrt{3}}{2}$	Stable
\mathcal{D}	$\left(\begin{cases} \beta > -\sqrt{\frac{3}{2}} \\ 0 < \lambda < \sqrt{6} \end{cases} \right) \vee \left(\begin{cases} \beta \neq -\sqrt{\frac{3}{2}} \\ \lambda < 0 \end{cases} \vee \begin{cases} \beta < -\sqrt{\frac{3}{2}} \\ 0 < \lambda < \sqrt{6} \end{cases} \vee \begin{cases} \beta \neq -\sqrt{\frac{3}{2}} \\ \lambda > \sqrt{6} \end{cases} \right)$	Unstable \vee Saddle
\mathcal{E}	$\left\{ -\sqrt{\frac{2}{3}} \leq \beta < -\frac{1}{\sqrt{2}} \vee -\frac{1}{\sqrt{2}} < \beta \leq -\frac{1}{\sqrt{3}} \vee \begin{cases} \frac{1}{\sqrt{3}} \leq \beta < \frac{1}{\sqrt{2}} \vee \frac{1}{\sqrt{2}} < \beta \leq \sqrt{\frac{2}{3}} \\ \lambda < -4\beta \vee -4\beta < \lambda < 0 \vee \lambda > 0 \end{cases} \right.$	Saddle
\mathcal{F}	$\left\{ -\sqrt{\frac{3}{2}} < \beta < -\frac{1}{\sqrt{2}} \vee -\frac{1}{\sqrt{2}} < \beta < 0 \vee \begin{cases} 0 < \beta < \frac{1}{\sqrt{2}} \vee \frac{1}{\sqrt{2}} < \beta < \sqrt{\frac{3}{2}} \\ \lambda < \frac{-3-2\beta^2}{2\beta} \vee \frac{-3-2\beta^2}{2\beta} < \lambda < 0 \vee \lambda > 0 \end{cases} \right.$	Saddle

TABLE XIV: Detailed characterization of critical points for NMC SFDM.

Point	x	y	λ_ϕ	Ω_r	ω_{eff}	Accelerated expansion	Ω_ϕ	ω_ϕ	Ω_b
\mathcal{A}	0	0	λ_ϕ	1	$\frac{1}{3}$	No	0	—	0
\mathcal{B}	0	0	λ	1	$\frac{1}{3}$	No	0	—	0
\mathcal{C}	0	1	0	0	-1	Yes	1	-1	0
\mathcal{D}	1	0	λ	0	1	No	1	1	0
\mathcal{E}	$-\frac{1}{\sqrt{6}\beta}$	0	λ	$1 - \frac{1}{2\beta^2}$	$\frac{1}{3}$	No	$\frac{1}{6\beta^2}$	1	$\frac{1}{3\beta^2}$
\mathcal{F}	$-\sqrt{\frac{2}{3}}\beta$	0	λ	0	$\frac{2}{3}\beta^2$	No	$\frac{2}{3}\beta^2$	1	$1 - \frac{2}{3}\beta^2$

Appendix C: Free parameters space diagrams - existence of the late-time acceleration

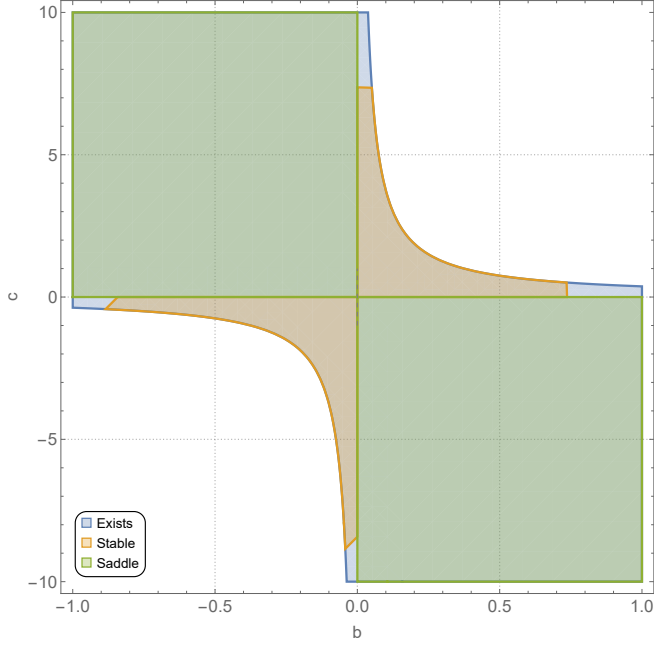


FIG. 1: Existence and character of the late-time acceleration (attractor) for the cyclic ekpyrotic NMC model. The free parameters space is spanned by the SF potential parameters b and c in (66).

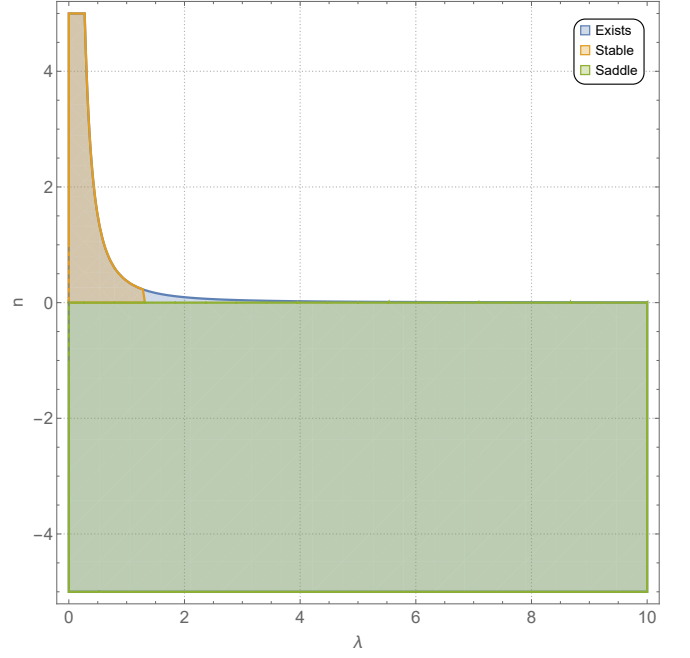


FIG. 2: Existence and character of the late-time acceleration (attractor) for the quintessence NMC model. The free parameters space is spanned by the SF potential parameters n and λ in (74).

Appendix D: 3D dynamical systems diagrams

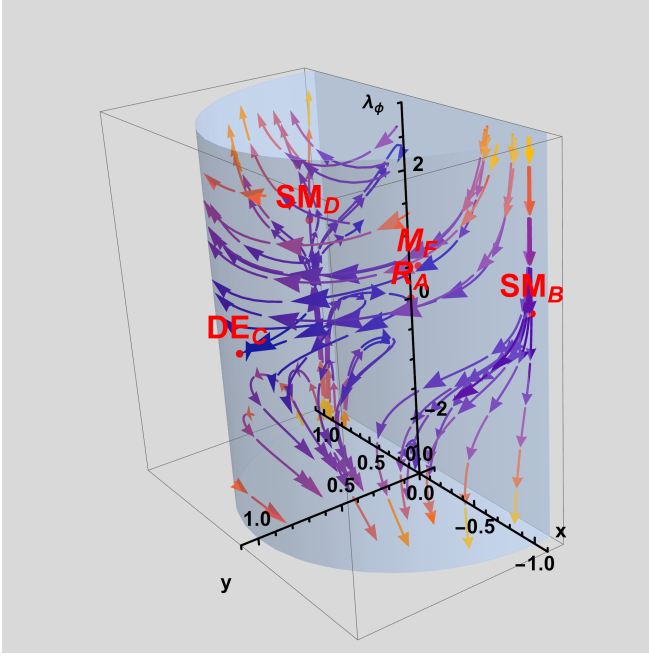


FIG. 3: 3D dynamical system diagram in the case of the NMC axions/ALPs model for $\beta = 10^{-1}$ and $\lambda_\phi = 0^a$.

^a The numerical value for λ_ϕ is only valid for the critical point \mathcal{A} .

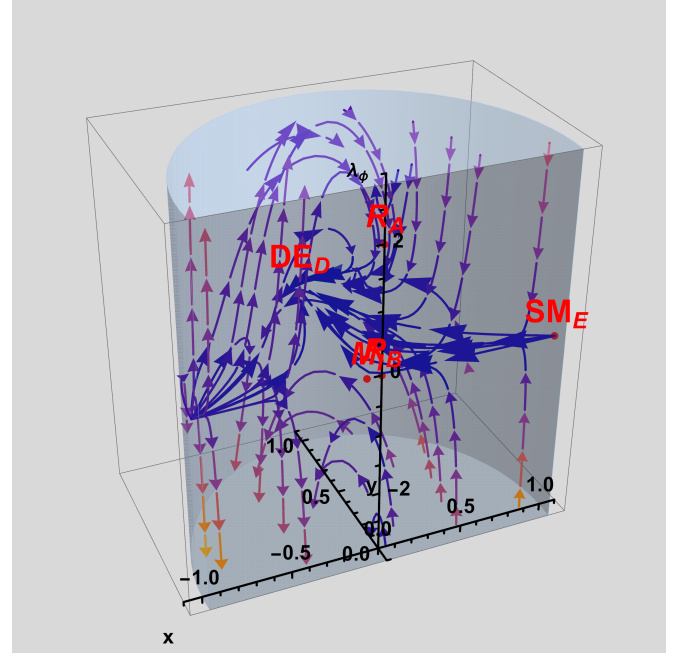


FIG. 5: 3D dynamical system diagram in the case of the NMC ekpyrotic/exponential SF with Λ model for $\beta = 10^{-1}$, $c = 10$ and $\lambda_\phi = 2$.

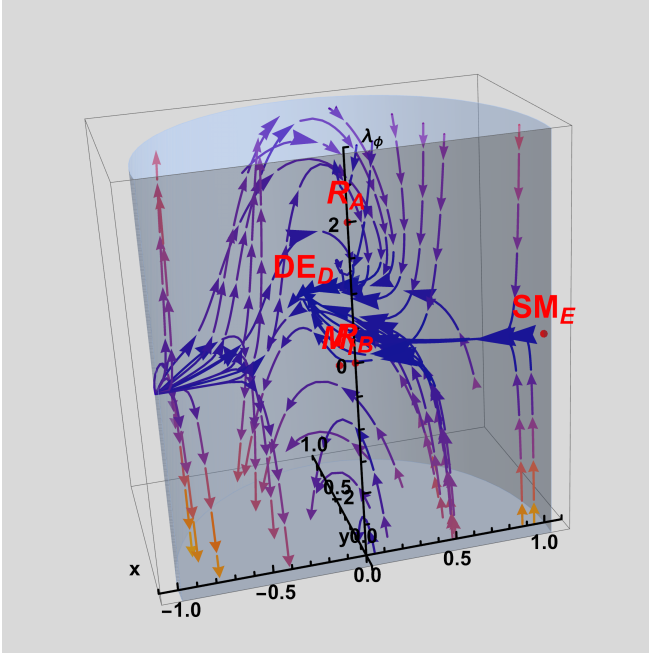


FIG. 4: 3D dynamical system diagram in the case of the NMC cyclic ekpyrotic model for $\beta = 10^{-1}$, $b = -5 \times 10^{-3}$, $c = 10$ and $\lambda_\phi = 2$. It is possible to observe a cyclic behaviour in the model for a number of selected values of the free parameters.

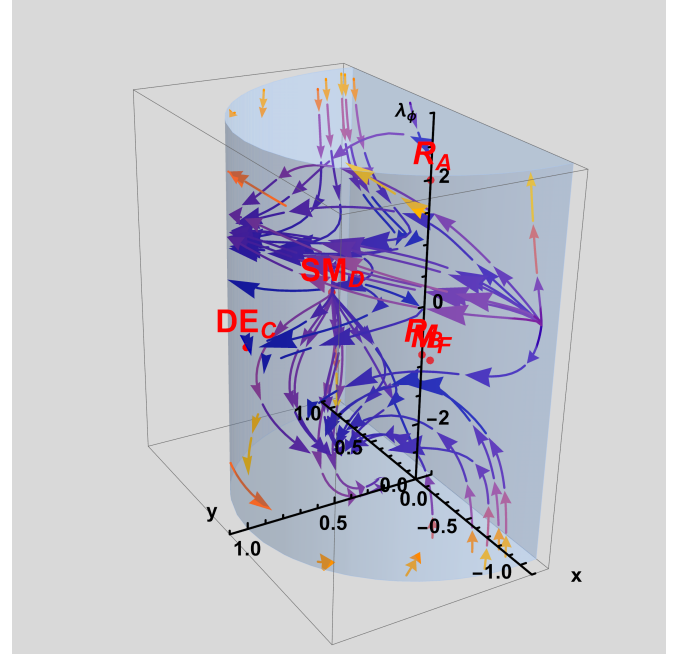


FIG. 6: 3D dynamical system diagram in the case of the NMC quintessence model for $\beta = 10^{-1}$, $n = -2$, $\lambda = 4 \times 10^{-1}$ and $\lambda_\phi = 2$.

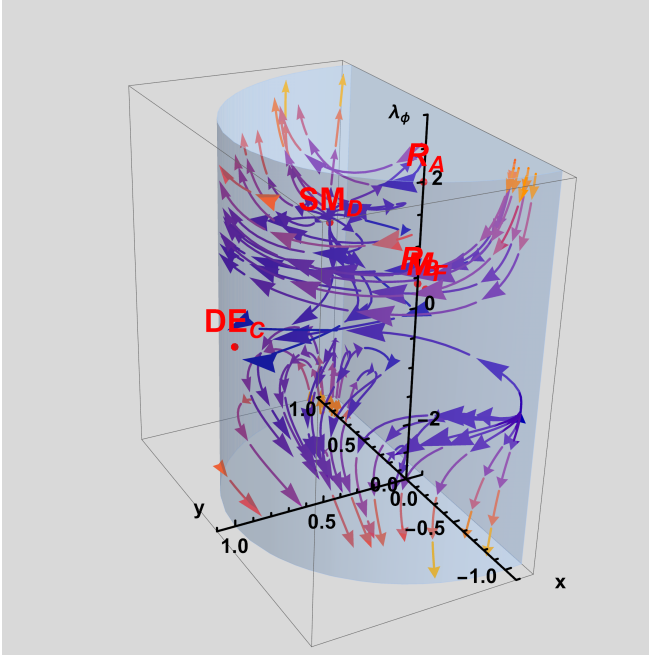


FIG. 7: 3D dynamical system diagram in the case of the NMC SFDM model for $\beta = 10^{-1}$, $\lambda = 4 \times 10^{-1}$ and $\lambda_\phi = 2$.

-
- [1] S. Weinberg, The Cosmological Constant Problem, *Rev. Mod. Phys.* **61**, 1 (1989).
 - [2] S. M. Carroll, The Cosmological constant, *Living Rev. Rel.* **4**, 1 (2001), arXiv:astro-ph/0004075.
 - [3] T. Padmanabhan, Cosmological constant: The Weight of the vacuum, *Phys. Rept.* **380**, 235 (2003), arXiv:hep-th/0212290.
 - [4] J. Martin, Everything You Always Wanted To Know About The Cosmological Constant Problem (But Were Afraid To Ask), *Comptes Rendus Physique* **13**, 566 (2012), arXiv:1205.3365 [astro-ph.CO].
 - [5] M. P. Hobson, G. P. Efstathiou, and A. N. Lasenby, *General Relativity: An Introduction for Physicists* (Cambridge University Press, 2006).
 - [6] R. J. Adler, B. Casey, and O. C. Jacob, Vacuum catastrophe: An Elementary exposition of the cosmological constant problem, *Am. J. Phys.* **63**, 620 (1995).
 - [7] P. J. E. Peebles and B. Ratra, The Cosmological Constant and Dark Energy, *Rev. Mod. Phys.* **75**, 559 (2003), arXiv:astro-ph/0207347.
 - [8] L. Amendola and S. Tsujikawa, *Dark Energy: Theory and Observations* (Cambridge University Press, 2015).
 - [9] P. Brax, What makes the Universe accelerate? A review on what dark energy could be and how to test it, *Rept. Prog. Phys.* **81**, 016902 (2018).
 - [10] N. Frusciante and L. Perenon, Effective field theory of dark energy: A review, *Phys. Rept.* **857**, 1 (2020), arXiv:1907.03150 [astro-ph.CO].
 - [11] G. Bertone, D. Hooper, and J. Silk, Particle dark matter: Evidence, candidates and constraints, *Phys. Rept.* **405**, 279 (2005), arXiv:hep-ph/0404175.
 - [12] M. Taoso, G. Bertone, and A. Masiero, Dark Matter Candidates: A Ten-Point Test, *JCAP* **03**, 022, arXiv:0711.4996 [astro-ph].
 - [13] J. Silk *et al.*, *Particle Dark Matter: Observations, Models and Searches*, edited by G. Bertone (Cambridge Univ. Press, Cambridge, 2010).
 - [14] G. Bertone and D. Hooper, History of dark matter, *Rev. Mod. Phys.* **90**, 045002 (2018), arXiv:1605.04909 [astro-ph.CO].
 - [15] G. Bertone and T. Tait, M. P., A new era in the search for dark matter, *Nature* **562**, 51 (2018), arXiv:1810.01668 [astro-ph.CO].
 - [16] G. Jungman, M. Kamionkowski, and K. Griest, Supersymmetric dark matter, *Phys. Rept.* **267**, 195 (1996), arXiv:hep-ph/9506380.
 - [17] L. Roszkowski, E. M. Sessolo, and S. Trojanowski, WIMP dark matter candidates and searches—current status and future prospects, *Rept. Prog. Phys.* **81**, 066201 (2018), arXiv:1707.06277 [hep-ph].
 - [18] T. Matos and L. A. Urena-Lopez, A Further analysis of a cosmological model of quintessence and scalar dark matter, *Phys. Rev. D* **63**, 063506 (2001), arXiv:astro-ph/0006024.
 - [19] L. Hui, J. P. Ostriker, S. Tremaine, and E. Witten, Ultralight scalars as cosmological dark matter, *Phys. Rev. D* **95**, 043541 (2017), arXiv:1610.08297 [astro-ph.CO].
 - [20] E. G. M. Ferreira, Ultra-light dark matter, *Astron. Astrophys. Rev.* **29**, 7 (2021), arXiv:2005.03254 [astro-ph.CO].
 - [21] D. F. J. Kimball and K. van Bibber, eds., *The Search for Ultralight Bosonic Dark Matter* (Springer, 2023).
 - [22] D. J. E. Marsh, Axion Cosmology, *Phys. Rept.* **643**, 1 (2016), arXiv:1510.07633 [astro-ph.CO].
 - [23] F. Chadha-Day, J. Ellis, and D. J. E. Marsh, Axion dark matter: What is it and why now?, *Sci. Adv.* **8**, abj3618 (2022), arXiv:2105.01406 [hep-ph].
 - [24] C. O'Hare, Cosmology of axion dark matter, *PoS COSMICWISPerS*, 040 (2024).
 - [25] W. Hu, R. Barkana, and A. Gruzinov, Cold and fuzzy dark matter, *Phys. Rev. Lett.* **85**, 1158 (2000), arXiv:astro-ph/0003365.
 - [26] M. Abdul Karim *et al.* (DESI), DESI DR2 Results II: Measurements of Baryon Acoustic Oscillations and Cosmological Constraints, (2025), arXiv:2503.14738 [astro-ph.CO].
 - [27] T. M. C. Abbott *et al.* (DES), Dark Energy Survey: implications for cosmological expansion models from the final DES Baryon Acoustic Oscillation and Supernova data, (2025), arXiv:2503.06712 [astro-ph.CO].
 - [28] C. Li, J. Wang, D. Zhang, E. N. Saridakis, and Y.-F. Cai, Quantum Gravity Meets DESI: Dynamical Dark Energy in Light of the Trans-Planckian Censorship Conjecture, (2025), arXiv:2504.07791 [astro-ph.CO].
 - [29] R. Brandenberger, Why the DESI Results Should Not Be A Surprise, (2025), arXiv:2503.17659 [astro-ph.CO].
 - [30] F. B. M. d. Santos, J. Morais, S. Pan, W. Yang, and E. Di Valentino, A New Window on Dynamical Dark Energy: Combining DESI-DR2 BAO with future Gravitational Wave Observations, (2025), arXiv:2504.04646 [astro-ph.CO].
 - [31] W. Giarè, T. Mahassen, E. Di Valentino, and S. Pan, An overview of what current data can (and cannot yet) say about evolving dark energy, *Phys. Dark Univ.* **48**, 101906 (2025), arXiv:2502.10264 [astro-ph.CO].
 - [32] W. Giarè, Dynamical Dark Energy Beyond Planck? Constraints from multiple CMB probes, DESI BAO and Type-Ia Supernovae, (2024), arXiv:2409.17074 [astro-ph.CO].
 - [33] W. Giarè, M. Najafi, S. Pan, E. Di Valentino, and J. T. Firouzjaee, Robust preference for Dynamical Dark Energy in DESI BAO and SN measurements, *JCAP* **10**, 035, arXiv:2407.16689 [astro-ph.CO].
 - [34] W. Giarè, M. A. Sabogal, R. C. Nunes, and E. Di Valentino, Interacting Dark Energy after DESI Baryon Acoustic Oscillation Measurements, *Phys. Rev. Lett.* **133**, 251003 (2024), arXiv:2404.15232 [astro-ph.CO].
 - [35] E. Di Valentino *et al.*, The CosmoVerse White Paper: Addressing observational tensions in cosmology with systematics and fundamental physics, (2025), arXiv:2504.01669 [astro-ph.CO].
 - [36] E. Di Valentino, O. Mena, S. Pan, L. Visinelli, W. Yang, A. Melchiorri, D. F. Mota, A. G. Riess, and J. Silk, In the realm of the Hubble tension—a review of solutions, *Class. Quant. Grav.* **38**, 153001 (2021), arXiv:2103.01183 [astro-ph.CO].
 - [37] E. Di Valentino and D. Brout, eds., *The Hubble Constant Tension*, Springer Series in Astrophysics and Cosmology (Springer, 2024).

- [38] A. H. Guth, The Inflationary Universe: A Possible Solution to the Horizon and Flatness Problems, *Phys. Rev. D* **23**, 347 (1981).
- [39] A. D. Linde, A New Inflationary Universe Scenario: A Possible Solution of the Horizon, Flatness, Homogeneity, Isotropy and Primordial Monopole Problems, *Phys. Lett. B* **108**, 389 (1982).
- [40] A. A. Starobinsky, A New Type of Isotropic Cosmological Models Without Singularity, *Phys. Lett. B* **91**, 99 (1980).
- [41] R. H. Brandenberger, Inflationary cosmology: Progress and problems, in *IPM School on Cosmology 1999: Large Scale Structure Formation* (1999) arXiv:hep-ph/9910410.
- [42] J. Martin and R. H. Brandenberger, The TransPlanckian problem of inflationary cosmology, *Phys. Rev. D* **63**, 123501 (2001), arXiv:hep-th/0005209.
- [43] U. H. Danielsson, A Note on inflation and transPlanckian physics, *Phys. Rev. D* **66**, 023511 (2002), arXiv:hep-th/0203198.
- [44] R. H. Brandenberger and J. Martin, Trans-Planckian Issues for Inflationary Cosmology, *Class. Quant. Grav.* **30**, 113001 (2013), arXiv:1211.6753 [astro-ph.CO].
- [45] J. Khoury, B. A. Ovrut, P. J. Steinhardt, and N. Turok, The Ekpyrotic universe: Colliding branes and the origin of the hot big bang, *Phys. Rev. D* **64**, 123522 (2001), arXiv:hep-th/0103239.
- [46] E. I. Buchbinder, J. Khoury, and B. A. Ovrut, New Ekpyrotic cosmology, *Phys. Rev. D* **76**, 123503 (2007), arXiv:hep-th/0702154.
- [47] J.-L. Lehnert, Ekpyrotic and Cyclic Cosmology, *Phys. Rept.* **465**, 223 (2008), arXiv:0806.1245 [astro-ph].
- [48] A. Ijjas, J.-L. Lehnert, and P. J. Steinhardt, General mechanism for producing scale-invariant perturbations and small non-Gaussianity in ekpyrotic models, *Phys. Rev. D* **89**, 123520 (2014), arXiv:1404.1265 [astro-ph.CO].
- [49] A. Ijjas and P. J. Steinhardt, Classically stable non-singular cosmological bounces, *Phys. Rev. Lett.* **117**, 121304 (2016), arXiv:1606.08880 [gr-qc].
- [50] A. Ijjas and P. J. Steinhardt, Fully stable cosmological solutions with a non-singular classical bounce, *Phys. Lett. B* **764**, 289 (2017), arXiv:1609.01253 [gr-qc].
- [51] A. Ijjas and P. J. Steinhardt, Bouncing Cosmology made simple, *Class. Quant. Grav.* **35**, 135004 (2018), arXiv:1803.01961 [astro-ph.CO].
- [52] P. J. Steinhardt, N. Turok, and N. Turok, A Cyclic model of the universe, *Science* **296**, 1436 (2002), arXiv:hep-th/0111030.
- [53] A. Ijjas and P. J. Steinhardt, A new kind of cyclic universe, *Phys. Lett. B* **795**, 666 (2019), arXiv:1904.08022 [gr-qc].
- [54] R. Penrose, Before the big bang: An outrageous new perspective and its implications for particle physics, *Conf. Proc. C* **060626**, 2759 (2006).
- [55] R. Penrose, *Cycles of Time: An Extraordinary New View of the Universe* (The Bodley Head, 2010).
- [56] R. Penrose, Difficulties with inflationary cosmology, *Annals N. Y. Acad. Sci.* **571**, 249 (1989).
- [57] A. Ijjas, P. J. Steinhardt, and A. Loeb, Inflationary paradigm in trouble after Planck2013, *Phys. Lett. B* **723**, 261 (2013), arXiv:1304.2785 [astro-ph.CO].
- [58] A. Ijjas, P. J. Steinhardt, and A. Loeb, Inflationary schism, *Phys. Lett. B* **736**, 142 (2014), arXiv:1402.6980 [astro-ph.CO].
- [59] A. Ijjas and P. J. Steinhardt, Implications of Planck2015 for inflationary, ekpyrotic and anamorphic bouncing cosmologies, *Class. Quant. Grav.* **33**, 044001 (2016), arXiv:1512.09010 [astro-ph.CO].
- [60] M. Postolak, Did the Big Bang and cosmic inflation really happen? (A tale of alternative cosmological models), (2024), arXiv:2404.18503 [physics.pop-ph].
- [61] M. Novello and S. E. P. Bergliaffa, Bouncing Cosmologies, *Phys. Rept.* **463**, 127 (2008), arXiv:0802.1634 [astro-ph].
- [62] D. Battefeld and P. Peter, A Critical Review of Classical Bouncing Cosmologies, *Phys. Rept.* **571**, 1 (2015), arXiv:1406.2790 [astro-ph.CO].
- [63] R. Brandenberger and P. Peter, Bouncing Cosmologies: Progress and Problems, *Found. Phys.* **47**, 797 (2017), arXiv:1603.05834 [hep-th].
- [64] J. D. Barrow, D. Kimberly, and J. Magueijo, Bouncing universes with varying constants, *Class. Quant. Grav.* **21**, 4289 (2004), arXiv:astro-ph/0406369.
- [65] C. Cheung, P. Creminelli, A. L. Fitzpatrick, J. Kaplan, and L. Senatore, The Effective Field Theory of Inflation, *JHEP* **03**, 014, arXiv:0709.0293 [hep-th].
- [66] D. Baumann and L. McAllister, *Inflation and String Theory*, Cambridge Monographs on Mathematical Physics (Cambridge University Press, 2015) arXiv:1404.2601 [hep-th].
- [67] T. S. Bunch and P. C. W. Davies, Quantum Field Theory in de Sitter Space: Renormalization by Point Splitting, *Proc. Roy. Soc. Lond. A* **360**, 117 (1978).
- [68] C. Caprini and D. G. Figueroa, Cosmological Backgrounds of Gravitational Waves, *Class. Quant. Grav.* **35**, 163001 (2018), arXiv:1801.04268 [astro-ph.CO].
- [69] M. Maggiore, *Gravitational Waves. Vol. 2: Astrophysics and Cosmology* (Oxford University Press, 2018).
- [70] R. Roshan and G. White, Using gravitational waves to see the first second of the Universe, *Rev. Mod. Phys.* **97**, 015001 (2025), arXiv:2401.04388 [hep-ph].
- [71] V. Mukhanov and S. Winitzki, *Introduction to quantum effects in gravity* (Cambridge University Press, 2007).
- [72] L. E. Parker and D. Toms, *Quantum Field Theory in Curved Spacetime: Quantized Field and Gravity*, Cambridge Monographs on Mathematical Physics (Cambridge University Press, 2009).
- [73] R. C. Tolman, *Relativity, Thermodynamics and Cosmology* (Clarendon Press, Oxford, 1934).
- [74] J. D. Bekenstein, Black holes and entropy, *Phys. Rev. D* **7**, 2333 (1973).
- [75] G. W. Gibbons and S. W. Hawking, Cosmological Event Horizons, Thermodynamics, and Particle Creation, *Phys. Rev. D* **15**, 2738 (1977).
- [76] I. Prigogine, J. Geheniau, E. Gunzig, and P. Nardone, Thermodynamics and cosmology, *Gen. Rel. Grav.* **21**, 767 (1989).
- [77] T. Padmanabhan, Thermodynamical Aspects of Gravity: New insights, *Rept. Prog. Phys.* **73**, 046901 (2010), arXiv:0911.5004 [gr-qc].
- [78] M. Visser and C. Barcelo, Energy conditions and their cosmological implications, in *3rd International Conference on Particle Physics and the Early Universe* (2000) pp. 98–112, arXiv:gr-qc/0001099.
- [79] S. W. Hawking and G. F. R. Ellis, The physical significance of curvature, in *The Large Scale Structure of Space-Time: 50th Anniversary Edition*, Cambridge

- Monographs on Mathematical Physics (Cambridge University Press, 2023) p. 78–116.
- [80] A. A. Coley, *Dynamical systems and cosmology* (Kluwer, Dordrecht, Netherlands, 2003).
 - [81] J. Wainwright and G. F. R. Ellis, *Dynamical Systems in Cosmology* (Cambridge University Press, 1997).
 - [82] S. Wiggins, *Introduction to Applied Nonlinear Dynamical Systems and Chaos* (Springer-Verlag, 2003).
 - [83] L. Perko, *Differential Equations and Dynamical Systems*, Vol. 7 (Springer New York, 2001).
 - [84] O. Hrycyna and M. Szydlowski, Extended Quintessence with non-minimally coupled phantom scalar field, *Phys. Rev. D* **76**, 123510 (2007), arXiv:0707.4471 [hep-th].
 - [85] O. Hrycyna and M. Szydlowski, Non-minimally coupled scalar field cosmology on the phase plane, *JCAP* **04**, 026, arXiv:0812.5096 [hep-th].
 - [86] S. Bahamonde, C. G. Böhm, S. Carloni, E. J. Copeland, W. Fang, and N. Tamanini, Dynamical systems applied to cosmology: dark energy and modified gravity, *Phys. Rept.* **775-777**, 1 (2018), arXiv:1712.03107 [gr-qc].
 - [87] P. Ntelis and J. Levi Said, Exploring ϕ CDM model dynamics, *Eur. Phys. J. C* **85**, 218 (2025), arXiv:2502.03486 [gr-qc].
 - [88] G. Obied, H. Ooguri, L. Spodyneiko, and C. Vafa, De Sitter Space and the Swampland, (2018), arXiv:1806.08362 [hep-th].
 - [89] P. Agrawal, G. Obied, P. J. Steinhardt, and C. Vafa, On the Cosmological Implications of the String Swampland, *Phys. Lett. B* **784**, 271 (2018), arXiv:1806.09718 [hep-th].
 - [90] E. Palti, The Swampland: Introduction and Review, *Fortsch. Phys.* **67**, 1900037 (2019), arXiv:1903.06239 [hep-th].
 - [91] Y. Akrami, R. Kallosh, A. Linde, and V. Vardanyan, The Landscape, the Swampland and the Era of Precision Cosmology, *Fortsch. Phys.* **67**, 1800075 (2019), arXiv:1808.09440 [hep-th].
 - [92] M. van Beest, J. Calderón-Infante, D. Mirfendereski, and I. Valenzuela, Lectures on the Swampland Program in String Compactifications, *Phys. Rept.* **989**, 1 (2022), arXiv:2102.01111 [hep-th].
 - [93] H. Ooguri and C. Vafa, On the Geometry of the String Landscape and the Swampland, *Nucl. Phys. B* **766**, 21 (2007), arXiv:hep-th/0605264.
 - [94] E. W. Kolb and M. S. Turner, *The Early Universe*, Vol. 69 (Taylor and Francis, 2019).
 - [95] A. Riotto and M. Trodden, Recent progress in baryogenesis, *Ann. Rev. Nucl. Part. Sci.* **49**, 35 (1999), arXiv:hep-ph/9901362.
 - [96] M. Dine and A. Kusenko, The Origin of the matter - antimatter asymmetry, *Rev. Mod. Phys.* **76**, 1 (2003), arXiv:hep-ph/0303065.
 - [97] L. Canetti, M. Drewes, and M. Shaposhnikov, Matter and Antimatter in the Universe, *New J. Phys.* **14**, 095012 (2012), arXiv:1204.4186 [hep-ph].
 - [98] D. J. Kapner, T. S. Cook, E. G. Adelberger, J. H. Gundlach, B. R. Heckel, C. D. Hoyle, and H. E. Swanson, Tests of the gravitational inverse-square law below the dark-energy length scale, *Phys. Rev. Lett.* **98**, 021101 (2007), arXiv:hep-ph/0611184.
 - [99] C. M. Will, The Confrontation between General Relativity and Experiment, *Living Rev. Rel.* **17**, 4 (2014), arXiv:1403.7377 [gr-qc].
 - [100] C. Burrage and J. Sakstein, Tests of Chameleon Gravity, *Living Rev. Rel.* **21**, 1 (2018), arXiv:1709.09071 [astro-ph.CO].
 - [101] P. Touboul *et al.* (MICROSCOPE), MICROSCOPE Mission: Final Results of the Test of the Equivalence Principle, *Phys. Rev. Lett.* **129**, 121102 (2022), arXiv:2209.15487 [gr-qc].
 - [102] A. Borowiec and M. Postolak, Is it possible to separate baryonic from dark matter within the Λ -CDM formalism?, *Phys. Lett. B* **860**, 139176 (2025), arXiv:2309.10364 [gr-qc].
 - [103] A. Paliathanasis, Dynamical Analysis in Chameleon Dark Energy, *Fortsch. Phys.* **71**, 2300088 (2023), arXiv:2306.03880 [gr-qc].
 - [104] H. Kodama and M. Sasaki, Cosmological perturbation theory, *Progress of Theoretical Physics Supplement* **78**, 1 (1984).
 - [105] V. F. Mukhanov, H. A. Feldman, and R. H. Brandenberger, Theory of cosmological perturbations, *Physics Reports* **215**, 203 (1992).
 - [106] C.-P. Ma and E. Bertschinger, Cosmological perturbation theory in the synchronous and conformal Newtonian gauges, *Astrophys. J.* **455**, 7 (1995), arXiv:astro-ph/9506072.
 - [107] K. A. Malik and D. Wands, Cosmological perturbations, *Physics Reports* **475**, 1 (2009).
 - [108] D. Baumann, *Cosmology* (Cambridge University Press, 2022).
 - [109] R. Holman and A. J. Tolley, Enhanced Non-Gaussianity from Excited Initial States, *JCAP* **05**, 001, arXiv:0710.1302 [hep-th].
 - [110] I. Agullo and L. Parker, Non-gaussianities and the Stimulated creation of quanta in the inflationary universe, *Phys. Rev. D* **83**, 063526 (2011), arXiv:1010.5766 [astro-ph.CO].
 - [111] E. Wilson-Ewing, The Matter Bounce Scenario in Loop Quantum Cosmology, *JCAP* **03**, 026, arXiv:1211.6269 [gr-qc].
 - [112] J. Carr, *Applications of Centre Manifold Theory*, Vol. 35 (Springer US, 1981).
 - [113] N. Roy and N. Banerjee, Dynamical systems study of chameleon scalar field, *Annals of Physics* **356**, 452 (2015).
 - [114] R. Zaregonbadi, N. Saba, and M. Farhoudi, Cosmological solutions of chameleon scalar field model, *European Physical Journal C* **83**, 1 (2023).
 - [115] J. Khoury and A. Weltman, Chameleon cosmology, *Phys. Rev. D* **69**, 044026 (2004), arXiv:astro-ph/0309411.
 - [116] P. Brax, C. van de Bruck, A.-C. Davis, J. Khoury, and A. Weltman, Detecting dark energy in orbit: The cosmological chameleon, *Phys. Rev. D* **70**, 123518 (2004), arXiv:astro-ph/0408415.
 - [117] P. J. Steinhardt, L.-M. Wang, and I. Zlatev, Cosmological tracking solutions, *Phys. Rev. D* **59**, 123504 (1999), arXiv:astro-ph/9812313.
 - [118] I. Zlatev, L.-M. Wang, and P. J. Steinhardt, Quintessence, cosmic coincidence, and the cosmological constant, *Phys. Rev. Lett.* **82**, 896 (1999), arXiv:astro-ph/9807002.
 - [119] R. R. Caldwell, R. Dave, and P. J. Steinhardt, Cosmological imprint of an energy component with general equation of state, *Phys. Rev. Lett.* **80**, 1582 (1998), arXiv:astro-ph/9708069.

- [120] A. Suarez and T. Matos, Structure Formation with Scalar Field Dark Matter: The Fluid Approach, *Mon. Not. Roy. Astron. Soc.* **416**, 87 (2011), arXiv:1101.4039 [gr-qc].
- [121] M. Joyce, Electroweak Baryogenesis and the Expansion Rate of the Universe, *Phys. Rev. D* **55**, 1875 (1997), arXiv:hep-ph/9606223.
- [122] A. R. Liddle and D. H. Lyth, *Cosmological inflation and large scale structure* (Cambridge University Press, 2000).
- [123] D. Blas, J. Lesgourgues, and T. Tram, The Cosmic Linear Anisotropy Solving System (CLASS) II: Approximation schemes, *JCAP* **07**, 034, arXiv:1104.2933 [astro-ph.CO].
- [124] J. Torrado and A. Lewis, Cobaya: Code for Bayesian Analysis of hierarchical physical models, *JCAP* **05**, 057, arXiv:2005.05290 [astro-ph.IM].
- [125] J. A. S. Lima, Thermodynamics of decaying vacuum cosmologies, *Phys. Rev. D* **54**, 2571 (1996), arXiv:gr-qc/9605055.
- [126] A. Ashtekar and V. Petkov, eds., *Springer Handbook of Spacetime*, Springer Handbooks (Springer, Berlin, 2014).
- [127] J. Khoury and A. Weltman, Chameleon fields: Awaiting surprises for tests of gravity in space, *Phys. Rev. Lett.* **93**, 171104 (2004), arXiv:astro-ph/0309300.
- [128] B. Bertotti, L. Iess, and P. Tortora, A test of general relativity using radio links with the Cassini spacecraft, *Nature* **425**, 374 (2003).
- [129] R. Jackiw and S. Y. Pi, Chern-Simons modification of general relativity, *Phys. Rev. D* **68**, 104012 (2003), arXiv:gr-qc/0308071.
- [130] S. Alexander and N. Yunes, Chern-Simons Modified General Relativity, *Phys. Rept.* **480**, 1 (2009), arXiv:0907.2562 [hep-th].
- [131] M. Satoh, S. Kanno, and J. Soda, Circular Polarization of Primordial Gravitational Waves in String-inspired Inflationary Cosmology, *Phys. Rev. D* **77**, 023526 (2008), arXiv:0706.3585 [astro-ph].
- [132] T. Qiu, J. Evslin, Y.-F. Cai, M. Li, and X. Zhang, Bouncing Galileon Cosmologies, *JCAP* **10**, 036, arXiv:1108.0593 [hep-th].
- [133] J. Grain and A. Barrau, Cosmological footprints of loop quantum gravity, *Phys. Rev. Lett.* **102**, 081301 (2009), arXiv:0902.0145 [gr-qc].
- [134] P. D. Meerburg and E. Pajer, Observational Constraints on Gauge Field Production in Axion Inflation, *JCAP* **02**, 017, arXiv:1203.6076 [astro-ph.CO].
- [135] I. Agullo and N. A. Morris, Detailed analysis of the predictions of loop quantum cosmology for the primordial power spectra, *Phys. Rev. D* **92**, 124040 (2015), arXiv:1509.05693 [gr-qc].
- [136] V. Faraoni, E. Gunzig, and P. Nardone, Conformal transformations in classical gravitational theories and in cosmology, *Fund. Cosmic Phys.* **20**, 121 (1999), arXiv:gr-qc/9811047.
- [137] A. Y. Kamenshchik and C. F. Steinwachs, Question of quantum equivalence between Jordan frame and Einstein frame, *Phys. Rev. D* **91**, 084033 (2015), arXiv:1408.5769 [gr-qc].
- [138] E. Barausse *et al.*, Prospects for Fundamental Physics with LISA, *Gen. Rel. Grav.* **52**, 81 (2020), arXiv:2001.09793 [gr-qc].
- [139] K. G. Arun *et al.* (LISA), New horizons for fundamental physics with LISA, *Living Rev. Rel.* **25**, 4 (2022), arXiv:2205.01597 [gr-qc].
- [140] C. Caprini *et al.*, Detecting gravitational waves from cosmological phase transitions with LISA: an update, *JCAP* **03**, 024, arXiv:1910.13125 [astro-ph.CO].
- [141] J. K. Erickson, D. H. Wesley, P. J. Steinhardt, and N. Turok, Kasner and mixmaster behavior in universes with equation of state $w \geq 1$, *Phys. Rev. D* **69**, 063514 (2004), arXiv:hep-th/0312009.
- [142] J.-L. Lehnners, P. McFadden, N. Turok, and P. J. Steinhardt, Generating ekpyrotic curvature perturbations before the big bang, *Phys. Rev. D* **76**, 103501 (2007), arXiv:hep-th/0702153.
- [143] L. A. Boyle and P. J. Steinhardt, Probing the early universe with inflationary gravitational waves, *Phys. Rev. D* **77**, 063504 (2008), arXiv:astro-ph/0512014.
- [144] M. Zumalacarregui, Gravity in the Era of Equality: Towards solutions to the Hubble problem without fine-tuned initial conditions, *Phys. Rev. D* **102**, 023523 (2020), arXiv:2003.06396 [astro-ph.CO].
- [145] N. Aghanim *et al.* (Planck), Planck 2018 results. VI. Cosmological parameters, *Astron. Astrophys.* **641**, A6 (2020), [Erratum: *Astron. Astrophys.* 652, C4 (2021)], arXiv:1807.06209 [astro-ph.CO].
- [146] H.-Y. Schive, M.-H. Liao, T.-P. Woo, S.-K. Wong, T. Chiueh, T. Broadhurst, and W. Y. P. Hwang, Understanding the Core-Halo Relation of Quantum Wave Dark Matter from 3D Simulations, *Phys. Rev. Lett.* **113**, 261302 (2014), arXiv:1407.7762 [astro-ph.GA].
- [147] S. Weinberg, Entropy generation and the survival of protogalaxies in an expanding universe, *Astrophys. J.* **168**, 175 (1971).
- [148] C. Eckart, The Thermodynamics of irreversible processes. 3.. Relativistic theory of the simple fluid, *Phys. Rev.* **58**, 919 (1940).
- [149] W. Israel and J. M. Stewart, Transient relativistic thermodynamics and kinetic theory, *Annals Phys.* **118**, 341 (1979).
- [150] R. Maartens, Dissipative cosmology, *Class. Quant. Grav.* **12**, 1455 (1995).
- [151] W. Zimdahl, Bulk viscous cosmology, *Phys. Rev. D* **53**, 5483 (1996), arXiv:astro-ph/9601189.
- [152] R. Bousso, The Holographic principle, *Rev. Mod. Phys.* **74**, 825 (2002), arXiv:hep-th/0203101.
- [153] S. Wang, Y. Wang, and M. Li, Holographic Dark Energy, *Phys. Rept.* **696**, 1 (2017), arXiv:1612.00345 [astro-ph.CO].
- [154] J. D. Bekenstein, A Universal Upper Bound on the Entropy to Energy Ratio for Bounded Systems, *Phys. Rev. D* **23**, 287 (1981).
- [155] J. D. Bekenstein, How does the entropy / information bound work?, *Found. Phys.* **35**, 1805 (2005), arXiv:quant-ph/0404042.
- [156] R. Brustein and S. P. de Alwis, Moduli stabilization and supersymmetry breaking in effective theories of strings, *Phys. Rev. Lett.* **87**, 231601 (2001), arXiv:hep-th/0106174.
- [157] S. Nojiri and S. D. Odintsov, The Final state and thermodynamics of dark energy universe, *Phys. Rev. D* **70**, 103522 (2004), arXiv:hep-th/0408170.
- [158] E.-A. Kontou and K. Sanders, Energy conditions in general relativity and quantum field theory, *Class. Quant. Grav.* **37**, 193001 (2020), arXiv:2003.01815 [gr-qc].

- [159] R. Penrose, Gravitational collapse and space-time singularities, *Phys. Rev. Lett.* **14**, 57 (1965).
- [160] S. W. Hawking and G. F. R. Ellis, *The Large Scale Structure of Space-Time*, Cambridge Monographs on Mathematical Physics (Cambridge University Press, 2023).
- [161] R. Penrose, Singularities and time-asymmetry, in *General Relativity: An Einstein Centenary Survey*, edited by S. Hawking and W. Israel (Cambridge University Press, 1979) pp. 581–638, 1st ed.
- [162] E. Curiel, A Primer on Energy Conditions, *Einstein Stud.* **13**, 43 (2017), arXiv:1405.0403 [physics.hist-ph].
- [163] C. Barcelo and M. Visser, Twilight for the energy conditions?, *Int. J. Mod. Phys. D* **11**, 1553 (2002), arXiv:gr-qc/0205066.
- [164] L. H. Ford, Quantum Coherence Effects and the Second Law of Thermodynamics, *Proc. Roy. Soc. Lond. A* **364**, 227 (1978).
- [165] C. J. Fewster, Quantum energy inequalities, in *Wormholes, Warp Drives and Energy Conditions*, edited by F. S. N. Lobo (Springer International Publishing, Cham, 2017) pp. 215–254.
- [166] D. H. Lyth, What would we learn by detecting a gravitational wave signal in the cosmic microwave background anisotropy?, *Phys. Rev. Lett.* **78**, 1861 (1997), arXiv:hep-ph/9606387.
- [167] F. J. Tipler, Energy conditions and spacetime singularities, *Phys. Rev. D* **17**, 2521 (1978).
- [168] C. J. Fewster, Lectures on quantum energy inequalities, (2012), arXiv:1208.5399 [gr-qc].
- [169] A. Wehrl, General properties of entropy, *Rev. Mod. Phys.* **50**, 221 (1978).
- [170] V. Vedral, The role of relative entropy in quantum information theory, *Rev. Mod. Phys.* **74**, 197 (2002), arXiv:quant-ph/0102094.
- [171] I. Bars, P. J. Steinhardt, and N. Turok, Cyclic Cosmology, Conformal Symmetry and the Metastability of the Higgs, *Phys. Lett. B* **726**, 50 (2013), arXiv:1307.8106 [gr-qc].
- [172] S. Navas *et al.* (Particle Data Group), Review of particle physics, *Phys. Rev. D* **110**, 030001 (2024).
- [173] T.-H. Yeh, J. Shelton, K. A. Olive, and B. D. Fields, Probing physics beyond the standard model: limits from BBN and the CMB independently and combined, *JCAP* **10**, 046, arXiv:2207.13133 [astro-ph.CO].
- [174] A. D. Sakharov, Violation of CP Invariance, C asymmetry, and baryon asymmetry of the universe, *Pisma Zh. Eksp. Teor. Fiz.* **5**, 32 (1967).
- [175] A. G. Cohen, D. B. Kaplan, and A. E. Nelson, Progress in electroweak baryogenesis, *Ann. Rev. Nucl. Part. Sci.* **43**, 27 (1993), arXiv:hep-ph/9302210.
- [176] N. Manton and P. Sutcliffe, Saddle points – sphalerons, in *Topological Solitons*, Cambridge Monographs on Mathematical Physics (Cambridge University Press, 2004) p. 441–466.
- [177] A. G. Cohen and D. B. Kaplan, Thermodynamic Generation of the Baryon Asymmetry, *Phys. Lett. B* **199**, 251 (1987).
- [178] A. G. Cohen and D. B. Kaplan, SPONTANEOUS BARYOGENESIS, *Nucl. Phys. B* **308**, 913 (1988).
- [179] H. Davoudiasl, R. Kitano, G. D. Kribs, H. Murayama, and P. J. Steinhardt, Gravitational baryogenesis, *Phys. Rev. Lett.* **93**, 201301 (2004), arXiv:hep-ph/0403019.
- [180] Y. Akrami *et al.* (Planck), Planck 2018 results. X. Constraints on inflation, *Astron. Astrophys.* **641**, A10 (2020), arXiv:1807.06211 [astro-ph.CO].
- [181] V. A. Kostelecky and N. Russell, Data Tables for Lorentz and CPT Violation, *Rev. Mod. Phys.* **83**, 11 (2011), arXiv:0801.0287 [hep-ph].
- [182] *The Road to Reality : A Complete Guide to the Laws of the Universe* (Random House, 2005).
- [183] P. J. Steinhardt and N. Turok, Cosmic evolution in a cyclic universe, *Phys. Rev. D* **65**, 126003 (2002), arXiv:hep-th/0111098.
- [184] V. Faraoni, *Cosmology in scalar tensor gravity* (Springer Dordrecht, 2004).